UNSTEADY SUPERSONIC CASCADE THEORY INCLUDING NONLINEAR THICKNESS EFFECTS

William Richard Chadwick

NAVAL POSTGRADUATE SCHOOL
Monterey, California

THESIS

UNSTEADY SUPERSONIC CASCADE THEORY
INCLUDING NONLINEAR THICKNESS EFFECTS

by

William Richard Chadwick

June 1975

Thesis Advisor: M. Platzer

REPORT DOCUMENTATION PAGE

READ INSTRUCTIONS BEFORE COMPLETING FORM

1. REPORT NUMBER

2. GOVT ACCESSION NO.

3. RECIPIENT'S CATALOG NUMBER

4. TITLE (and Subtitle)
Unsteady Supersonic Cascade Theory Including Nonlinear Thickness Effects

5. TYPE OF REPORT & PERIOD COVERED
Doctor of Philosophy Thesis; June 1975

6. PERFORMING ORG. REPORT NUMBER

7. AUTHOR(s)
William Richard Chadwick

8. CONTRACT OR GRANT NUMBER(s)

9. PERFORMING ORGANIZATION NAME AND ADDRESS
Naval Postgraduate School
Monterey, California 93940

10. PROGRAM ELEMENT, PROJECT, TASK AREA & WORK UNIT NUMBERS

11. CONTROLLING OFFICE NAME AND ADDRESS
Naval Postgraduate School
Monterey, California 93940

12. REPORT DATE
June 1975

13. NUMBER OF PAGES
131

14. MONITORING AGENCY NAME & ADDRESS(if different from Controlling Office)

15. SECURITY CLASS. (of this report)
Unclassified

15a. DECLASSIFICATION/DOWNGRADING SCHEDULE

16. DISTRIBUTION STATEMENT (of this Report)

Approved for public release; distribution unlimited.

17. DISTRIBUTION STATEMENT (of the abstract entered in Block 20, if different from Report)

18. SUPPLEMENTARY NOTES

19. KEY WORDS (Continue on reverse side if necessary and identify by block number)

Unsteady supersonic cascade theory
Nonlinear thickness effects

20. ABSTRACT (Continue on reverse side if necessary and identify by block number)

Several problems are treated which arise in the study of generalized airforces in unsteady supersonic cascades having subsonic axial velocity. The finite cascade of oscillating wedges is first solved numerically. When the thickness is very small, the general nonlinear solution agrees with results based on the linear theory of characteristics, while for a single wedge oscillating near shock detachment it agrees closely

(20. ABSTRACT Continued)

with Carrier's exact solution. There is some indication that thickness effects are reduced by cascading. Next, the finite cascade of oscillating flat plates is solved analytically, to the third power of oscillation frequency. The generalized surface pressure is shown to agree with exact numerical results for moderate blade index, but diverges in the far field of the cascade. For comparison with the finite cascade, there is presented finally an elementary periodic solution for the infinite cascade. A simple relationship between the two basic cascade models is developed. The investigation is presently restricted to flow regions upstream of Mach wave reflections in the blade passages.

Unsteady Supersonic Cascade Theory Including Nonlinear Thickness Effects

by

William Richard Chadwick
Research Associate, Naval Surface Weapons Center
B.S., Royal College of Advanced Technology, 1957
M.S., Cranfield Institute of Technology, 1959
M.S., Catholic University of America, 1968

Submitted in partial fulfillment of the
requirements for the degree of

DOCTOR OF PHILOSOPHY

from the

NAVAL POSTGRADUATE SCHOOL
June 1975

ABSTRACT

Several problems are treated which arise in the study of generalized airforces in unsteady supersonic cascades having subsonic axial velocity. The finite cascade of oscillating wedges is first solved numerically. When the thickness is very small, the general nonlinear solution agrees with results based on the linear theory of characteristics, while for the single wedge oscillating near shock detachment it agrees closely with Carrier's exact solution. There is some indication that thickness effects are reduced by cascading. Next, the finite cascade of oscillating flat plates is solved analytically, to the third power of oscillation frequency. The generalized surface pressure is shown to agree with exact numerical results for moderate blade index, but diverges in the far field of the cascade. For comparison with the finite cascade, there is presented finally an elementary periodic solution for the infinite cascade. A simple relationship between the two basic cascade models is developed. The investigation is presently restricted to flow regions upstream of Mach wave reflections in the blade passages.

TABLE OF CONTENTS

SYMBOLS

a	speed of sound in undisturbed flow
b	dimensionless pivot, measured from leading edge
c	chord of blade or aerofoil
d	blade spacing (fig. 3.1)
$g(y)$	dimensionless lateral excursion amplitude of bow wave
f,h	arbitrary functions of the arguments $(x-\beta y)$ or $(\xi-\beta\eta)$
g,r	arbitrary functions of the argument $(\xi+\beta\eta)$
k	reduced frequency $(k=\omega c/U)$
l	chordwise stagger of adjacent blades (fig. 3.1)
m	chordwise stagger of adjacent leading edge Mach lines (fig. 3.1)
n	blade index
s	left running Mach wave $(s=x-\beta y)$
u_o, v_o	dimensionless horizontal and vertical perturbation velocities respectively (thickness problem)
u_1, v_1	dimensionless horizontal and vertical perturbation velocities respectively (unsteady angle-of-attack problem)
$\hat{u}_1, \hat{v}_1$	the quantities u_1 and v_1 immediately downstream of bow wave respectively
$w_n, \hat{w}_n$	dimensionless normal velocities immediately upstream and downstream of bow wave respectively
$w_t, \hat{w}_t$	dimensionless tangential velocities immediately upstream and downstream of bow wave respectively
$w_1(x)$	downwash velocity
v'	dimensionless normal velocity of bow shock in stationary coordinates

x,y	dimensionless cartesian coordinates ($x=X/c$, $y=Y/c$)
t	time ($t=TU/c$)
y	aerofoil surface ($y=Y/c$)
C_p^u, C_p^l	aerofoil pressure coefficient on upper and lower surface respectively
M	Mach number of inlet flow relative to blading
M_n	component of M normal to bow wave
U	velocity of inlet flow relative to blading
α_n	angle-of-attack of n^{th} blade
β	cotangent of Mach angle ($\beta^2=M^2-1$)
$\gamma_o(y)$	orientation of bow shock wave in steady flow
γ'	change in orientation of bow shock wave due to aerofoil motion
γ	adiabatic index
δ	wedge semi-vertex angle
$\zeta, \bar{\zeta}$	left and right running Mach waves respectively ($\zeta=\xi-\beta\eta$, $\bar{\zeta}=\xi+\beta\eta$)
θ	transformation variable
λ, μ	state variables (thickness problem)
ν	defined by equ. 2.43
ξ,η	dimensionless cartesian coordinates, generally used for n^{th} blade with origin at leading edge
ρ	density of undisturbed flow
ϕ	perturbation velocity potential
ϕ_o, ϕ_1	potentials due to thickness distribution and angle-of-attack respectively
μ	interblade phase angle
ψ	modified perturbation velocity potential
ΔC_p	total pressure loading coefficient ($\Delta C_p=C_p^l - C_p^u$)
ω	oscillation frequency

1 INTRODUCTION

1.1 General Problem Area

Significant improvements in the performance of the next generation of gas turbine engines seem possible with compressors having lighter discs and blades, with a smaller number of stages and increased pressure ratio perstage. This calls for increased tip speeds which give rise to supersonic flow relative to the blades, even when the axial flow is subsonic. With lighter blades operating in the low supersonic range close to the flutter boundary, the non-linear effects of blade thickness may also be important. In this regard unsteady airforce calculations are frequently advanced with the warning that thickness effects have not been considered.

Flutter problems have thus arisen which are quite different from those associated with stalled compressor blading. The onset of this phenomenon is characterized by a sudden increase in blade stress at the fundamental mode frequency. When flutter is encountered, it is also observed that all the blades oscillate at the same frequency, usually in the torsional mode, with some constant interblade phase angle [1].

With the above features in mind, the present work aims to provide methods for determining oscillating airforces in high-speed compressor stages for use in flutter calculations.

Both thickness effects and certain aspects of the linearized supersonic flow theory are considered. In order to study these problems, however, the actual flow through the compressor must be simplified. Thus, irreversible shock losses and viscous boundary layer interactions are neglected. However, the resulting potential flow field remains highly three-dimensional due to rotational effects and downwash induced by the blade-tip vortex system [2]. The fully three-dimensional case is too difficult to handle by present methods and further simplification is achieved by unwrapping the annulus of blades from the body of the compressor (see fig. 1.1). Thus, generalized airforces for flutter calculation purposes are at present calculated by determining the irrotational flow of a perfect gas through oscillating two-dimensional cascades.

Supersonic cascades are of the two types illustrated in fig. 1.1. When the axial velocity into the compressor stage is supersonic, the Mach lines of the effective inlet flow are swept back beyond the leading edge locus. This is the rectilinear cascade with the supersonic leading-edge locus condition, in which no disturbances exist upstream of the blade passages. The entire flow in this case is a periodic extension of the flow between the first two blades. The solution of this problem, using a Laplace transformation, was first given by Lane [3]. When the axial velocity is subsonic there results the subsonic leading edge locus

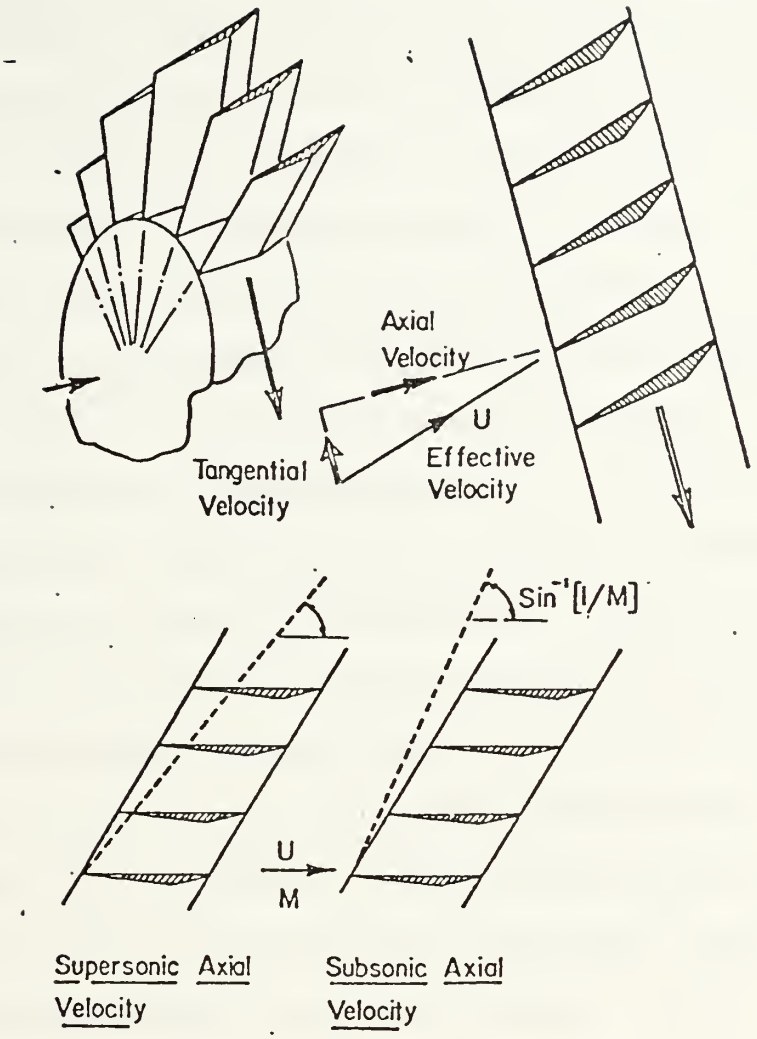

fig. 1.1 The two basic rectilinear cascades

condition, in which disturbances exist infinitely far upstream. This is the case of main practical interest and it has yet to be solved in closed form for general oscillation frequencies.

1.2 Rectilinear Cascade Theory - Recent Progress

Noteworthy of the progress which has recently been made with the above problem are the approaches of Platzer and Chalkley [4], Brix and Platzer [5], Verdon [6] and Nagashima and Whitehead [8]. Although somewhat different procedures were used in each case, namely characteristics [4,5], finite differences [6] and singularity distribution methods [8], the agreement between the methods is generally good. The dependent variable in these methods is the forced steady state amplitude of the velocity potential. However, the methods exhibit several disadvantages. First, convergence is slow and it is usually necessary to add the effect of a large number of aerofoils; Verdon shows regular oscillations in the amplitude of the unsteady lift and pitching moment out to blade index 30. Second, for large blade index, significant numerical errors are introduced in pressure loading, particularly when the blades oscillate in phase. Third, no mathematical proof exists to show that the limiting pressures are indeed representative of the infinite array.

An alternative numerical approach by Sisto and Ni [7] attacks the infinite cascade by directly introducing the boundary condition which ensures periodicity of the flow with blade index. Instead of solving the small perturbation wave equation for the forced steady state amplitude of the velocity potential, Sisto solves the complete set of unsteady flow equations using the time-marching technique. However, in

the example given, 1000 time-steps were needed for convergence [7]. The method, apparently, may be extended to include thickness effects.

The infinite cascade problem has recently been solved analytically to the first order in frequency by Kurosaka [9]. Using the streamwise coordinate x as the Laplace transformation variable, a general solution in integral form for $\phi(x,y)$ is obtained, which contains arbitrary functions for the initial conditions $\phi(o,y)$ and $\partial\phi/\partial x(o,y)$. The complexity of the initial value problem is reduced by representing $\phi(x,y)$ as the first two terms in a power series based on frequency. Reformulation as a simple integral equation follows by eliminating the unknown initial condition using the periodicity requirement in the cascade. The analysis is complicated and the equations of great length. The stability boundaries, for torsional oscillations at reduced frequency 0.1, are of little practical application in turbine flutter calculations. Comparison with any of the available finite cascade solutions would have been of more fundamental interest. A limitation of the theory is that when the blades oscillate in phase, the surface pressures become infinite; the lifting pressure, however, remains finite. This could indicate that a first-order power series in frequency is inadequate. Kurosaka is presently extending this work to include terms of higher order in frequency.* In a very recent paper, Verdon and

---

*Unpublished communication.

McCune present a singularity method for the infinite cascade [10]; further work, however, is required to clarify the numerical convergence aspects of the method.

The concern of the discussion to the present juncture has been with linearized supersonic flow theory. Thus, the above methods for predicting flutter in compressor stages have employed unsteady supersonic airforces calculated on the basis of flat-plate theory; the influence of blade thickness remains to be investigated. Thickness influences the steady flow about supersonic wings by causing a redistribution of pressure which usually changes the total lift force slightly and the pitching moment considerably. This well known experimental result is in agreement with Busemann's second-order potential flow theory [11]. The unsteady counterpart of the Busemann theory is the second-order potential flow theory of Van Dyke [12]. Van Dyke gives a solution for the slowly oscillating aerofoil of arbitrary profile expressed as a third-power series based on frequency, and a solution for the oscillating wedge which is exact in frequency. Teipel considers the unsteady supersonic aerofoil with arbitrary profile, attacking the problem numerically [13,14]. This method also assumes potential flow, with no entropy loss through the oscillating bow shock wave. However, shock losses may be of practical interest in high-speed compressor blading near shock detachment. These effects may fortunately be estimated by comparison with Carrier's exact solution for the oscillating wedge [15].

1.3 Present Investigation

The main aims of the present work were twofold: first it was desired to determine a numerical procedure for calculating the nonlinear effects of blade thickness in finite cascades, and second it was desired to investigate theoretically the features of the linear (flat plate) cascade. The nonlinear study employs a generalization of Teipel's method, briefly mentioned earlier in this sequel. However, the flow variables immediately behind the second oscillating bow shock wave, and indeed behind each succeeding wave, can no longer be determined simply by assuming steady upstream flow conditions. The flow is taken to be irrotational and isentropic and to satisfy the unsteady form of the nonlinear transonic small perturbation equation at all points in the field. Teipel's approach is to derive the unsteady boundary conditions behind the oscillating bow shock wave (an interesting strategem involving the Rankine Hugoniot equation is used) and to then develop the solution downstream using a nonlinear characteristics procedure. A concise account is given of Teipel's work, omitting considerable detail, but emphasizing fundamentals and important computational steps.

Before extending the basic method to the cascade problem, its accuracy in the low supersonic range near shock detachment was carefully investigated by comparison with Carrier's exact solution for the oscillating wedge. This elegant

solution involves evaluation of an infinite Bessel function series; perhaps as a consequence there are no published results on pressure distribution, or indeed results of any kind showing the effect of thickness on the main aerodynamic stability derivatives in the low supersonic range. Such results, given here for the oscillating wedge, are thus of fundamental interest, as well as providing the necessary base for comparison with the potential flow theory.

Agreement is found with Van Dyke's result, that thickness generally reduces the dynamic stability of the torsion mode. However, the magnitude of the effect on pressure distribution and various unsteady force derivatives, is more dramatically illustrated by the present results than by those of previous authors. In the case, for example, of slow oscillations about a forward pivot at low supersonic Mach number, it is shown that while the biconvex aerofoil exhibits a level of instability only slightly higher than that predicted by the classical linear theory of Garrick and Rubinow [16], the equivalent single wedge is drastically unstable.

An important limitation in scope was imposed throughout the present work by restricting attention to the flow in the cascade upstream of any Mach wave reflections in the blade passages. These flow regions are indicated in fig. 1.2 as the preinterference zone A and first blade passage zone B of the cascade; they frequently extend through most of the

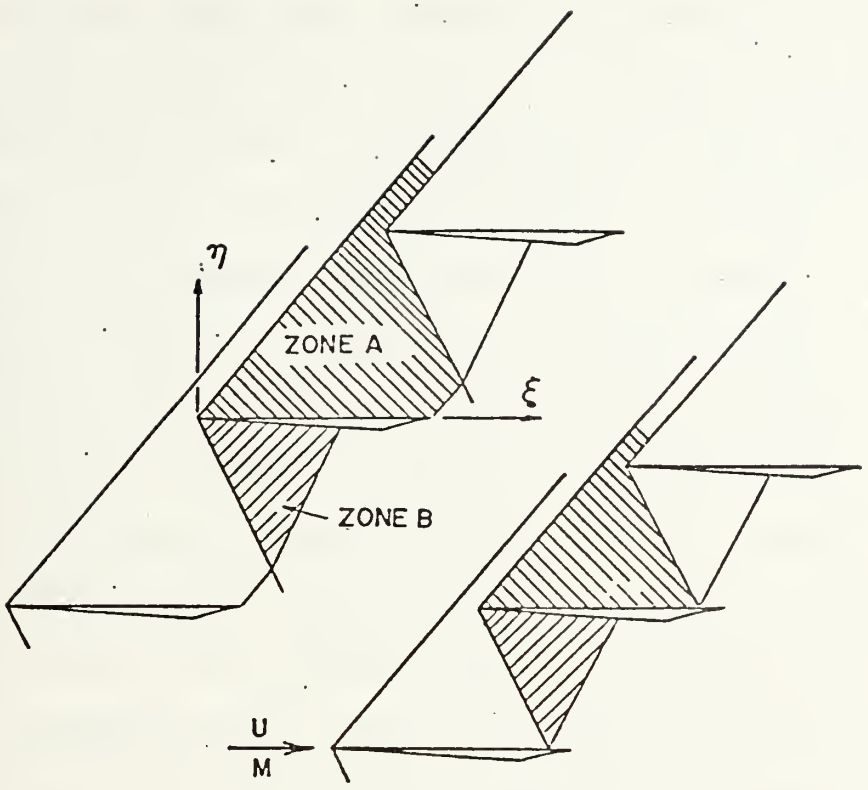

fig. 1.2 Preinterference and blade passage zones considered in the investigation

cascade. It is nevertheless to be emphasized that under no circumstances has attention been given to the trailing edge wake, which clearly influences the cascade exit flow [9,17].

Results for the finite cascade of oscillating wedges reduce correctly for vanishing blade thickness to those of Platzer and Verdon, mentioned earlier in this sequel.*

---

*Such exact limiting results, obtained from the general nonlinear thickness model, are extensively used in this dissertation for comparison with linear theory developments.

Also for this limiting case, certain simple forms of the general bow shock wave analysis are presented. Pressure distributions are given for two 5-percent thick wedges oscillating in phase for several oscillation frequencies. However, until the present solution is extended to the exit plane of the cascade the results are of limited use in practical flutter calculations. Nevertheless, reduced influence due to thickness for the second blade is indicated.

Section 3 presents a theoretical approach, using Laplace transformation, to the finite flat plate cascade. There is developed, to the third power in frequency, an analytical solution for the velocity potential together with closed-form expressions for unsteady pressure distribution. For two blades, the out-of-phase (damping) solution is shown to be accurate for reduced frequency 0.4 at $M = 1.25$ and for reduced frequency 0.7 at $M = 1.6$, well beyond the useful range of the first-order solution obtained by neglecting the cubic frequency term. On the other hand, the complete third-order theory is satisfactory out to blade index 9 for oscillations with reduced frequency 0.2 at $M = 1.6$. The theory also correctly predicts, when the blades oscillate in phase, a strong sinusoidal modulation of pressure with blade index. However, owing to an expansion of the Bessel function which assumes small values of the argument, the third-order solution diverges in the far field, failing to approach a finite limit with increasing blade index. When the higher order terms are removed, the first-order frequency solution

solution is relatively simple. In paragraph 3.4 there is given an alternative derivation of this important first-order solution for the finite cascade, based on Sauer's classical treatment of the oscillating flat plate in unbounded flow [18].

The coefficients of upper surface pressure and total pressure loading, according to the first-order theory, are found to be

$$C_{P_n}^{(u)} = C_{P_1}^{(u)} + i \frac{2km}{\beta^3} \sum_{p=1}^{n-1} e^{-p\mu}$$

$$\Delta C_{P_n} = 2C_{P_1}^{(u)} [e^{-i\mu} - 1] + i \frac{4k}{\beta} [\frac{M^2 d}{\beta} - m] e^{-i\mu}$$

for the n^{th} blade in the torsion mode when angle-of-attack is maximum. Here $C_{P_1}^{(u)}$ corresponds to the first blade; μ is interblade phase angle; k reduced frequency; d interblade spacing; and m the chordwise stagger of adjacent leading edge Mach lines (for the sonic leading-edge locus, m = 0, and $C_{P_n}^{(u)}$ is independent of blade index). To first-order frequency, the pressure loading for the finite cascade is therefore constant for all blades except the first, while for $\mu = 0$ it is independent of position along the chord and pivot axis location. The upper surface pressure, however, exhibits a continuing oscillation with blade index, except in the case

of zero interblade phase angle, when the out-of-phase component increases by the constant amount $2km/\beta^3$ from blade-to-blade.

There is derived in Section 4, using a much simpler approach than Kurosaka [9], an elementary periodic solution for the infinite cascade. When the condition of flow periodicity is imposed, the pressure loading coefficient for the infinite cascade is found to agree with ΔC_{P_n} given above, while for finite interblade phase angle the periodic solution for the surface pressure coefficient is precisely the mean value of the oscillatory series for $C_{P_n}^{(u)}$.

1.4 Important Note

Concerning the simple harmonic motion assumed for aerofoil angle of attack, the following should be emphasized. First, the time dependent angle of attack of the isolated blade, $\alpha_1 = \exp ikt$, where k is reduced frequency and t nondimensional time, assumes an oscillation amplitude of unity. This is consistent with the basic premise that all flow variables are linear functions of angle of attack and that the onset of flutter is characterized by oscillations of very small amplitude. Where significant nonlinearities are present (Section 2), they enter on account of aerofoil thickness. Second, the angle of attack of the n^{th} blade, at time zero, is denoted $\alpha_n = \alpha_1 \exp i(n-1)\mu$, where μ is interblade phase angle. Solutions for surface pressure consist of a real and an imaginary part, and throughout this dissertation final

results for the n^{th} blade are expressed at the instant when $\alpha_n = 1$, by multiplying by $\exp -i(n-1)\mu$. Accordingly, the real component of surface pressure is in-phase with the angle of attack of the n^{th} blade, while the imaginary component is the pressure which occurs at the instant when the blade presents zero angle of attack to the free stream with its trailing edge moving down.

This work was made possible for the author through the guidance of Professor Max F. Platzer of the Department of Aeronautics.

2 NONLINEAR THICKNESS EFFECTS

The methods which are being increasingly applied to the study of flutter in high-speed compressor stages employ generalized air forces calculated on the basis of linearized supersonic flow theory. Frequently, these methods are advanced with the warning that the results do not include nonlinear thickness effects. Accordingly, there is given in the present section, employing a generalization of Teipel's method for the single oscillating aerofoil, a numerical solution of the thickness problem for aerofoils oscillating in cascade. The method is intended for application in the low supersonic range near shock detachment, where thickness effects may be of considerable practical interest.

2.1 Aerofoil in Unbounded Supersonic Flow The Teipel Approach

The small perturbation equation describing the unsteady transonic flow of an irrotational fluid is given by Landahl [19]

$$\left[M^2 - 1 + \frac{U(\gamma+1)}{a^2}\frac{\partial\Phi}{\partial x}\right]\frac{\partial^2\Phi}{\partial x^2} - \frac{\partial^2\Phi}{\partial y^2} = -\frac{1}{a^2}\frac{\partial^2\Phi}{\partial T^2} - \frac{2M}{a}\frac{\partial^2\Phi}{\partial x \partial T} \qquad 2.1$$

where the nonlinear term involving the adiabatic index is shown in ref. 19 to be of vanishing significance for unsteady flows in which

$$k >> |M_L - 1| \qquad 2.2a$$

where k denotes reduced frequency and M_L local Mach number. The nonlinearity also vanishes for flows about bodies of small thickness, such that

$$k >> \delta^{2/3} \qquad 2.2b$$

where δ is the larger of the quantities thickness-to-chord ratio or oscillation amplitude. The present aim is to investigate the effect of thickness on the unsteady flow in low-supersonic compressor stages for blade vibration frequencies within the critical flutter range. Previous work, based on linearized supersonic flow theory, indicates that this range extends to k = 1.5 [20].

A clear understanding of Teipel's treatment of equ. 2.1 for the case of the biconvex aerofoil oscillating in unbounded supersonic flow is essential before considering the cascade problem. Accordingly, there is presented below a concise account of the Teipel method. This account, based on translations of the German by the present writer, strongly emphasizes the fundamentals of Teipel's analysis, highlights important computational steps, but omits considerable detail. Further, while Teipel employs the chord length c = 2 with origin at midchord and works in dimensional variables, these conventions are not adopted in the present study.

2.1.1 Characteristic equations

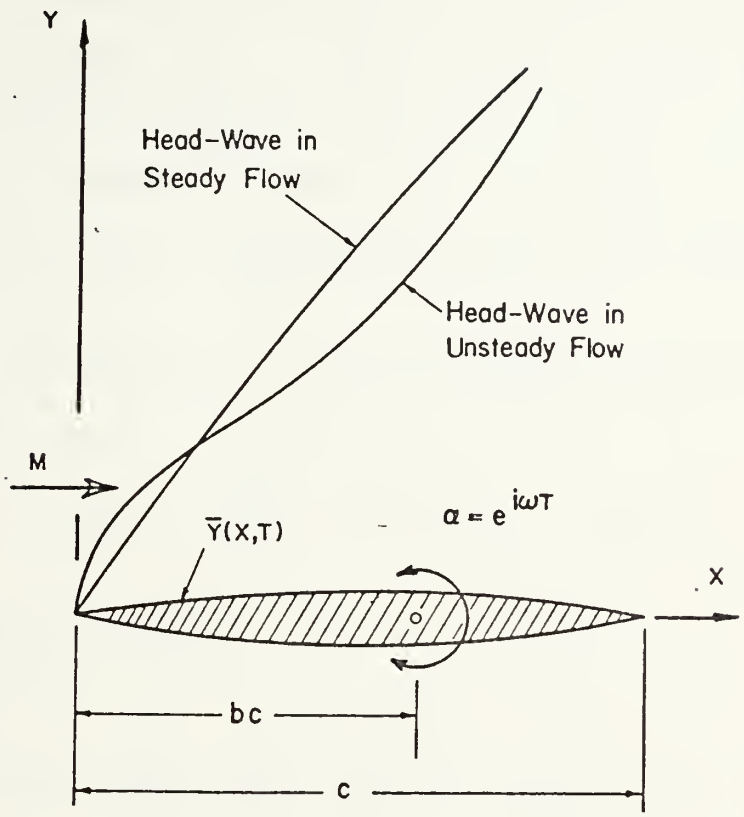

fig. 2.1 Biconvex aerofoil in torsion mode

With reference to fig. 2.1, the basic problems involved in solving equ. 2.1 are threefold. First, a solution must be found which satisfies the differential equation at all points within the disturbed flow field. Second, it must satisfy the usual linearized form of the unsteady boundary condition, which requires tangential flow along the aerofoil surface

$$\frac{\partial \Phi}{\partial Y} = U \frac{\partial \bar{Y}}{\partial X} + \frac{\partial \bar{Y}}{\partial T} \quad ; \quad Y = 0 \qquad 2.3$$

Third, the appropriate boundary conditions must be satisfied along the oscillating head wave which separates the disturbed from the undisturbed flow. The remainder of this paragraph outlines the Teipel approach for solving equ. 2.1 subject to the tangency condition of equ. 2.3. Paragraph 2.1.2 gives the head-wave analysis and paragraph 2.1.3 the computational steps.

Upon introducing the nondimensional variables

$$x = \frac{X}{c} , \quad y = \frac{Y}{c} , \quad t = \frac{TU}{c} , \quad \phi = \frac{\Phi}{cU} \qquad 2.4$$

equs. 2.1 and 2.3 become

$$\left[M^2 - 1 + M^2(\gamma+1)\right] \frac{\partial \phi}{\partial x} \frac{\partial^2 \phi}{\partial x^2} - \frac{\partial^2 \phi}{\partial y^2} = -M^2 \frac{\partial^2 \phi}{\partial t^2} - 2M^2 \frac{\partial^2 \phi}{\partial x \partial t} \qquad 2.5a$$

$$\frac{\partial \phi}{\partial y} = \frac{\partial \bar{y}}{\partial x} + \frac{\partial \bar{y}}{\partial t} \quad ; \quad y = 0 \qquad 2.5b$$

where $\bar{Y} = \bar{Y}(x,t)$, as shown in fig. 2.1, and $\bar{y} = \bar{Y}/c$.

Consider torsional oscillations $\alpha = \exp(i\omega T)$ about the pivot $x = b$, and define a reduced frequency

$$k = \frac{\omega c}{U} \qquad 2.6$$

Then there may be written for the total potential $\phi(x,y,t)$ the sum of a steady thickness term $\phi_o(x,y)$ and an unsteady angle-of-attack term $\phi_1(x,y)$

$$\phi(x,y,t) = \phi_o(x,y) + \phi_1(x,y)e^{ikt} \qquad 2.7$$

whereupon the differential equation and tangency condition become

$$\left[M^2 - 1 + M^2(\gamma+1)\frac{\partial\phi_o}{\partial x}\right]\frac{\partial^2\phi_o}{\partial x^2} - \frac{\partial^2\phi_o}{\partial y^2} = 0 \qquad 2.8a$$

$$\frac{\partial\phi_o}{\partial y} = \frac{\partial\bar{y}(x)}{\partial x} \quad ; \quad y = 0 \qquad 2.8b$$

$$\left[M^2-1+M^2(\gamma+1)\frac{\partial\phi_o}{\partial x}\right]\frac{\partial^2\phi_1}{\partial x^2} - \frac{\partial^2\phi_1}{\partial y^2} + \left[M^2(\gamma+1)\frac{\partial^2\phi_o}{\partial x^2}\right]\frac{\partial\phi_1}{\partial x}$$

$$- M^2k^2\phi_1 + i2kM^2\frac{\partial\phi_1}{\partial x} = 0 \qquad 2.9a$$

$$\frac{\partial\phi_1}{\partial y} = -[1 + ik(x-b)] \qquad 2.9b$$

where ϕ_1 denotes the amplitude of the forced steady-state velocity potential and $\bar{y}(x)$ the aerofoil profile, nondimensionalized through division by the chord. In deriving equ. 2.9a, ϕ_{1xx} is neglected in comparison with ϕ_{oxx}, in agreement with the assumption of very small amplitude oscillations. The hyperbolic differential equation (2.8a) is nonlinear, due to the term involving the adiabatic index . However, the solution procedure using nonlinear characteristics is

straightforward. The potential $\phi_o(x,y)$ represents the steady-state flow (assumed to be entirely supersonic) about a thin aerofoil (assumed to be symmetrical) at zero angle of attack.

The hyperbolic differential equation (2.9a) is linear – since ϕ_o is known. Furthermore, since the coefficients of the second-order derivatives are those in equation 2.8a, the characteristic directions in both problems are identical. The potential $\phi_1(x,y)$ represents the unsteady flow due to angle-of-attack.

The basic approach, using the method of characteristics is now apparent. First, equation 2.8 is solved. The compatibility relations for ϕ_o are extremely simple. However, they must be applied along characteristic lines in the (x,y) plane with varying slope. Second, employing appropriate compatibility relations for ϕ_1, the characteristic mesh derived for the steady problem (in the region formed between the head wave and the upper surface of the aerofoil) is used to develop the unsteady solution.

The characteristic lines of equ. 2.8a have the slope

$$\left(\frac{\partial y}{\partial x}\right)_{\alpha,\beta} = \pm \lambda^{-1/2} \qquad 2.10$$

along which the state variables change according to the compatibility relations

$$\lambda^{3/2} \mp \mu = \text{const.} \qquad 2.11$$

where the constant for the left running α characteristics (upper sign) will be denoted by C^{α} and that for the right running β characteristics (lower sign) by C^{β}, as shown in fig. 2.2. The state variables have the meaning

$$\lambda = M^2 - 1 + (\gamma + 1)\, M^2\, u_o \qquad 2.12a$$

$$\mu = \frac{3}{2}(\gamma + 1)\, M^2\, v_o \qquad 2.12b$$

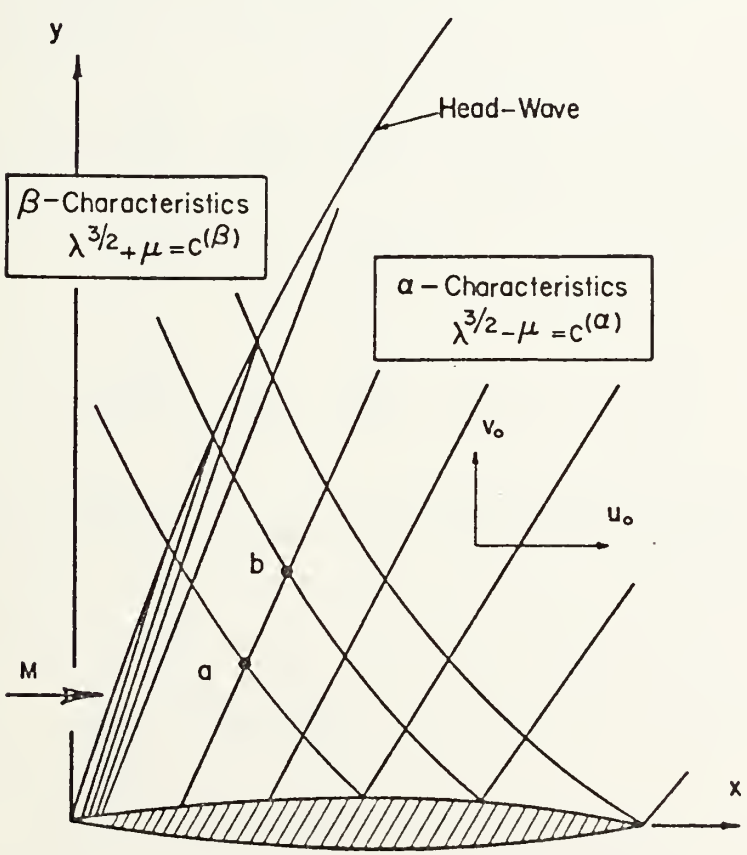

fig. 2.2 The characteristic mesh

where $u_o = \partial\phi_o/\partial x$ and $v_o = \partial\phi_o/\partial y$ are nondimensional horizontal and vertical perturbation velocities, respectively. Along the profile μ is known, from the tangency condition imposed by equ. 2.8b. The curvature of the head wave and the structure of the entire simple wave flow thus follow with little difficulty from equ. 2.10 to 2.12. Observe, for example, that the compatibility relations demand λ and μ constant along all α characteristics, which are therefore straight lines in the (x,y) plane. This important result follows if the β compatibility equation is assumed to remain valid through the bow shock wave.* For then there may be written, referring to fig. 2.2

$$\lambda_a^{3/2} + \mu_a = \lambda_\infty^{3/2}$$

$$\lambda_b^{3/2} + \mu_b = \lambda_\infty^{3/2}$$

$$\lambda_a^{3/2} - \mu_a = \lambda_b^{3/2} - \mu_b$$

where λ_∞ occurs in the undisturbed flow and $\mu_\infty = 0$. There follows

$$\lambda_a = \lambda_b$$

$$\mu_a = \mu_b$$

---

*Oswatitsch considers the problem, and by comparison with exact shock polar results shows that the use of equ. 2.11 leads to a maximum possible error in λ of 6% [21].

and from equ. 2.10 the result that the α characteristics are straight lines. The computational procedure for dealing with the ϕ_o problem is now straightforward and will be given in paragraph 2.1.3, as mentioned previously. Using equ. 2.12a, the differential equation describing the ϕ_1 problem may be written

$$\lambda \frac{\partial^2 \phi_1}{\partial x^2} - \frac{\partial^2 \phi_1}{\partial y^2} + \frac{\partial \lambda}{\partial x} \frac{\partial \phi}{\partial x} - M^2 k^2 \phi_1 + i2kM^2 \frac{\partial \phi_1}{\partial x} = 0 \qquad 2.13$$

whereupon, along the characteristic lines previously defined in equ. 2.10, the following compatibility relations can be shown to hold

$$\left[\frac{\partial u_1}{\partial x}\right]_{\alpha,\beta} \mp \frac{1}{\sqrt{\lambda}} \left[\frac{\partial v_1}{\partial x}\right]_{\alpha,\beta} + \frac{1}{\lambda}\left[\frac{\partial \lambda}{\partial x} + i2kM^2\right] u_1 - \frac{k^2 M^2}{\lambda} \phi_1 = 0 \qquad 2.14$$

where $u_1 = \partial\phi_1/\partial_x$, $v_1 = \partial\phi_1/\partial y$ are respectively nondimensional horizontal and vertical perturbation velocities for the unsteady problem. The state variable λ is known everywhere. In equ. 2.14 the second-order term in frequency somewhat complicates a numerical solution since, as is clear, the potential ϕ_1 itself must be determined throughout the field (by integrating the velocities).

Teipel's rather involved treatment of $\partial\lambda/\partial x$ can be simplified using a geometrical interpretation. At the point Q(x,y) in fig. 2.3

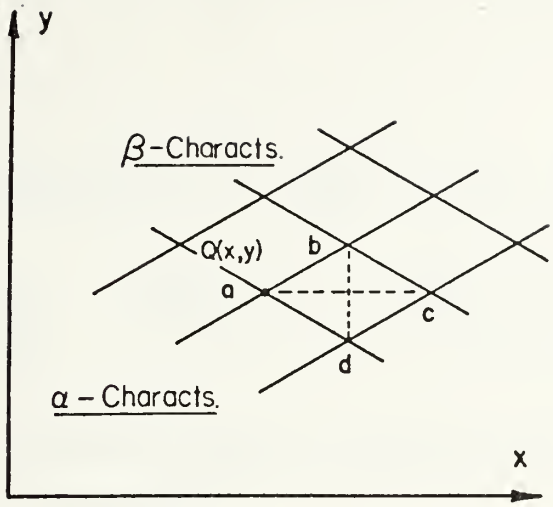

fig. 2.3 Geometrical interpretation of $\partial\lambda/\partial x$

$$\left[\frac{\partial\lambda}{\partial x}\right]_Q = \frac{\lambda_c - \lambda_a}{x_c - x_a} \quad ; \quad \text{limit} \quad x_c \to x_a$$

However, from a result of paragraph 2.1.1, the state variable λ is constant along an α characteristic. Accordingly, writing $\lambda_d = \lambda_c$ in the above equation and using an obvious approximation for the denominator

$$\left[\frac{\partial\lambda}{\partial x}\right]_Q = \frac{1}{2}\,\frac{\lambda_d - \lambda_a}{x_d - x_a} \quad ; \quad \text{limit} \quad x_d \to x_a$$

which is simply

$$\frac{\partial\lambda}{\partial x} = \frac{1}{2}\left[\frac{\partial\lambda}{\partial x}\right]_\beta \qquad 2.15$$

The compatibility equations for the unsteady problem thus become

$$du_1 - \frac{dv_1}{\sqrt{\lambda}} + \frac{u_1}{2\lambda}\left(\frac{\partial\lambda}{\partial x}\right)_\beta dx + i\,\frac{2kM^2}{\lambda}\,u_1\,dx - \frac{k^2M^2}{\lambda}\,\phi_1 dx = 0 \qquad 2.16a$$

$$du_1 + \frac{dv_1}{\sqrt{\lambda}} + \frac{u_1}{2\lambda} + i\,\frac{2kM^2}{\lambda}\,u_1\,dx - \frac{k^2M^2}{\lambda}\,\phi_1\,dx = 0 \qquad 2.16b$$

along α and β characteristics, respectively. Also, since $d\phi_1 = \partial\phi_1/\partial x dx + \partial\phi_1/\partial y dy$

$$\phi_1{}^b = \phi_1{}^a + \int_a^b (u_1 dx + v_1 dy) \qquad 2.17$$

Further details of important computational steps are given in paragraph 2.1.3.

2.1.2 Bow Shock Wave Analysis

There are two important boundaries associated with the $\phi_1(x,y)$ problem. One is the aerofoil surface along which the flow must be tangent and along which $v_1(x,o)$ is therefore given by equ. 2.9b. The other is the oscillating shock wave which emanates from the leading edge of the aerofoil. Fluid particles in the undisturbed flow, passing through this oblique moving shock, will have their properties suddenly changed. Accounting for entropy losses, this change could be calculated using the shock polar [22]. However, the flow is assumed to be isentropic and no account is

taken of irreversible shock losses. Accordingly, the flow variables immediately behind the head wave are derived using the isentropic Rankine Hugoniot relations. The more exact shock polar is not employed.

Teipel's analysis of the unsteady head wave is in fact surprisingly straightforward, when the equation for the change in gas speed through a moving normal shock is given. Such a weak shock is shown in fig. 2.4, moving from left-to-right with the speed W relative to the undisturbed inlet flow. Denoting the velocity of the latter w_n, the shock thus has the velocity $(W + w_n)$ in stationary coordinates. The one-dimensional continuity and momentum equations then lead to the expression given by (2.18) for $\hat{w}_n$, the gas speed following passage through the shock. Here it is to be assumed that the velocities w_n, $\hat{w}_n$ and W have been normalized through division by U. An outline of Teipel's elegant use of this result follows:

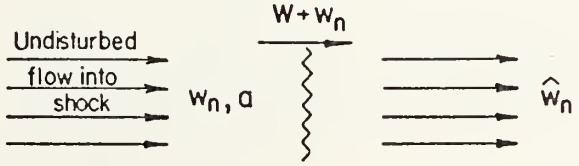

$$\hat{w}_n = w_n + \frac{2W}{\gamma+1}\left(1 - \frac{a^2/U^2}{W^2}\right) \qquad 2.18$$

fig. 2.4 Flow through normal shock

The locus of the oscillating head wave, as it might appear with the aerofoil at small positive incidence in a low frequency torsional mode, is shown in fig. 2.5. For a wedge, the orientation γ_o of the head wave in steady flow is constant. However, for the biconvex section shown, $\gamma_o = \gamma_o(y)$. Consider P(x,y) on the oscillating head wave in the immediate neighbourhood of the leading edge. Then, notwithstanding the variation of γ_o with y, the approximate horizontal coordinate of P is

$$x_p = y_p \cot \gamma_o + g(y)\ e^{ikt} \qquad 2.19$$

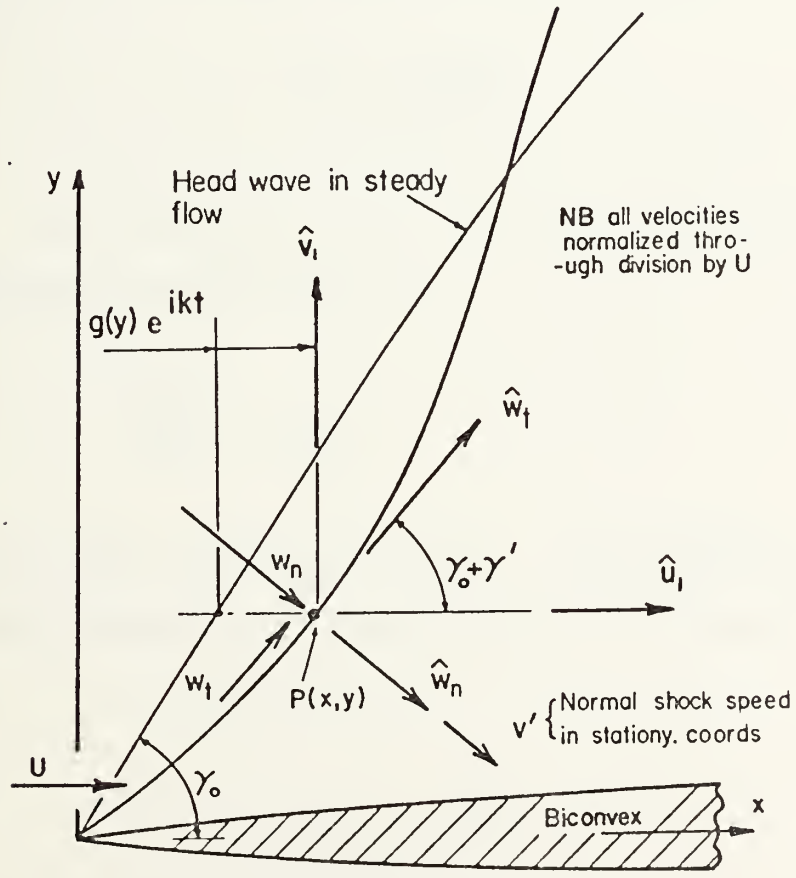

fig. 2.5 Geometry of oscillating bow wave

where the nondimensional, complex, shock excursion amplitude g(y) has been multiplied by exp(ikt) in accordance with the basic assumption involving harmonic time dependence. Omitting this time dependence, the slope at P(x,y) is

$$\left[\frac{\partial x}{\partial y}\right]_p = \cot \gamma_o + \frac{dg}{dy} = \cot (\gamma_o + \gamma') \qquad 2.20$$

where fig. 2.5 shows the small angle γ'. Employing an elementary trigonometrical expansion and taking $\tan \gamma' = \gamma'$, the change in the orientation of the head wave relative to its position in steady flow may thus be approximated by

$$\gamma' = - \sin^2 \gamma_o \frac{dg}{dy} \qquad 2.21$$

The nondimensionless velocity assumed for P(x,y) in stationary coordinates is

$$\frac{dx_p}{dt} = ikg(y) \qquad 2.22$$

from equ. 2.19, omitting exp(ikt). Multiplying by $\sin \gamma_o$, the normal velocity of the head wave in stationary coordinates is

$$v' = ik \sin \gamma_o \, g(y) \qquad 2.23$$

which is to be associated directly with the shock speed $(W + w_n)$ in fig. 2.4. It therefore follows from equ. 2.18 that the gas speed $\hat{w}_n$ immediately behind and normal to the head wave is given by

$$\hat{w}_n - w_n = \frac{2(v' - w_n)}{\gamma + 1}\left[1 - \frac{a^2/u^2}{(v' - w_n)^2}\right] \qquad 2.24$$

But

$$w_n = \sin(\gamma_o + \gamma') \doteq \sin\gamma_o + \gamma'\cos\gamma_o \qquad 2.25$$

whereupon

$$\hat{w}_n - w_n = \frac{2(v'-w_n)}{\gamma+1} + \frac{2a^2}{(\gamma+1)U^2\sin^2\gamma_o}\left[1+\frac{\gamma'\cos\gamma_o - v')}{\sin\gamma_o}\right]^{-1} \qquad 2.26$$

Employing the Binomial theorem, and after some simplification, the main result of the Teipel head wave analysis may be written

$$\hat{w}_n = \frac{\gamma-1}{\gamma+1}\sin\gamma_o\left[1+\frac{2/M_n^2}{\gamma-1}\right] + \frac{\gamma-1}{\gamma+1}\cos\gamma_o\left[1-\frac{2/M_n^2}{\gamma-1}\right]\gamma' + \frac{2}{\gamma+1}\left[1+\frac{1}{M_n^2}\right]v' \qquad 2.27$$

$$M_n = \frac{U\sin\gamma_o}{a} \qquad 2.28$$

where the second-order terms γ' and v' are given above in terms of the head-wave displacement $g(y)$. The tangential velocity of the fluid is unchanged on passing through the head wave and consequently

$$\hat{w}_t = w_t = \cos \gamma_o - \gamma' \sin \gamma_o \qquad 2.29$$

It is now required to find the dimensionless perturbation velocities $\partial\phi_1/\partial x$ and $\partial\phi_1/\partial y$ immediately behind the head wave, these being the desired boundary value quantities for the solution of the ϕ_1 problem. Formally introducing the overhat notation to denote quantities immediately behind the bow wave

$$\hat{u}_1 = (\hat{w}_n \sin\gamma + \hat{w}_t \cos\gamma) - (\hat{w}_n \sin\gamma_o + \hat{w}_t \cos\gamma_o) \qquad 2.30a$$

$$\hat{v}_1 = (-\hat{w}_n \cos\gamma + \hat{w}_t \sin\gamma) - (-\hat{w}_n \cos\gamma_o + \hat{w}_t \sin\gamma_o) \qquad 2.30b$$

where the two groups of terms on the right of equ. 2.30 represent fluid velocities behind the head wave (a) in unsteady flow and (b) in steady flow. Of course, $\gamma = \gamma_o + \gamma'$. The remaining work is routine. Neglecting squares and products of γ' and v', there is obtained finally

$$\hat{u}_1 = m_1 \frac{dg}{dy} + i m_2 g \qquad 2.31a$$

$$\hat{v}_1 = n_1 \frac{dg}{dy} + in_2 g \qquad 2.31b$$

$$m_1 = \frac{2}{\gamma+1} \sin 2\gamma_o \sin^2 \gamma_o$$

$$m_2 = \frac{2k}{\gamma+1} (1+1/M_n^2) \sin^2 \gamma_o \qquad 2.32$$

$$n_1 = \frac{-2}{\gamma+1} (\cos 2\gamma_o + 1/M_n^2) \sin^2 \gamma_o$$

$$n_2 = \frac{-2k}{\gamma+1} (1+1/M_n^2) \cot \gamma_o \sin^2 \gamma_o$$

The more formidable looking equations of ref. 14 result when the orientation of the head wave is expressed in the form

$$\tan \gamma_o = \frac{2}{\sqrt{\lambda} + \sqrt{\lambda_\infty}} \qquad 2.33$$

an important observation, which follows from the slope of the left-running characteristics in equ. 2.10, and is equivalent to averaging the Mach angles before and after leading-edge compression.

Equations 2.31a and 2.31b are simultaneous ordinary differential equations for the unsteady head-shock profile. They are expressed in terms of the unknown dimensionless perturbation velocities $\hat{u}_1$ and $\hat{v}_1$ immediately behind the shock. The coefficients m and n are functions of y in general

because of the curvature of the steady shock boundary. They are known from the solution of the ϕ_o problem.

2.1.3 Computational Procedure

Certain mathematical aspects of the unsteady transonic flow about a thin aerofoil have been discussed. It is now desired to translate these considerations into a procedure for solving the problem numerically. With regard to the steady state or ϕ_o problem, the following sequence of steps may be used:

(i) Guess the point P_a

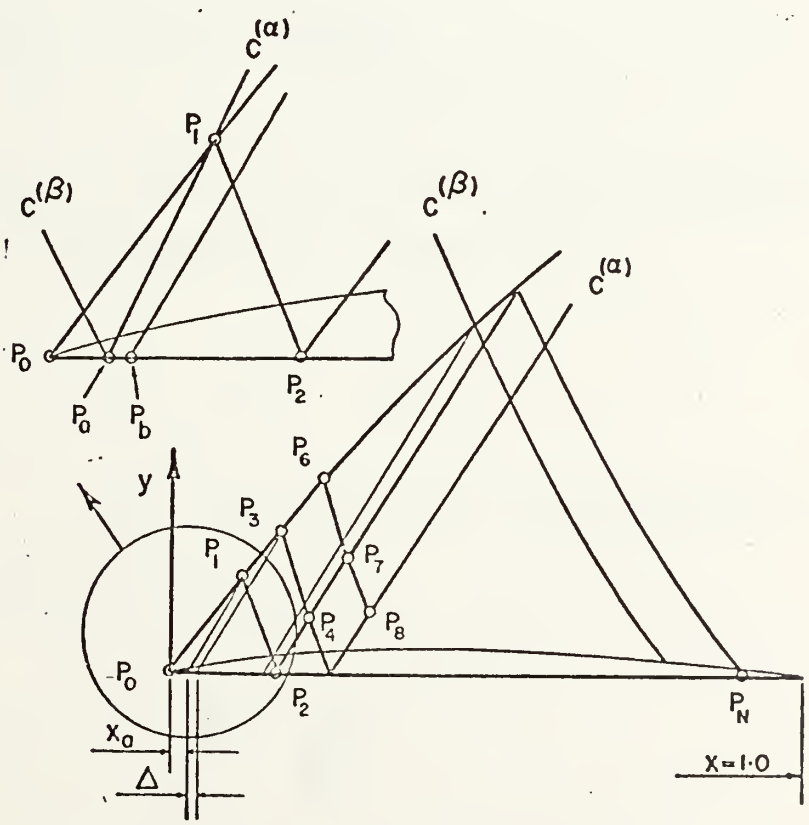

fig. 2.6 Construction procedure for characteristic lines and steady-state bow wave

(ii) There may be written, corresponding to the α and β characteristics which meet at P_a

$$\hat{\lambda}_1^{3/2} - \hat{\mu}_1 = \lambda a^{3/2} - \mu_a = C^{\alpha}$$

$$\lambda_\infty^{3/2} + \mu_\infty = \lambda_a^{3/2} + \mu_a = C^{\beta}$$

from equ. 2.11, and where, as noted previously, the overhat denotes a quantity immediately behind the head wave. But from the steady tangency condition of equ. 2.12b

$$\mu_a = \frac{3}{2} (\gamma+1) M^2 \left(\frac{\partial \bar{y}}{\partial x}\right)_{x_a}$$

Further, $\hat{\mu}_1 = \mu_a$ and $\hat{\lambda}_1 = \lambda_a$ since the two states are on the same α characteristic. Accordingly

$$\hat{\lambda}_1 = (\lambda_\infty^{3/2} - \mu_a)^{2/3}$$

(iii) Construct the α characteristic through P_a with slope from equ. 2.10

$$\frac{dy}{dx} = \frac{1}{\sqrt{\hat{\lambda}_1}}$$

(iv) Construct the initial segment of the head wave between the leading edge point P_o and P_1 with slope

$$\frac{dy}{dx} = \frac{4}{2\sqrt{\lambda_\infty} + \sqrt{\hat{\lambda}_1} + \sqrt{\hat{\lambda}_o}}$$

which is equivalent to averaging the Mach lines before and after leading edge compression. This is not the segment of an α characteristic. Hence, P_1 on the head wave is determined.

(v) The state variable μ_2 must satisfy the tangency condition and is a known function of x_2, as in step (ii). Along the β characteristic through P_2

$$\lambda_1^{3/2} + \mu_a = \lambda_2^{3/2} + \mu_2 = C^\beta$$

$$\frac{y_1}{x_2 - x_1} = \frac{2}{\sqrt{\lambda_1} + \sqrt{\lambda_2}}$$

and hence x_2 and λ_2 follow by a simple iteration procedure.

(vi) Guess Δ (thereby determining P_b) and repeat steps (ii)-to-(v).

Determination of the general mesh point P_4 is obvious. The above sequence of steps is repeated until the entire characteristic mesh is formed and the ϕ_o problem solved.

Some experience is useful in determining a suitable initial point P_a and the x-wise increment Δ.* In the case of a simple wedge or flat plate aerofoil, the head wave is straight and the state variables constant throughout the flow field; consequently the complexity of the ϕ_o problem is greatly reduced.

The same characteristic mesh applies to the unsteady ϕ_1 problem. Here, it will be recalled, there is available the following information: First, the unsteady tangency condition of equ. 2.9b for $\hat{v}_1(x,o)$; second, the compatibility relations of equs. 2.16a and 2.16b, which identify small differential changes in the state variables $u_1(x,y)$ and $v_1(x,y)$ along the α and β characteristics, respectively; and third, the first-order ordinary differential equations (2.31a and 2.31b) for g(y), the amplitude of the oscillating head wave, measured from steady state. For a typical problem the shaded area of fig. 2.7 is of infinitesimal dimension, as should be clear from the information in the footnote *. Accordingly, the leading edge values of $\hat{u}_1$ and $\hat{v}_1$ are assumed to apply throughout this small region. Let $\hat{v}_1(P_o)$, or v_o for convenience, denote the dimensionless vertical perturbation velocity immediately behind the head shock at the leading edge. Then from equ. 2.9b

---

*Typical values for M = 1.2, τ = 0.025 and M = 1.15, τ = 0.0125 were x_a = 0.0017, Δ = 0.0055 and x_a = 0.0088, Δ = 0.00425, respectively; with fourteen mesh points P_o, P_2, P_5 ... P_n.

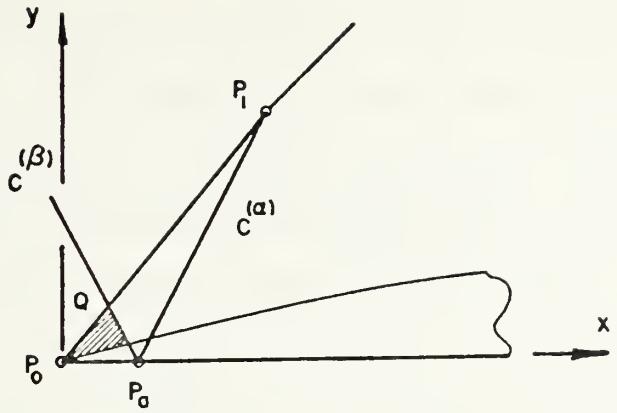

fig. 2.7 Initial step for the unsteady problem

$$v_o = -(1 - ikb)$$

where b is the dimensionless pivot. From equ. 2.31

$$u_o = \frac{m_1}{n_1} v_o$$

since g(o) = 0. Also from equ. 2.31

$$(u_1+u_o)/2 = m_1 \frac{g_1-g_o}{y_1-y_o} + im_2(g_1+g_o)/2 \qquad **$$

$$(v_1+v_o)/2 = n_1 \frac{g_1-g_o}{y_1-y_o} + in_2(g_1+g_o)/2 \qquad **$$

while from equ. 2.16a

$$u_1-u_o-\frac{v_1-v_o}{\sqrt{\lambda_1}} + \frac{(u_1+u_o)(\lambda_1-\lambda_o)}{2\lambda_1(x_a-x_Q)}(x_1-x_a) + i\frac{kM^2}{\lambda_1}(u_1+u_o)(x_1-x_a)$$

$$-\frac{k^2M^2}{\lambda_1}\left\{\phi_a+\frac{(x_1-x_a)}{2}(u_1+u_o)+(v_1+v_o)/\sqrt{\lambda_1}\right\}(x_1-x_a) = 0$$

where ϕ_a would be taken as zero for the single aerofoil in unbounded flow. The three algebraic equations (**) determine u_1, v_1, and g_1 at the mesh point P_1.* By similarly applying these equations to the points P_3, P_6, P_{10} (assume $\hat{u}_1(P_1)$ and $\hat{v}_1(P_1)$ apply at the intersection of the α characteristic through P_b with the β characteristic through P_1), the unsteady boundary conditions along the entire head wave may be determined. Subsequently, the compatibility relations (equs. 2.16a and 2.16b) give the entire unsteady flow field.

2.2 Discussion of Results for Flat Plate, Wedge and Biconvex Aerofoils

The linearized pressure coefficient on the upper surface of the aerofoil is

$$\frac{p^u - p^\infty}{1/2\rho u^2} = -\frac{2}{u}\left[\frac{\partial \Phi}{\partial x} + \frac{1}{u}\frac{\partial \Phi}{\partial t}\right] = -2[u_o + e^{ikt}(u_1 + ik\phi_1)] \qquad 2.34$$

where u_o and u_1 are dimensionless horizontal perturbation velocities due to aerofoil thickness and angle-of-attack, respectively. The thickness or steady state component of pressure is entirely real and of no direct interest. The unsteady component, which varies in accordance with the assumed harmonic time dependence, is complex and will be written, omitting the term exp(ikt)

---

*Again it is to be noted that u_1, v_1 and g_1 should in fact be denoted $\hat{u}_1(P_1)$, $\hat{v}_1(P_1)$ and $g(P_1)$.

$$C_P^{(u)} = -2(u_1 + ik\phi_1) \qquad 2.35$$

The present aim is to study the effect of thickness on $C_P^{(u)}$. Therefore, it is appropriate to first discuss the meaning of the real and imaginary parts. The real part, $R_e[C_P^{(u)}]$, is the pressure which occurs as the oscillation starts. It is the component of unsteady aerodynamic pressure which is in-phase with the angle-of-attack (aerodynamic stiffness). The imaginary part, $I_m[C_P^{(u)}]$, is the pressure at the instant the aerofoil presents zero angle-of-attack to the free stream with the trailing edge moving down. It is due to aerofoil rotation about the pivot and therefore out-of-phase with the angle-of-attack (aerodynamic damping).

A mathematical model describing Teipel's method has been formulated and results compared (a) with Teipel calculations for a family of biconvex aerofoils in the low supersonic range [13], and (b) with Carrier's exact solution for the oscillating wedge [15]. Some disagreement was found with Teipel, which could not be resolved. As shown in fig. 2.8 for a 2% thick biconvex aerofoil oscillating in the torsion mode about midchord this disagreement is in $I_m[C_P^{(u)}]$, the component of pressure which is out-of-phase with the angle-of-attack. Similar results were obtained for most of the torsion and plunge modes considered in ref. 13. However, in the case of vanishing aerofoil thickness, the present model agrees with Teipel, and indeed with the classical linear

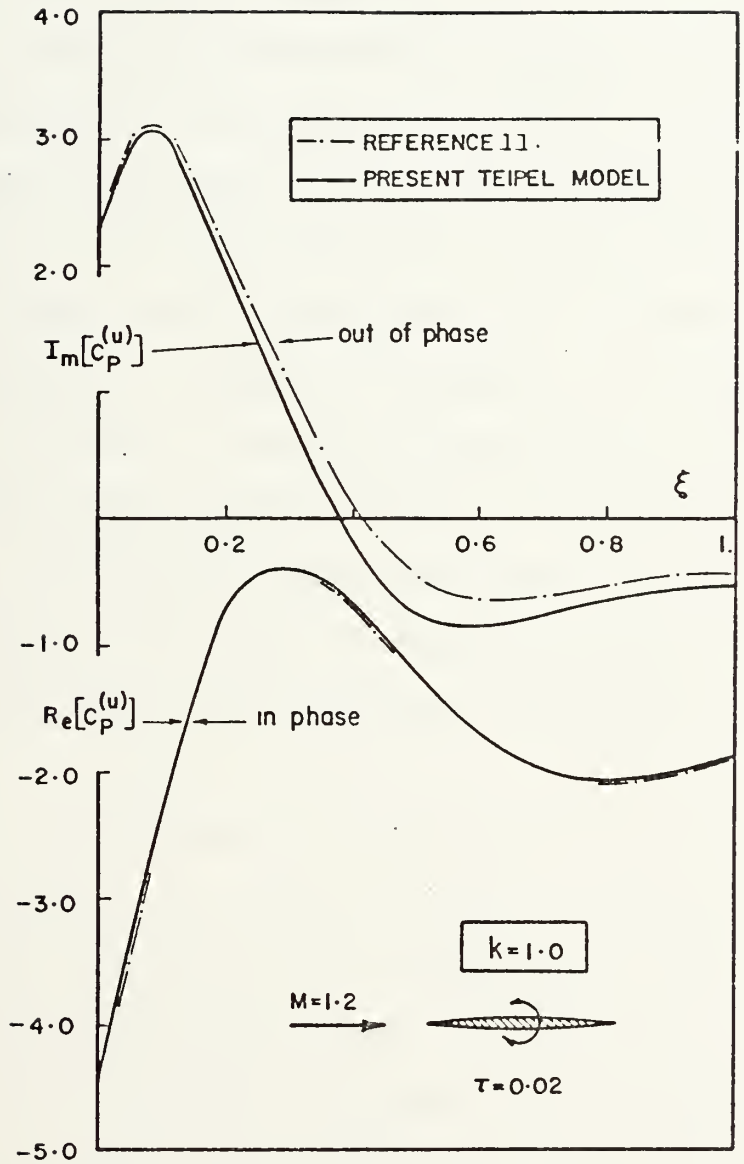

fig. 2.8 Pressure distribution for 2% thick biconvex aerofoil pivoted at mid-chord

theory of Garrick and Rubinow [16]. The structure of Teipel's nonlinear characteristics mesh is based on 13-points across the chord. A similar number was found to be satisfactory for all of the unsteady aerofoil motions considered in the present investigation.

As already mentioned Teipel assumes isentropic flow with no entropy loss through the head shock. In view of the envisaged application of the basic method to compressor blade rows in the low-supersonic range, where irreversible shock losses could be important, this assumption requires investigation. Carrier's solution for the wedge, oscillating about its apex in unbounded supersonic flow, is exact in thickness and therefore accounts correctly for entropy losses in the fluid provided the amplitude of oscillation is small (the solution is linear in angle-of-attack). It provides an obvious basis for comparison with the potential-flow theory.

The Carrier analysis is difficult and the final solution is expressed as an infinite series of Bessel functions of the first kind with certain coefficients which are to be determined successively from three simultaneous algebraic recurrence relations. Consequently, the computation involved is considerable, which may account for the fact that no pressure distributions based on the theory are available. Reference should be made, however, to exact calculations by Van Dyke of the stability derivative m_α for a 5% thick oscillating wedge. These are published in ref. 23, which extends Carrier's solution to include pivots other than the apex.

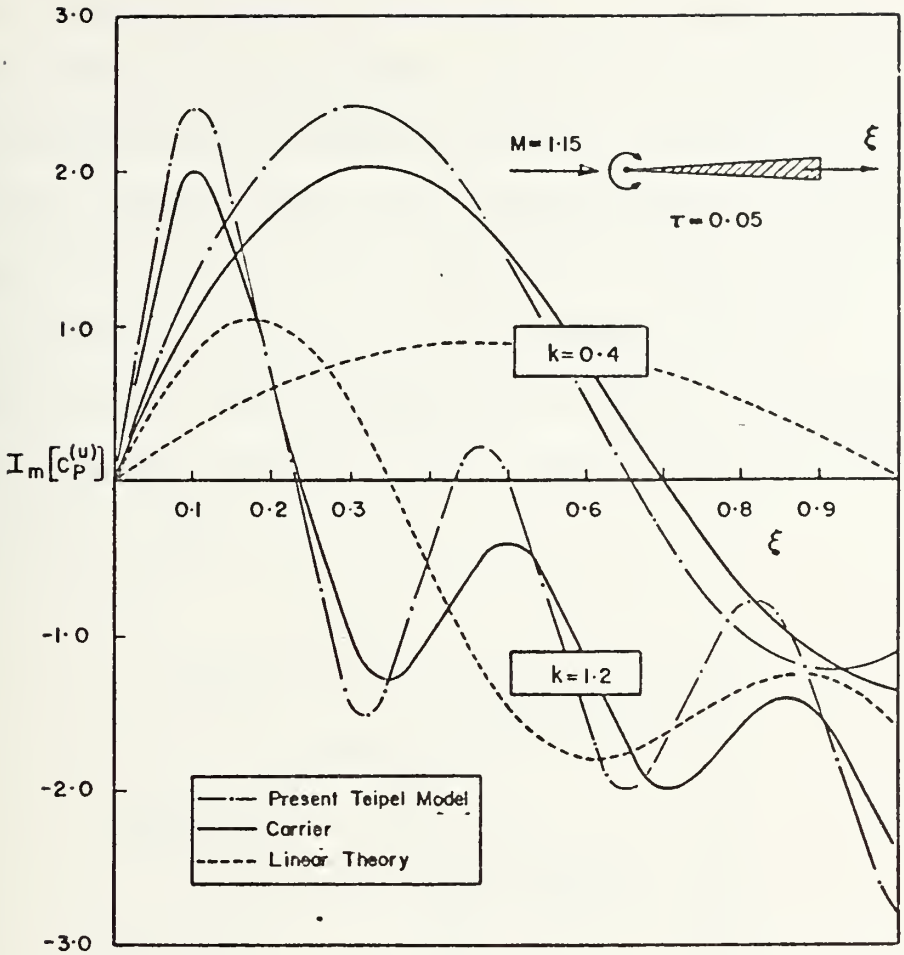

fig. 2.9 Pressure distribution for 5% wedge pivoted at apex

Figure 2.9 presents the component of pressure which is out-of-phase with the angle-of-attack for a 5% thick wedge oscillating about its apex. The free-stream Mach number is 1.15, only slightly above that for shock detachment. Therefore, the results should highlight possible limitations of the potential-flow method. There are two fundamental observations. First, the strong effect of thickness, particularly

at the low oscillation frequency, and second the performance of the present Teipel model, which is considered excellent.

Calculations on the shape of the oscillating bow shock wave are given in fig. 2.10, which shows the dimensionless lateral amplitude of the wave at the instant when the aerofoil is at maximum incidence. It is clear that the flat-plate theory, which forms the basis for Jones' work on the oscillating biconvex aerofoil [24], fails entirely to predict the shock wave locus.

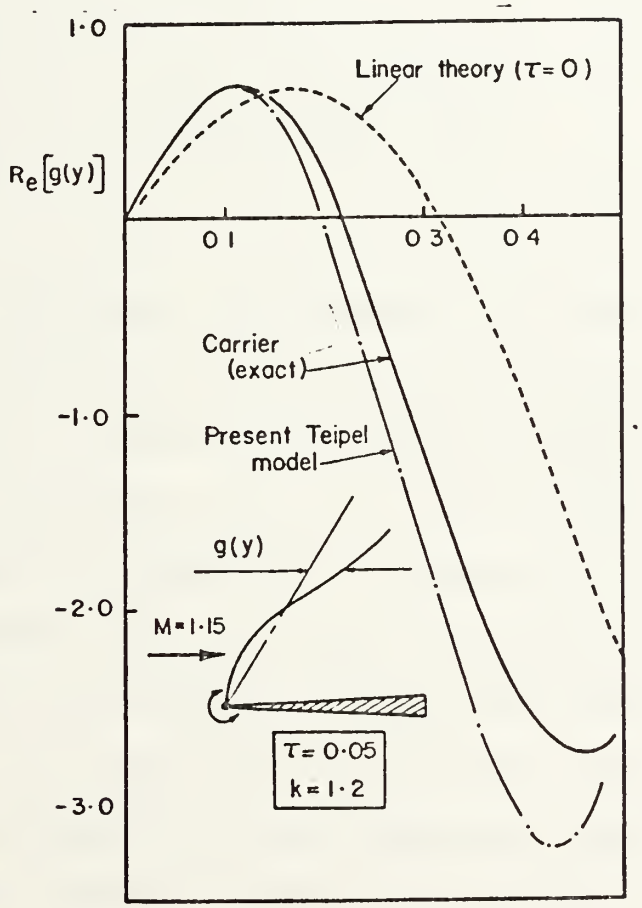

fig. 2.10 Locus of the oscillating bow wave

The main results of the present paragraph show the effect of thickness on several stability coefficient derivatives for the oscillating wedge. The British notation has been used to define the derivatives

$$m_{\dot{\alpha}} = I_m \left[\frac{1}{k} \int_0^1 (b-\xi)\, C_P^{(u)}\, d\xi \right] \qquad 2.36a$$

$$m_{\alpha} = R_e \left[\int_0^1 (b-\xi)\, C_P^{(u)}\, d\xi \right] \qquad 2.36b$$

$$l_{\alpha} = R_e \left[\int_0^1 C_P^{(u)}\, d\xi \right] \qquad 2.36c$$

which are, of course, the dynamic and static moment derivatives and the lift derivative for the aerofoil, respectively. Dynamically unstable oscillations about the pivot will thus have $-m_{\dot{\alpha}} < 0$, and the absence of a positive static restoring moment will correspond to $-m_{\alpha} < 0$. The damping moment derivative $-m_{\dot{\alpha}}$ is plotted against oscillation frequency in fig. 2.11 for several low supersonic Mach numbers. As is well known, the linear theory predicts unstable oscillations at low frequency, under certain conditions. This is clearly illustrated in the figure for each of the Mach numbers considered. Thickness effects are seen to increase the possibility of instability for oscillations

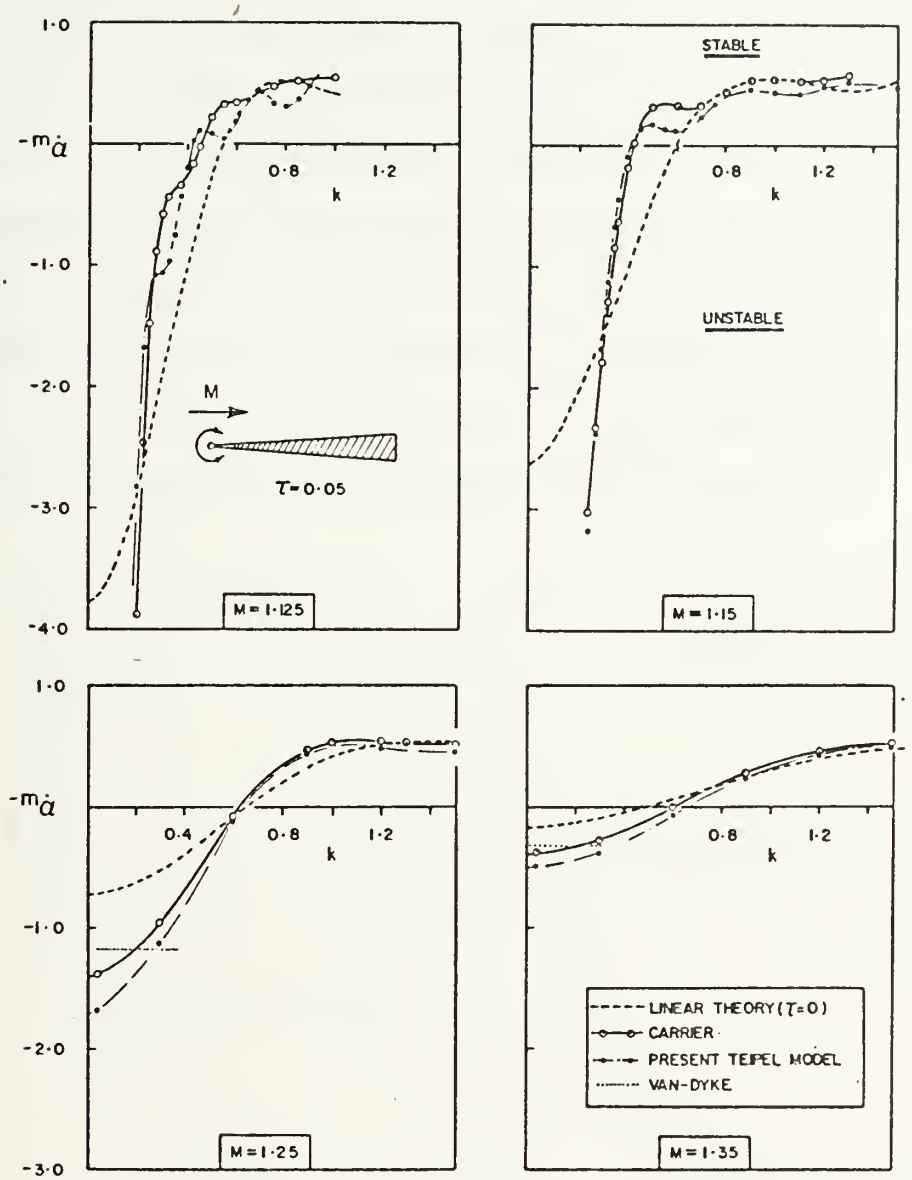

fig. 2.11 Damping moment coefficient for 5% thick wedge pivoted at apex

of very low frequency. However, as the frequency increases, the effect is reversed. At the higher frequencies, in accordance with Landahl's observation noted earlier (equ. 2.2), there is no significant effect due to thickness. Close to the

shock detachment Mach number, thickness effects cause a highly nonlinear modulation in the curves of $-m_\alpha$ versus k. The curves of restoring moment and lift coefficient, shown in fig. 2.12, exhibit similar features. The prediction by the present Teipel model of these interesting nonlinearities, in close agreement with the exact solution, seems adequately to justify the basic isentropic-flow method. Also given in figs. 2.11 and 2.12 is Van Dyke's second-order thickness solution for very low oscillation frequencies [12].

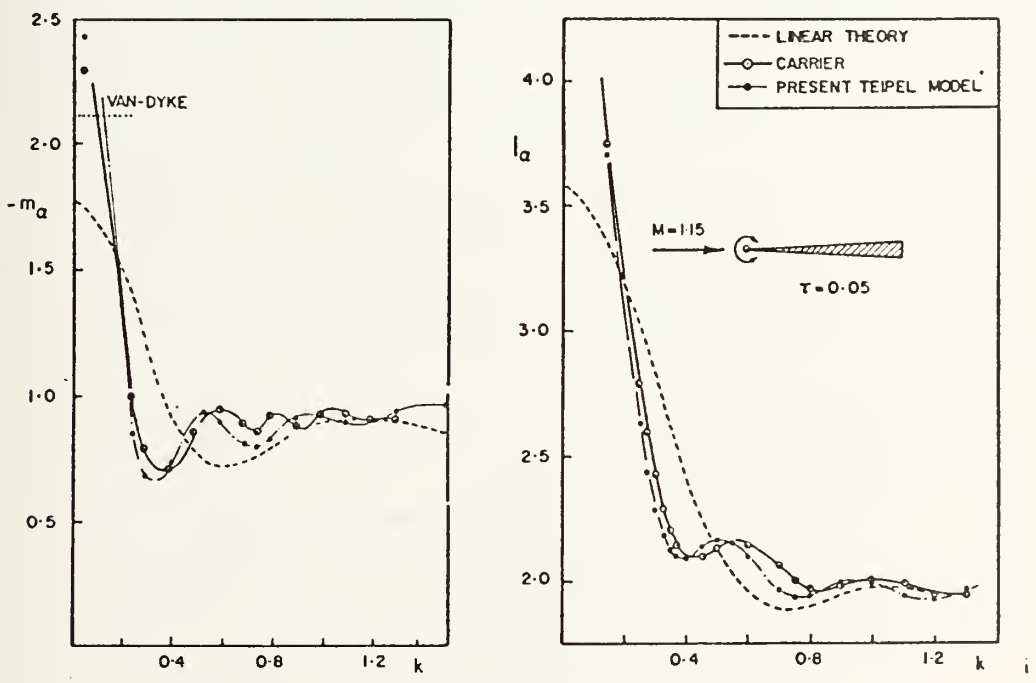

fig. 2.12 Restoring moment and lift coefficients for 5% thick wedge pivoted at apex

The results discussed above seem to justify Teipel's assumption of isentropic flow for the oscillating aerofoil, even at Mach numbers close to shock detachment. They also

give a useful indication of general thickness effects for the wedge oscillating about its apex. Of more practical interest, however, are the pressure distributions given in fig. 2.13 for a 2 1/2% thick biconvex aerofoil pivoted at the leading edge, midchord, and trailing edge positions, respectively.

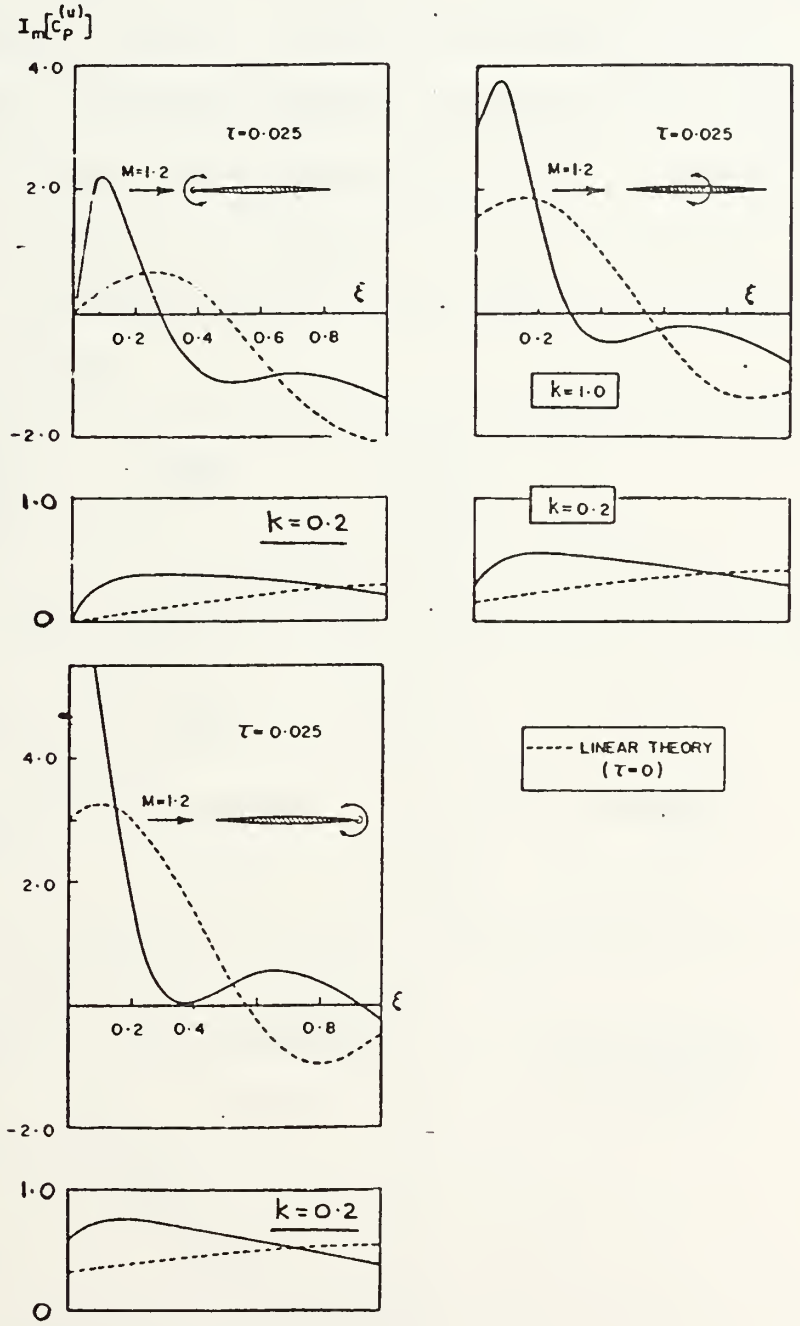

fig. 2.13 Pressure distribution for 2.5% thick biconvex aerofoil

As in the case of the wedge, thickness effects are highly significant at the lower of the two frequencies considered. At the higher oscillation frequency, however, they seem to be important only in bringing about a marked change in the local distribution of pressure. The total out-of-phase aerodynamic force and moment are evidently in reasonable agreement with linear theory. This is shown more clearly in fig. 2.14, which illustrates the damping moment coefficient for these three torsional modes. The possibility is also indicated in fig. 2.14 of a significant increase in the stability of the biconvex aerofoil, compared with the flat plate, for oscillations about rearward pivots.

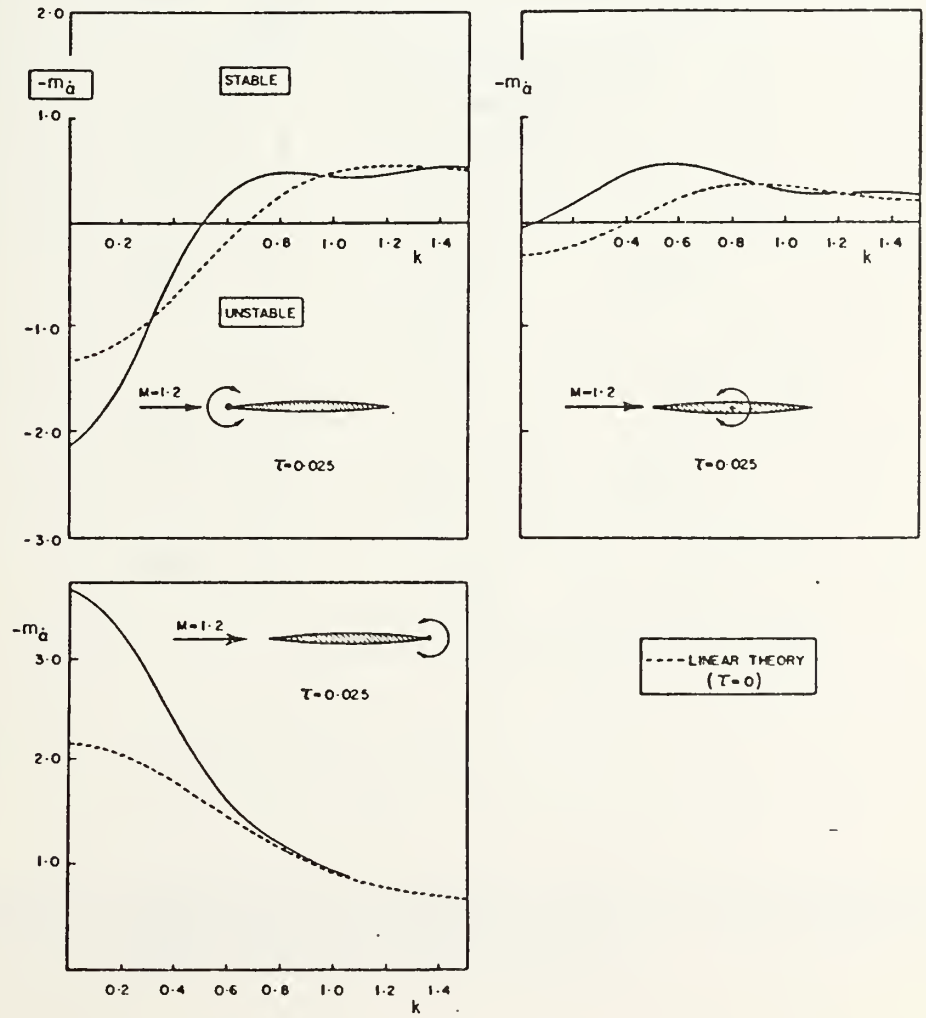

fig. 2.14 Damping moment coefficient for 2.5% biconvex aerofoil

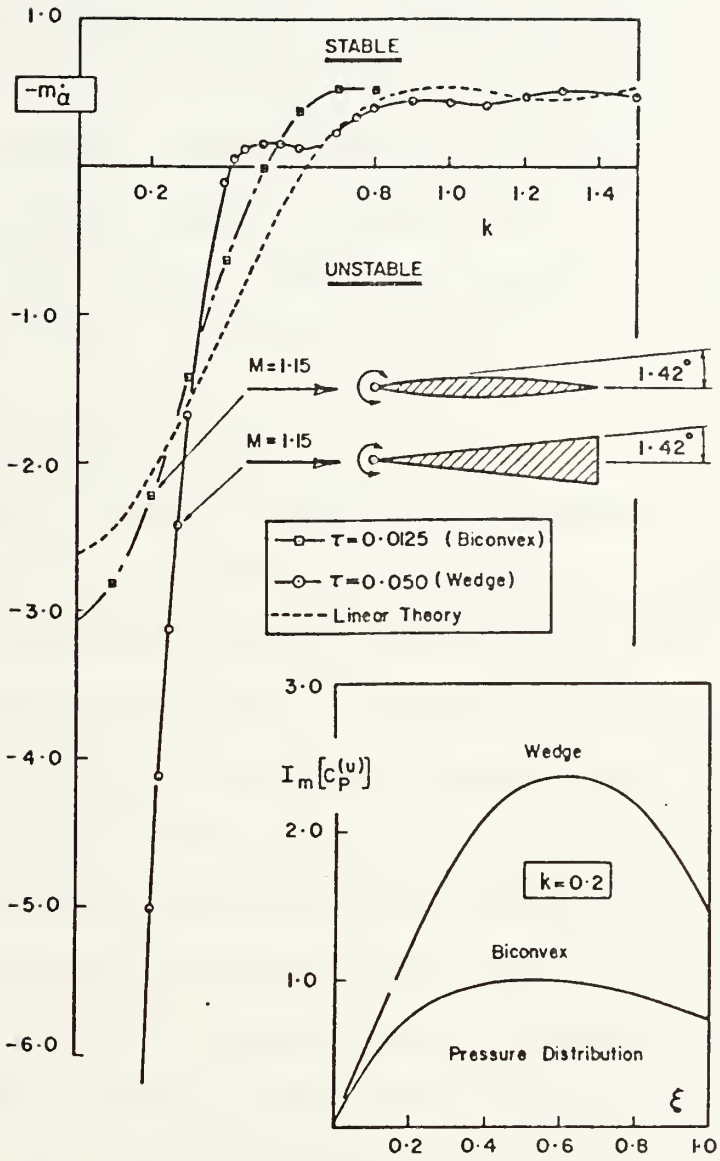

fig. 2.15 Comparison of damping moment coefficients for wedge and biconvex aerofoil

When the thickness ratios of the wedge and circular arc or biconvex aerofoils are 4:1, they will cause the same deflection of the airstream at their leading edges and consequently they will have the same shock detachment Mach number. The damping moment coefficients are therefore compared in fig. 2.15 for a 5% thick wedge and a 1 1/4% thick biconvex aerofoil. The strong instability of the wedge, oscillating slowly about a forward pivot, is shown most clearly in this figure. Thickness effects are much less important for the 'equivalent' biconvex section.

2.3 Aerofoils in Cascade

The transonic small perturbation equation is assumed to describe the flow throughout the cascade. Consequently, the same basic method of solution outlined for the single oscillating aerofoil will apply. However, in determining the unsteady airforces acting on the second blade, there must be contended with the fact that the flow immediately upstream of the second oscillating bow shock wave is no longer uniform, as is the case for the third blade, and so on. This, the remaining problem of significance, is treated in paragraph 2.3.2. First, however, there must be considered a steady ϕ_o problem. For the cascade of wedges this is a simple one.

2.3.1 The steady ϕ_o problem

Consider the region shown in fig. 2.16, downstream of the second right-running bow shock wave but upstream of the first trailing edge expansion wave. Denote this region

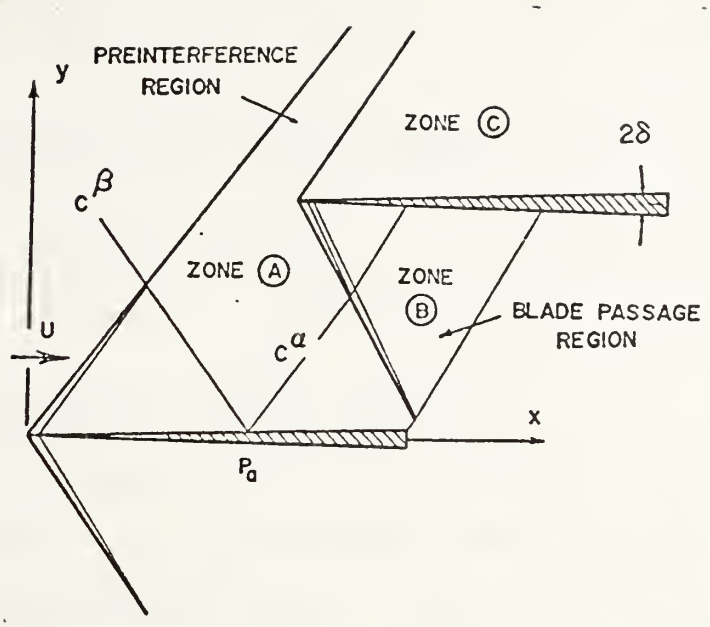

fig. 2.16 Preinterference and blade passage zones

of the blade passage, zone B. The compatibility equation for the right-running β wave through P_a is

$$\lambda_\infty^{3/2} = \lambda_a^{3/2} + \frac{3}{2}(\gamma+1)\, M^2\delta \qquad 2.37a$$

while that for the left-running α wave reads

$$\lambda_a^{3/2} - \frac{3}{2}(\gamma+1)\, M^2\delta = \lambda_b^{3/2} + \frac{3}{2}(\gamma+1)\, M^2\delta \qquad 2.37b$$

which follow from the elementary characteristics formulas given previously. The state variable λ, which determines the steady horizontal velocity u_o according to equ. 2.12a is thus

$$\lambda_a = \left[(M^2 - 1)^{3/2} - \frac{3}{2}(\gamma+1)\, M^2\delta\right]^{2/3} \qquad 2.38a$$

in the preinterference region (zone A), and

$$\lambda_b = \left[(M^2 - 1)^{3/2} - \frac{9}{2}(\gamma+1)\, M^2\delta\right]^{2/3} \qquad 2.38b$$

in the blade passage region (zone B).

It is worthwhile at this juncture to briefly compare this transonic small perturbation theory with the theories of Ackeret and Prandtl-Meyer. The pressure coefficient $C_P = -2u_o$, according to the transonic perturbation theory is

$$C_{P_a} = \frac{-2}{(\gamma+1)M^2}\left\{\left[(M^2-1)^{3/2} - \frac{3}{2}(\gamma+1)\, M^2\delta\right]^{2/3} - (M^2-1)\right\} \qquad 2.39a$$

on the upper surface of the isolated blade, and

$$C_{P_b} = \frac{-2}{(\gamma+1)M^2}\left\{\left[(M^2-1)^{3/2} - \frac{9}{2}(\gamma+1)\, M^2\delta\right]^{2/3} - (M^2-1)\right\} \qquad 2.39b$$

on the lower surface of the second blade. By taking a Binomial theorem expansion for large M (or small δ) there is obtained the Ackeret theory, $C_{P_a} = 2\delta/(M^2-1)^{1/2}$ and $C_{P_b} = 3C_{P_a}$.

The transonic and Prandtl-Meyer pressure coefficients, which are nonlinear functions of the streamline deflection angle δ, are compared with the Ackeret theory below

	Transonic Small Perturbation	Ackeret	Prandtl Meyer
C_{P_a}	0.0486	0.04654	0.05065
C_{P_b}	0.1649	0.13962	0.16066

M = 1.25, Semiwedge Angle δ = 1°

The slopes of the α and β characteristics in zone B are $\pm\lambda_b^{-1/2}$, respectively. Also, following the procedure for averaging $\sqrt{\lambda}$ upstream and downstream of the shock, the orientation of the right-running bow wave separating this zone from zone A is $-2/(\sqrt{\lambda_a} + \sqrt{\lambda_b})$.

This essentially completes the solution of the ϕ_o problem. Zone C immediately above the second blade need not be considered, since a streamline of the steady flow passing through the second left-running bow shock wave clearly experiences no further disturbance. Indeed, the upper bow wave from the second blade is now an α characteristic of the zone A field. Blade-to-blade periodicity of the ϕ_o solution in zone C must follow. A typical characteristic mesh with the Kantrowitz condition (discussed later) imposed on the steady inlet flow, is shown in fig. 2.17.

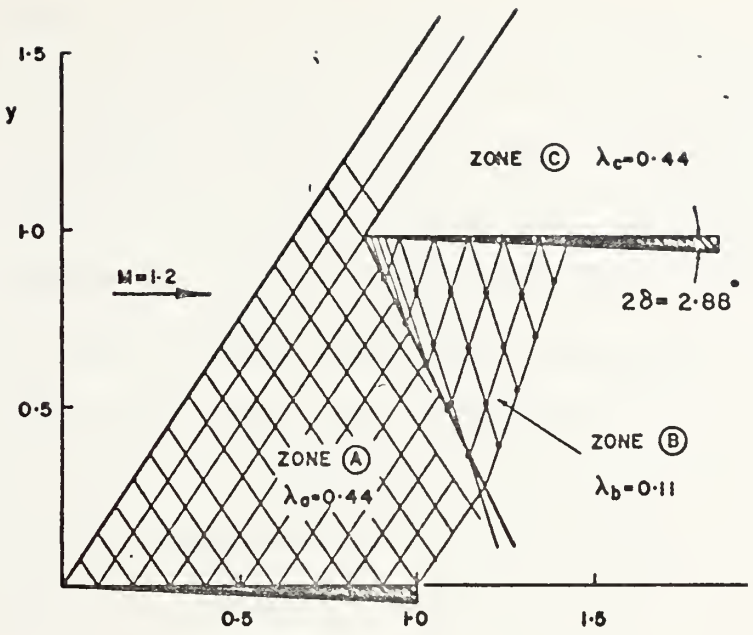

fig. 2.17 Characteristic mesh for interacting wedge flows

2.3.2 The unsteady ϕ_1 problem

The flow is assumed to remain supersonic throughout the cascade and consequently the unsteady compatibility relations derived previously apply everywhere. Indeed, they simplify somewhat for the cascade of oscillating wedges, since $\partial\lambda/\partial x$ is zero. Accordingly, along α and β characteristics, respectively

$$du_1 - dv_1/\sqrt{\lambda} + i2kM^2u_1/\lambda\, dx - k^2M^2\phi_1/\lambda\, dx = 0 \qquad 2.40a$$

$$du_1 + dv_1/\sqrt{\lambda} + i2kM^2u_1/\lambda\, dx - k^2M^2\phi_1/\lambda\, dx = 0 \qquad 2.40b$$

where the state variable λ will assume the value λ_a in zones A and C and λ_b in zone B. It is desired to determine the change in velocity as the fluid passes through the oscillating bow wave from zone A into zone C, assuming isentropic conditions. Thus, denote $u^*(x,y,t)$ and $v^*(x,y,t)$ the horizontal and vertical velocities immediately upstream of $P(x,y)$ on the head wave. The components of u^* are $1 + u_o$ and $u_1 \exp(ikt)$, and for v^* they are δ and $v_1 \exp(ikt)$, where u_1 and v_1 are known functions of x and y from the zone A solution of the single aerofoil problem, and δ is the semi-wedge angle. It therefore follows, expressing u_o in terms of λ_a according to equ. 2.12a, that the velocity into the bow wave may be written

$$u^* = \left[1 + \frac{\lambda_a - (M^2-1)}{(\gamma+1)M^2} \right] + u_1(x,y)e^{ikt} \qquad 2.41a$$

$$v^* = \delta + v_1(x,y)e^{ikt} \qquad 2.41b$$

As with the single biconvex aerofoil (except that the steady shock profile is now straight and γ_o consequently is a constant) denote the orientation of the unsteady bow shock wave at $P(x,y)$ by $\gamma_o+\gamma'$, as shown in fig. 2.18. Then the dimensionless normal and tangential velocity components into the shock are

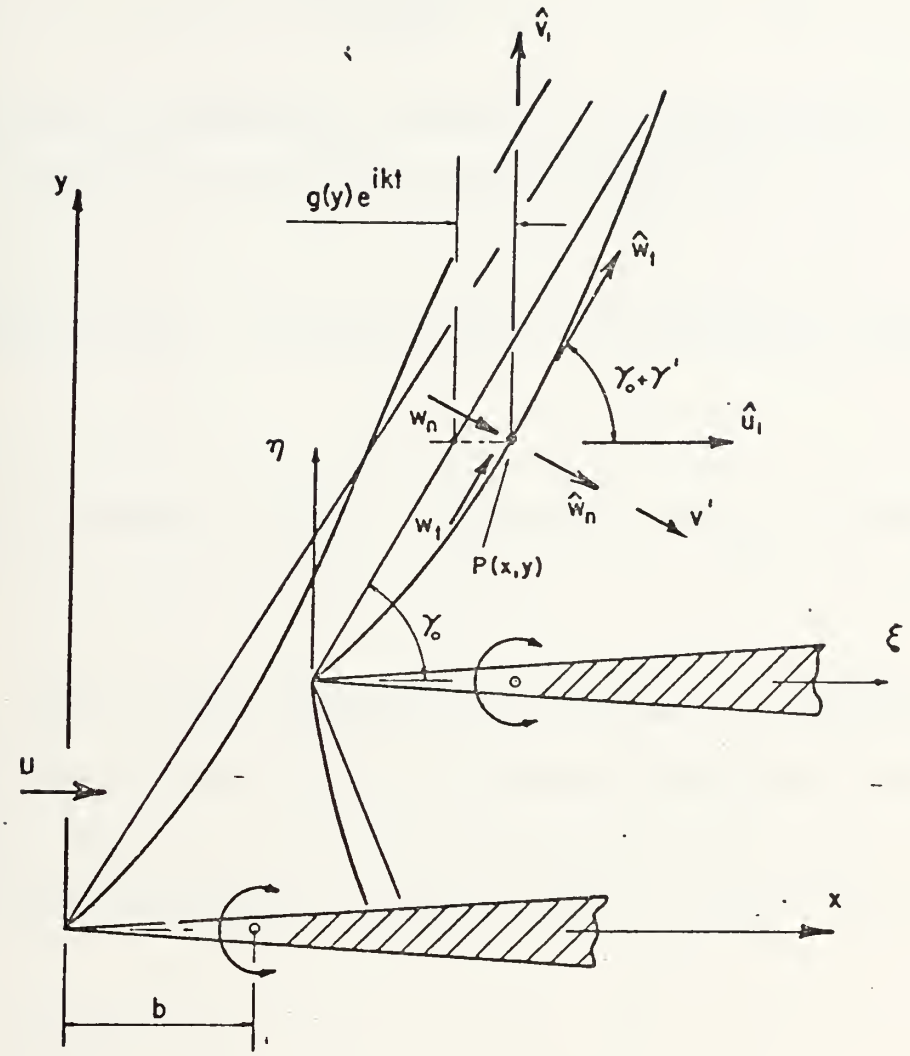

fig. 2.18 Geometry of oscillating bow wave for second blade

$$w_n = (v+u_1)\sin(\gamma_o+\gamma') - (\delta+v_1)\cos(\gamma_o+\gamma') \qquad 2.42a$$

$$w_t = (v+u_1)\cos(\gamma_o+\gamma') + (\delta+v_1)\sin(\gamma_o+\gamma') \qquad 2.42b$$

omitting exp(ikt) but keeping in mind that this harmonic time dependence applies to all unsteady functions, and where the following notation has been used

$$\nu = 1 + \frac{\lambda_a - (M^2-1)}{(\gamma+1)M^2} \qquad 2.43$$

Neglecting second-order products of γ' with u_1, v_1, and δ, equs. 2.42a and 2.42b may be approximated by

$$w_n = \nu\sin\gamma_o - \delta\cos\gamma_o + (u_1\sin\gamma_o - v_1\cos\gamma_o + \nu\gamma'\cos\gamma_o) \qquad 2.44a$$

$$w_t = \nu\cos\gamma_o + \delta\sin\gamma_o + (u_1\cos\gamma_o + v_1\sin\gamma_o - \nu\gamma'\sin\gamma_o) \qquad 2.44b$$

The normal component of gas speed $\hat{w}_n$ immediately behind the moving bow wave is obtained using the Rankine-Hugoniot equation in the form developed previously. Thus, employing the present expression for w_n, equ. 2.24 becomes

$$\hat{w}_n - w_n = \frac{2}{\gamma+1}(v'-w_n) + \frac{2a^2}{(\gamma+1)a^2U^2\sin\gamma_o}\left[1 + \frac{u_1\sin\gamma_o + \nu\gamma'\cos\gamma_o - v_1\cos\gamma_o - \delta\cos\gamma_o - v'}{\nu\sin\gamma_o}\right]^{-1} \qquad 2.45$$

where v' is the normal velocity of the head wave in stationary coordinates. The Binomial theorem yields

$$\hat{w}_n = \frac{\gamma-1}{\gamma+1}\,\nu\sin\gamma_o\left[1+\frac{2/M_n^2}{(\gamma-1)\nu^2}\right] + \frac{\gamma-1}{\gamma+1}\,\nu\cos\gamma_o\left[1-\frac{2/M_n^2}{(\gamma-1)\nu^2}\right]\gamma'$$

$$+ \frac{2}{\gamma+1}\left[1+\frac{1/M_n^2}{\nu^2}\right]v'$$

$$+ \frac{\gamma-1}{\gamma+1}\,(u_1\sin\gamma_o - v_1\cos\gamma_o - \delta\cos\gamma_o)\left[1-\frac{2/M_n^2}{(\gamma-1)\nu^2}\right] \qquad 2.46$$

after some simplification, and where, as previously defined, M_n is the normal inlet Mach number of the steady flow and the quantities γ' and v' are of small order compared with γ_o and U. The unsteady velocities u_1 and v_1 are known in zone A immediately upstream of the second bow wave. Thus, with $\hat{w}_t = w_t$ (equ. 2.44b), the components of velocity immediately behind the second left-running bow wave can be determined. These are the required boundary value quantities for the solution of the unsteady characteristics problem in zone C. They are obtained from $\hat{w}_n$ and $\hat{w}_t$ using a simple orthogonal transformation (2.30). Neglecting such high-order terms as $\gamma' u_1$, $v' u_1$, and $\gamma'\delta$, the following simultaneous ordinary differential equations can thus be determined

$$\hat{u}_1 = m_1\,dg/dy + im_2 g + m_3 u_1 + m_4 v_1 \qquad 2.47a$$

$$\hat{v}_1 = n_1\,dg/dy + in_2 g + n_3 u_1 + n_4 v_1 \qquad 2.47b$$

in terms of the complex lateral amplitude of the oscillating bow shock wave g(y). The velocities $u_1(x,y)$ and $v_1(x,y)$ are known from the solution of the unsteady ϕ_1 problem, while the coefficients m and n are known from the solution of the steady ϕ_o problem. For the wedge, in which case the locus of the steady bow shock wave is a straight line, the m and n are constant. They are given, with $\gamma_o = \gamma_o(y)$ in the general case, as

$$
\begin{aligned}
m_1 &= \frac{2\nu}{\gamma+1} \sin 2\gamma_o \sin^2\gamma_o \\
m_2 &= \frac{2k}{\gamma+1}\left[1 + \frac{1/M_n^2}{\nu^2}\right]\sin^2\gamma_o \\
m_3 &= \cos^2\gamma_o + \frac{\gamma-1}{\gamma+1}\sin^2\gamma_o\left[1 - \frac{2/M_n^2}{(\gamma-1)\nu^2}\right] \\
m_4 &= \frac{\sin 2\gamma_o}{2} - \frac{\gamma-1}{\gamma+1}\frac{\sin 2\gamma_o}{2}\left[1 - \frac{2/M_n^2}{(\gamma-1)\nu^2}\right] \\
n_1 &= \frac{-2\nu}{\gamma+1}\left[\cos 2\gamma_o + \frac{1/M_n^2}{\nu^2}\right]\sin^2\gamma_o \\
n_2 &= \frac{-2k}{\gamma+1}\left[1 + \frac{1/M_n^2}{\nu^2}\right]\cot\gamma_o \sin^2\gamma_o \\
n_3 &= m_4 \\
n_4 &= \sin^2\gamma_o + \frac{\gamma-1}{\gamma+1}\cos^2\gamma_o\left[1 - \frac{2/M_n^2}{(\gamma-1)\nu^2}\right]
\end{aligned}
\qquad 2.48
$$

The above equations reduce to those of paragraph 2.1.2 when $\nu = 1$ and the unsteady perturbation velocities are $u_1 = 0$ and $v_1 = 0$. The unsteady shock locus $g(y)$ and the required $\hat{u}_1(x,y)$ and $\hat{v}_1(x,y)$ are determined simultaneously in a manner similar to that described previously (by employing equ. 2.47 and the α compatibility formula 2.40a). However, if the torsional mode of the second blade leads that of the first so that its oscillation is described by $\alpha_2 = \exp[i(kt+\mu)]$, where μ is the interblade phase angle, then the unsteady flow tangency condition will read

$$\frac{\partial \phi_1}{\partial \eta} = - \left[1+ik(\rho-b)\right] e^{i\mu} \; ; \quad \eta = 0 \qquad 2.49$$

which is a simple modification of equ. 2.9b. The vertical perturbation velocity $\hat{v}_1$ immediately behind the bow wave at the leading edge of the second blade, $g(o) = 0$, is therefore known and there may be determined consequently the corresponding value of $\hat{u}_1$

$$\hat{u}_1 = - \frac{m_1}{n_1}(1-ikb)e^{i\mu} + \frac{(m_3 n_1 - m_1 n_3)}{n_1} u_1 + \frac{(m_4 n_1 - m_1 n_4)}{n_1} v_1 \qquad 2.50$$

Thus has been presented the basic analysis necessary for the determination of the unsteady aerodynamic force on the upper surface of the second blade in zone C. Nothing

new is involved in extending the procedure to succeeding blades. It is necessary, however, to indicate how the analysis should be modified to yield the appropriate unsteady boundary conditions behind the lower bow wave, following which the zone B field can be determined. As may easily be verified, defining g(y) as an upstream perturbation, the changes necessary reduce simply to reversing the algebraic signs of m_2, m_4 and n_1 in the shock geometry equations, which in this case must be solved in conjunction with the β compatibility relation (2.40b) to yield the required $\hat{u}_1(x,y)$, $\hat{v}_1(x,y)$.

2.3.3 Limiting Cases

There are several interesting limiting situations which arise in the case of vanishing blade thickness. With $\nu = 1$ and $M_n = 1$, the shock geometry equations, written for conditions immediately behind the upper and lower waves at the leading edge of the second blade, are

$$\hat{u}_1 = -\frac{2}{\gamma+1}\sin 2\gamma_o \gamma'_{u,1} + u_1\left[\cos^2\gamma_o + \frac{\gamma-3}{\gamma+1}\sin^2\gamma_o\right] \pm \frac{2v_1}{\gamma+1}\sin 2\gamma_o \qquad 2.51a$$

$$\hat{v}_1 = \pm\frac{4}{\gamma+1}\cos^2\gamma_o \gamma'_{u,1} + v_1\left[\sin^2\gamma_o + \frac{\gamma-3}{\gamma+1}\cos^2\gamma_o\right] \pm \frac{2u_1}{\gamma+1}\sin 2\gamma_o \qquad 2.51b$$

where the upper sign is to be taken for the upper wave and where γ'_u is the perturbation in the orientation of the upper shock (relative to γ_o) very close to the leading edge; it

is considered to be a constant. Similarly γ_1' denotes a perturbation to the lower wave. Both are positive for upstream excursions of the unsteady shock relative to its steady-state position. The $\hat{u}_1$ and $\hat{v}_1$ are dimensionless perturbations on the blade immediately behind the bow wave and the u_1 and v_1 similar quantities immediately upstream of this point; the latter are zero, of course, for the first blade. Now $\hat{v}_1$ is known from the unsteady tangency condition; for small amplitude in-phase torsional oscillations about the pivot b it is simply

$$\hat{v}_1 = -(1-ikb)\alpha \qquad 2.52$$

Case (i) Isolated blade

It follows immediately, with $u_1 = v_1 = 0$, that

$$\gamma'_{u,l} = \pm \frac{\gamma+1}{4} \alpha \sec^2\gamma_o(1-ikb) \qquad 2.53$$

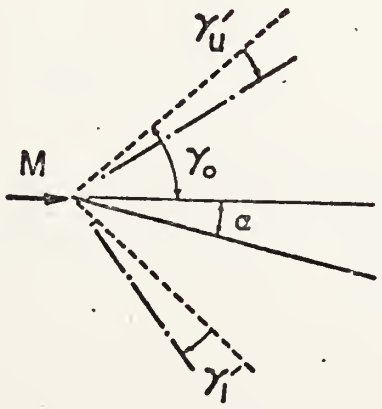

$$\hat{u}_1 = \pm \alpha \tan\gamma_o(1-ikb) \qquad 2.54$$

The significance of these equations is as follows: The general shock polar [Ref. 22 page 177], upon assuming the turning angle of the flow δ is so small that there may be written the relation $\tan(\xi-\delta) = \tan \xi - \delta\sec^2\xi$, may in turn be written

$$\frac{\gamma+1}{2} \delta \tan \xi = \sin^2\xi - \sin^2\gamma_o \qquad 2.55$$

where ξ is the shock angle (measured from the direction of the free stream). Writing $(-\alpha)$ for δ and with $(\gamma_o + \gamma_u')$ for ξ, where γ_u' is second order, equation 2.53 results. The isentropic-flow assumptions are thus seen to be consistent with the linearized shock polar. The pressure coefficient immediately behind the oscillating shock wave at the leading edge of the blade is

$$\hat{C}_p = \pm 2\alpha/\beta(1-ikb) \qquad 2.56$$

a result which, it is important to note, is exact in frequency.* This is simple Ackeret theory with $\Delta C_p = 4\alpha/\beta$ at maximum

---

*See equ. 3.13 of the next Section.

angle-of-attack, and $\Delta C_p = -4\alpha kb/\beta$ when the aerofoil is at zero angle-of-attack with the trailing edge moving down.

Case (ii) Second blade with $k = 0$ and $\mu = 180°$

The tangency condition for the second blade reduces to $v = \alpha$, while the flow induced by the first blade is $u_1 = \alpha \tan\gamma_o$ and $v_1 = -\alpha$. Consequently, the shock geometry equation (3.51b) yields

$$\gamma_u' = \alpha \sec^2\gamma_o(\gamma-1)/2 \qquad 2.57a$$

$$\gamma_l' = -\alpha \sec^2\gamma_o(\gamma+3-4\cos^2\gamma_o)/2 \qquad 2.57b$$

which, as shown in fig. 2.20, are positive and negative angles, respectively. Substituting equ. 2.57 into the shock geometry equation (2.51a) and simplifying results in the velocity perturbations $-\alpha \tan\gamma_o$ and $3\alpha \tan\gamma_o$ on the

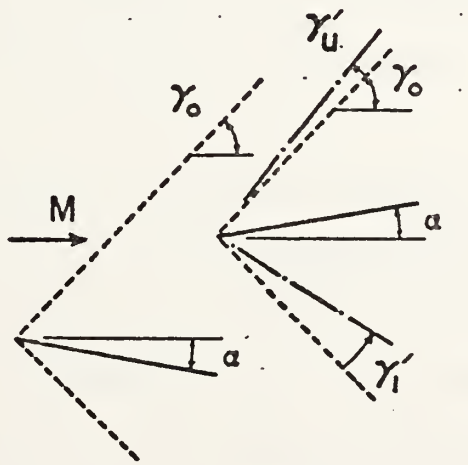

upper and lower surfaces respectively of the second blade. The pressure loading is therefore $\Delta C_p = -8\alpha \tan\gamma_o$.

2.3.4 Results

A mathematical model based on the nonlinear analysis has been formulated. During the model validation phase several flow solutions were obtained for the oscillating wedge cascade for various combinations of the Mach number, oscillation frequency, pivot location and thickness-chord ratio. These results, however, are of limited practical interest until the solution is extended to include the cascade exit flow. Consequently, only a representative example of these preliminary calculations is given, showing the nonlinear effects of thickness on two 5% thick wedges oscillating in-phase about a 33% chord pivot at M = 1.2. The inlet flow is parallel to the suction surfaces of the wedges; otherwise, in the case k = 0, steady equilibrium rotation of the compressor blading is not possible. Kantrowitz gives a clear explanation of this unique incidence condition in Ref. 25.

The results, for several reduced frequencies, are given in fig. 2.21. For the isolated blade, at k = 0.1, the strong destabilizing influence of thickness on the out-of-phase air loads is clear. For the second blade, however, depending on the outcome of calculations downstream of ξ = a, which are beyond the scope of the present investigation, it seems highly likely from the results in fig. 2.21

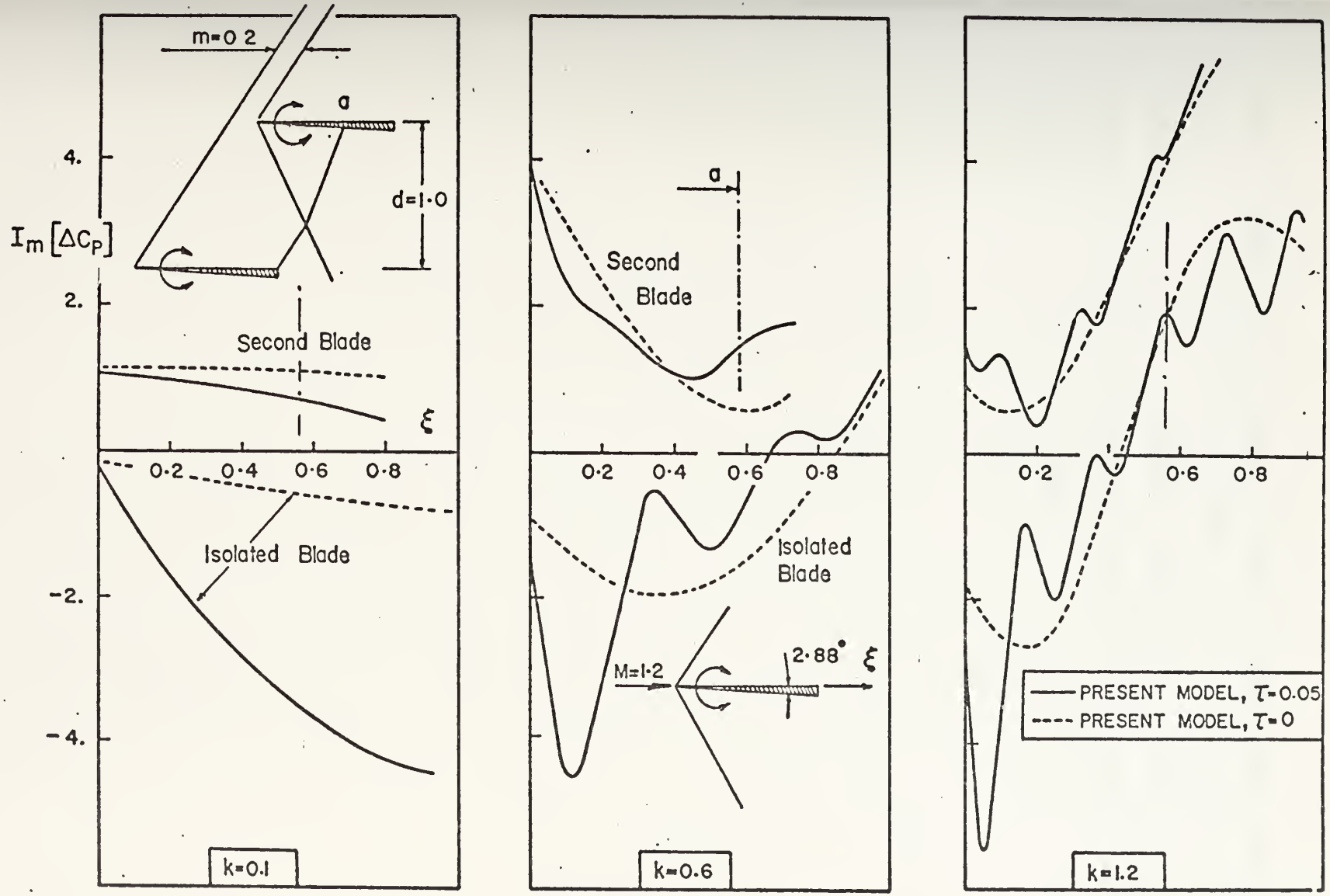

fig. 2.21 Preinterference lift distribut on for two 5% thick wedges pivoted at 33% chord

that thickness effects may be stabilizing. The magnitude of the nonlinearity in the case of the second blade is certainly reduced. At higher oscillation frequencies, nonlinear thickness effects are seen to cause only local variations in pressure loading.

3 FINITE SUPERSONIC CASCADE WITH A SUBSONIC LEADING EDGE. A THIRD-ORDER THEORY IN FREQUENCY

The finite rectilinear cascade was originally solved during the course of this investigation to first order in oscillation frequency, using both Laplace transformation and by generalization of Sauer's solution for the slowly oscillating aerofoil in unbounded flow [18]. However, the pressure loading was found to remain constant for all the blades of the cascade (except the first) while the unsteady surface pressures, for the case of oscillations with zero phase difference between the blades, diverged in the far field. Kurosaka obtains a similar unbounded result for the infinite cascade [9]. The work of the present section was undertaken mainly to determine if these limitations of the first-order analysis could be avoided by seeking a solution of higher order in oscillation frequency.

The velocity potential is first derived exactly to third order in frequency for a single aerofoil oscillating in unbounded supersonic flow. The cascade with two blades is then solved by requiring continuity of the potential along the left and right running bow waves emanating from the leading edge of the second blade and by suitably modifying the flow tangency condition to account for the downwash induced by the first blade. The general case of n-blades is then given.

3.1 Isolated Blade in Unbounded Flow

The linearized equations describing the flow field, unsteady flow tangency condition and pressure coefficient for the oscillating rectilinear cascade shown in fig. 3.1 are

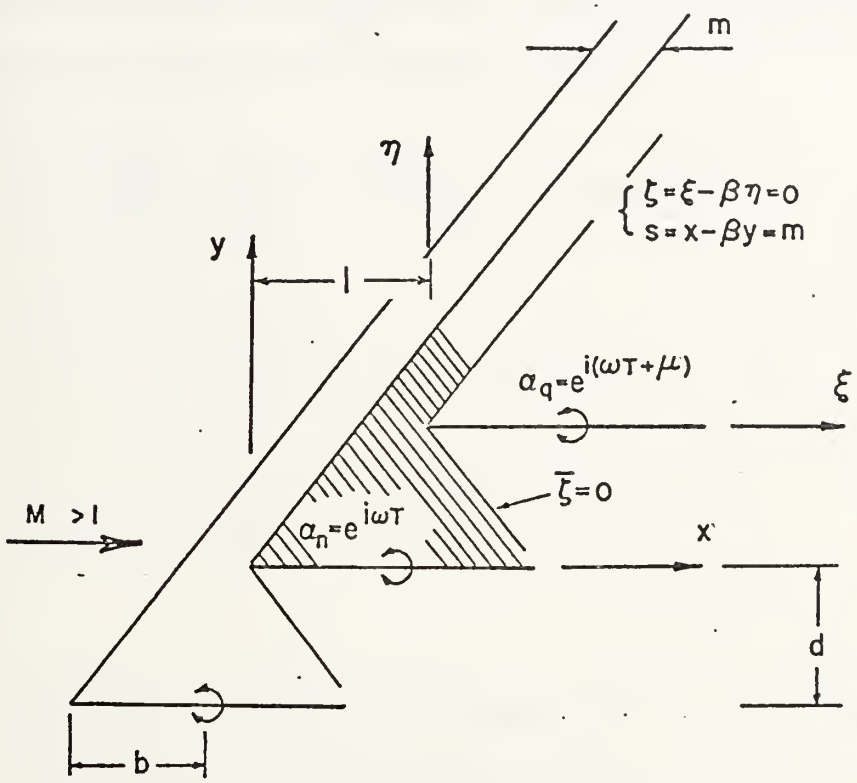

fig. 3.1 Cascade geometry

$$(M^2-1)\frac{\partial^2\Phi}{\partial X^2}-\frac{\partial^2\Phi}{\partial Y^2}=-\frac{1}{a^2}\frac{\partial^2\Phi}{\partial T^2}-\frac{2M}{a}\frac{\partial^2\Phi}{\partial X\partial T} \qquad 3.1a$$

$$\frac{\partial\Phi}{\partial Y}=U\frac{\partial\bar{Y}}{\partial X}+\frac{\partial\bar{Y}}{\partial T} \qquad 3.1b$$

$$C_P=-\frac{2}{U}\left[\frac{\partial\Phi}{\partial X}+\frac{1}{U}\frac{\partial\Phi}{\partial T}\right] \qquad 3.1c$$

where $\bar{Y}$ defines the aerofoil surface. Consider small amplitude torsional oscillations $\alpha_1 = \exp(i\omega T)$ about the pivot $x = b$ and introduce the dimensionless variables

$$x = \frac{X}{c}\ ,\quad y = \frac{Y}{c}\ ,\quad t = \frac{TU}{c}\ ,\quad k = \frac{\omega c}{U}\ ,\quad \phi = \frac{\Phi}{cU} \qquad 3.2$$

The above equations, written for the flow in the preinterference zone of the first blade, become

$$\beta^2 \frac{\partial^2 \phi_1}{\partial x^2} - \frac{\partial^2 \phi_1}{\partial y^2} = k^2 M^2 \phi_1 - i2kM^2 \frac{\partial \phi_1}{\partial x} \qquad 3.3a$$

$$\frac{\partial \phi_1}{\partial y} = -\ [1 + ik(x-b)]\ ;\quad y = 0 \qquad 3.3b$$

$$C_{P_1} = -2\ [\frac{\partial \phi_1}{x} + ik\phi_1] \qquad 3.3c$$

The partial differential equation for the unsteady velocity potential may be transformed to a more convenient form through

$$\phi_1 = \psi_1 e^{-i\theta x} \qquad 3.4a$$

$$\theta = \frac{M^2 k}{\beta^2} \qquad 3.4b$$

In terms of the modified potential there results

$$\beta^2 \frac{\partial^2 \psi_1}{\partial x^2} - \frac{\partial^2 \psi_1}{\partial y^2} + \left(\frac{\beta\theta}{M}\right)^2 \psi_1 = 0 \qquad 3.5a$$

$$\frac{\partial \psi_1}{\partial y} = -w_1(x) \; ; \quad y = 0 \qquad 3.5b$$

$$C_{P_1} = 2e^{-i\theta x} \left[\frac{i\theta}{M^2} - \frac{\partial}{\partial x}\right] \psi_1 \qquad 3.5c$$

where the downwash velocity is

$$w_1(x) = e^{i\theta x} \left[1 + i \frac{\beta^2 \theta}{M^2} (x-b)\right] \qquad 3.6$$

Taking the Laplace transform of equ. 3.5a with respect to the streamwise coordinate x and noting that the initial conditions $\psi_1(0,y)$ and $\partial\psi_1/\partial x(0,y)$ are zero

$$\frac{\partial^2 \psi_1(p)}{\partial y^2} - \beta^2 (p^2 + \theta^2/M^2) \; \psi_1(p) = 0 \qquad 3.7$$

$\psi_1(p)$ denoting the transformed dependent variable. The solution is

$$\psi_1(p) = A_1(p)e^{-\beta y(p^2+\theta^2/M^2)^{\frac{1}{2}}} + B_1(p)e^{\beta y(p^2+\theta^2/M^2)^{\frac{1}{2}}} \quad 3.8$$

where the condition $B_1(p) = 0$ must be imposed to ensure that the flow remains undisturbed upstream of the left-running bow wave $x-\beta y = 0$. The constant $A_1(p)$ follows from the flow tangency condition of equ. 3.5b, whereupon the modified potential becomes

$$\psi_1(p) = \frac{w_1(p)}{\beta(p^2+\theta^2/M^2)^{\frac{1}{2}}} e^{-\beta y(p^2+\theta^2/M^2)^{\frac{1}{2}}} \quad 3.9$$

Inversion is accomplished using standard tables together with the convolution theorem

$$\psi_1(x,y) = \frac{1}{\beta}\int_0^s w_1(u)\, J_o(x,y,u)\, du \quad 3.10a$$

where J_o is the Bessel function of the first kind

$$J_o(x,y,u) = J_o\left[\frac{\theta}{M}\sqrt{(x-u)^2-\beta^2y^2}\right] \quad 3.10b$$

$$s = x - \beta y \quad 3.11$$

It is now to be assumed that the solution may be expressed as a power series based on frequency up to terms involving the cube of the frequency parameter θ. Accordingly, expanding the integrand of equ. 3.10 and performing the integration

$$\psi_1(x,y) = a_1 s + i\theta s[b_1 s+b_2] + \theta^2 s^2 [c_1 s+c_2+c_3 x]$$

$$+ i\theta^3 s^3 [d_1 s^2+d_2 s+x(d_3 s+d_4)] \qquad 3.12a$$

where

$$a_1 = 1/\beta$$

$$b_1 = (2M^2-1)/2M^2\beta \qquad d_1 = -(8M^4-12M^2+3)/48M^4\beta$$

$$b_2 = -\beta^2 b/M^2\beta \qquad d_2 = \beta^4 b/6M^4\beta$$

$$c_1 = -\beta^2/2M^2\beta \qquad d_3 = (2M^2-1)/12M^4\beta$$

$$c_2 = \beta^2 b/2M^2\beta \qquad d_4 = \beta^2 b/4M^4\beta$$

$$c_3 = -1/4M^2\beta \qquad 3.12$$

and $\psi_1(x,y) = 0$ for $s < 0$. The upper surface pressure coefficient for the flat plate oscillating in unbounded supersonic flow, exact to the third power of the oscillation frequency, follows by substituting equ. 3.12a into equ. 3.5c with $k = \beta^2\theta/M^2$

$$C_{P_1}^{(u)} = -\frac{2}{\beta} + i\frac{2k}{\beta^3}\left[(2-M^2)x + \beta^2 b\right] + \frac{k^2}{2\beta^5}\left[(M^2+2)x + 4\beta^2 b\right]x$$

$$+ i\frac{k^3M^2}{2\beta^7}\left[-\frac{(M^2+4)}{3}x + 3\beta^2 b\right]x^2 \qquad 3.13$$

3.2 Cascade with Two Blades

Introduce the coordinates ξ and η, where

$$\zeta = \xi - \eta \qquad 3.14$$

and consider the problem of determining the velocity potential $\phi_2(\xi,\eta)$ in the preinterference zone immediately above the second blade (the shaded region in fig. 3.1). The differential equation and tangency condition are

$$\beta^2\frac{\partial^2\phi_2}{\partial\xi^2} - \frac{\partial^2\phi_2}{\partial\eta^2} = k^2M^2\phi_2 - i2kM^2\frac{\partial\phi_2}{\partial\xi} \qquad 3.15a$$

$$\frac{\partial\phi_2}{\partial\eta} = -e^{i\mu}[1 + ik(\xi-b)] \quad ; \quad \eta = 0 \qquad 3.15b$$

where the oscillation of the second blade, upon introducing the interblade phase angle μ, is described as $\alpha_2 = \alpha_1\exp(i\mu)$. The potential must be continuous along the second left-running Mach wave separating the preinterference zones of the first and second blades. Accordingly

$$\phi_2(\zeta=0) = \phi_1(s=m) = \psi_1(s=m)e^{-i\theta x} \qquad 3.16$$

Consider the following transformation of dependent variable

$$\phi_2(\xi,\eta) = \psi_2(\xi,\eta)e^{-i\theta x} \qquad 3.17$$

where, as shown in fig . 3.1, $x = \xi+1$. This is different than the transformation of equ. 3.4 on account of the phase lag $\exp(-i\theta 1)$, which ensures that along the second bow wave $\zeta = 0$ (or $s = m$) the continuity of ϕ implies the continuity of ψ. Accordingly, there may be written

$$\psi_2(\zeta=0) = \psi_1(s=m) \qquad 3.18$$

In terms of the modified potential, the differential equation, tangency condition and pressure coefficient are now

$$\beta^2 \frac{\partial^2\psi_2}{\partial\xi^2} - \frac{\partial^2\psi_2}{\partial\eta^2} + \left(\frac{\beta\theta}{M}\right)^2 \psi_2 = 0 \qquad 3.19a$$

$$\frac{\partial\psi_2}{\partial\eta} = -w_1(\xi) \exp i(\mu+\theta 1) \qquad 3.19b$$

$$C_{P_2} = 2\left[\frac{i\theta}{M^2}\psi_2 - \frac{\partial\psi_2}{\partial\xi}\right] \exp\left\{-i\left[\theta(\xi+1)+\mu\right]\right\} \qquad 3.19c$$

where, by introducing $\exp(-i\mu)$ in equ. 3.19c, the pressure coefficient is given at the instant when the second blade is at maximum angle-of-attack.

Take the Laplace transform in the streamwise sense

$$\frac{\partial^2 \psi_2(p)}{\partial \eta^2} - \beta^2 (p^2+\theta^2/M^2) \psi_2(p) = f(p,\eta) \qquad 3.20$$

where the non-homogeneous form results from the fact that the flow along the line $\xi=0$ is now disturbed by the first blade. The appropriate initial conditions could, in fact, be obtained for $d < \eta < m/\beta$ from equ. 3.12a, while for $\eta > m/\beta$ (free-stream) they are zero. It may be noted in passing that m, shown in fig. 3.1, is the chordwise stagger of adjacent leading edge Mach lines in the cascade and that the limit $m=0$ corresponds to the sonic leading-edge locus condition. A particular integral for the present problem could thus be obtained by employing the Heavyside unit step function, as in Kurosaka [9]. In this case an integral may be written down immediately from the continuity requirement of equ. 2.18

$$\psi_2(p) = \psi_1(p) + A_2(p) e^{-\beta\eta(p^2+\theta^2/M^2)^{\frac{1}{2}}} + B_2(p) e^{\beta\eta(p^2+\theta^2/M^2)^{\frac{1}{2}}} \qquad 3.21$$

Further, since the inverse of the second term on the right vanishes for $\zeta < 0$, there must follow $B_2(p) = 0$ for $\psi_2(\zeta=0) = \psi_1(s=m)$.

The constant $A_2(p)$ follows from the downwash condition imposed by equ. 3.19b

$$-w_1(p)e^{i(\mu+\theta 1)} = \frac{\partial \psi_1}{\partial y}(p) - \beta(p^2+\theta^2/M^2)A_2(p) \; ; \; y=d \qquad 3.22$$

whereupon the general solution of equ. 3.20 is

$$\psi_2(p) = \psi_1(p) + \frac{w_1(p)e^{i(\mu+\theta 1)} + \psi_1'(p)}{(p^2+\theta^2/M^2)^{\frac{1}{2}}} e^{-\beta\eta(p^2+\theta^2/M^2)^{\frac{1}{2}}} \qquad 3.23a$$

where $$\psi_1' = \frac{\partial \psi_1}{\partial y} \; ; \quad x = u+1 \; , \; y=d \qquad 3.23b$$

The inverse is

$$\psi_2(\xi,\eta) = \psi_1(x,y) + \frac{1}{\beta}\int_0^{\zeta}\left[w_1(u)e^{i(\mu+\theta 1)} + \psi_1'\right] J_o(\xi,\eta,u)\, du \qquad 3.24$$

where the integral vanishes for $\zeta < 0$.

Recalling equ. 3.10a, this may be written in the form

$$\psi_2(\xi,\eta) = \psi_1(x,y) + \psi_1(\xi,\eta)e^{i(\mu+\theta 1)} + I(\xi,\eta) \qquad 3.25a$$

where $I(\xi,\eta)$ is to be determined by integrating the product of the Bessel function and the downwash function for the first blade ψ_1', which is known from the solution of the preceding paragraph. That is

$$I(\xi,\eta) = \frac{1}{\beta} \int_0^{\zeta} \psi_1' J_o(\xi,\eta,u)\, du \qquad 3.25b$$

Neglecting terms of order θ^4 in the expansion of the Bessel function

$$I(\xi,\eta) = -\int_0^{\zeta} \Big\{ a_1 + i\theta\Big[2b_1(u+m) + b_2\Big] + \theta^2(u+m)\Big[3c_1(u+m) + 2c_2 + 2c_3(u+1)\Big] + i\theta^3(u+m)\Big[4d_1(u+m)^2 + 3d_2(u+m) + 3d_3(u+m)(u+1) + 2d_4(u+1)\Big]\Big\} \Big\{1 - \frac{\theta^2}{4M^2}\Big[(\xi-u)^2 - \beta^2\eta^2\Big]\Big\}\, du \qquad 3.26$$

Performing the integration and defining an interference potential $\psi_{12}(\xi,\eta)$, it is found that

$$\psi_2(\xi,\eta) = \psi_1(\xi,\eta)\, e^{i(\mu+\theta 1)} + \psi_{12}(\xi,\eta) \qquad 3.27a$$

where the interference term is

$$\psi_{12}(\xi,\eta) = a_1 m + i\theta m\left[b_1 m + b_2\right] + \theta^2 m\left[c_1 m^2 + c_2 m + c_3(\zeta\bar{\zeta} + mx)\right]$$

$$+ i\theta^3 m\left[d_1 m^3 + d_2 m^2 + d_3 m(3/2\,\zeta\bar{\zeta} + mx) + d_4(\zeta\bar{\zeta} + mx)\right]$$

$$\bar{\zeta} = \xi + \beta\eta \qquad 3.28$$

Equation 3.27 is the required expression for the modified velocity potential, exact to the third power of the oscillation frequency parameter θ. It is easily shown to satisfy the transformed differential equation and tangency condition, while along the leading edge bow wave $\bar{\zeta} = 0$ it may be seen to reduce to ψ_1.

The upper surface pressure coefficient for the second blade now follows by operating on $\psi_2(\xi,\eta)$ according to equ. 3.19c. The final result, exact to the third power of oscillation frequency is

$$C_{P_2}^{(u)} = C_{P_1}^{(u)} + C_{P_{12}}^{(u)} e^{-i\mu} \qquad 3.29a$$

where the interference pressure coefficient due to the aerodynamic interaction of the first blade may be evaluated as

$$C_{P_{12}} = \frac{i2km}{\beta^3} + \frac{k^2 m}{2\beta^5} \left\{ 6M^2\xi + \left[m(M^2+2) + 4M^2\beta d + 4b\beta^2 \right] \right\}$$

$$+ \frac{ik^3 M^2 m}{2\beta^7} \left\{ -(4M^2+1)\xi^2 + \left[-m(M^2+4) - 6M^2\beta d - 6b\beta^2 \right] \xi \right.$$

$$\left. + \left[-m^2(M^2+4)/3 - m\beta d(M^2+3) - b\beta^2(3m+4d\beta) \right] \right\} \qquad 3.29b$$

being independent of interphase blade angle μ and vanishing for the cascade with the sonic leading edge locus condition ($m = 0$). The imaginary part of this result, the unsteady pressure which is out-of-phase with angle-of-attack, is given in fig. 3.2 for two blades oscillating in-phase about the pivots at b. The inlet Mach number is 1.1. The results labeled characteristics are exact in frequency and were derived by neglecting thickness terms in the nonlinear oscillating head shock model described in Section 2.

The low supersonic Mach number strongly emphasizes nonlinear frequency effects in these calculations; as shown later, the third-order theory gives satisfactory results out to much higher frequencies in the higher supersonic range. For the cascade considered here, the interference pressure coefficient $C_{P_{12}}^{(u)}$ compares in magnitude with the pressure coefficient $C_{P_1}^{(u)}$ for the isolated blade. At $k = 0.075$, the

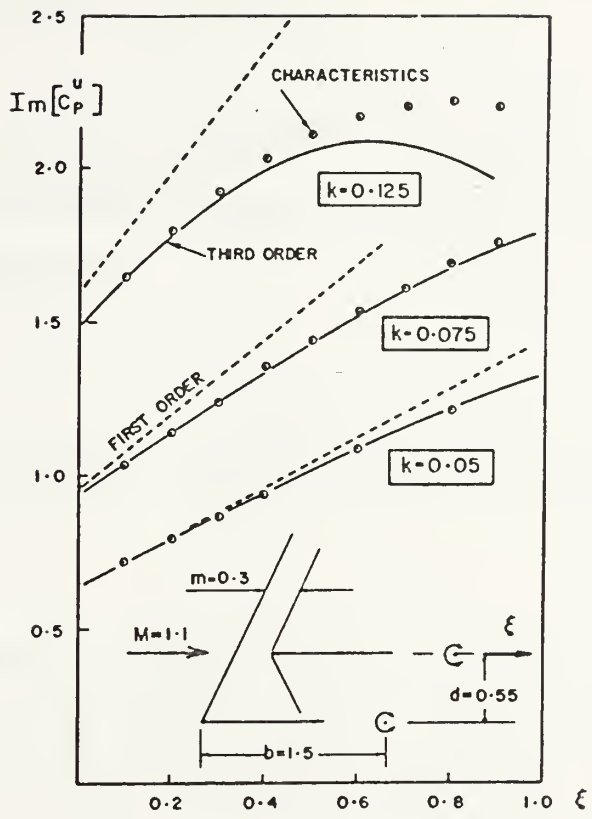

fig. 3.2 Upper surface pressure distribution for second blade (zero interblade phase angle)

out-of-phase upper surface lift coefficient for the second blade is 1.42; for the same blade oscillating in unbounded supersonic flow it is 1.06.

Turning now to the blade passage zone downstream of the second right-running bow wave, for $\eta < 0$ and $\zeta > 0$ (see fig. 3.1). The differential equation for the modified velocity potential, unsteady tangency condition and pressure coefficient given by the set of equs. 3.19 still apply. Also

$$\psi_2(\bar{\zeta}=0) = \psi_1(s=2\xi+m) \qquad 3.30$$

ensures continuity of potential along the bow wave $\bar{\zeta} = 0$. In this case the general solution, given by inverting equ. 3.21, reduces to

$$\psi_2(\xi,\bar{\eta}) = \psi_1(x,y) - \frac{1}{\beta}\int_0^{\bar{\zeta}} \left[w_1(u)e^{i(\mu+\theta 1)} + \psi_1'\right] J_o(\xi,\bar{\eta},u)\, du \qquad 3.31$$

where the integral vanishes for $\bar{\zeta} < 0$; ψ_1' is given by equ. 3.23b; and the over-bar ($\bar{\eta}$) is used to distinguish the blade-passage from the preinterference zone. The important difference between equs. 3.24 (preinterference zone) and 3.31 (blade-passage zone) is the sign attached to the integral; however, increased complexity is to be expected in the present case because of the reflection of left-running waves from the lower surface of the second blade. Some simplification is nevertheless possible as only the difference in potential through the blade surface is now required. Accordingly

$$\psi_2(\xi,0^-) = \psi_1(x,d) - \psi_1(\xi,0)e^{i(\mu+\theta 1)} + I(\xi,0) \qquad 3.32$$

where ψ_1 is given by equ. 3.12a and $I(\xi,0)$ by equ. 3.26.

From a previous result

$$\psi_2(\xi,0^+) = \psi_1(x,d) + \psi_1(\xi,0)e^{i(\mu+\theta l)} + I(\xi,0) \qquad 3.25a$$

whereupon it follows that

$$\Delta\psi_2(\xi) = -2\left[\psi_1(\xi,0)e^{i(\mu+\theta l)} + I(\xi,0)\right] \qquad 3.33$$

The pressure loading coefficient is therefore given by evaluating

$$\Delta C_{P_2} = -2C_{P_1}^{(u)} - 4\left[\frac{i\theta}{M^2} I(\xi,0) - \frac{\partial I}{\partial \xi}\right] \exp -i\left[\theta(\xi+1) + \mu\right] \qquad 3.34$$

the reduction of which, to the expression given below, is somewhat simplified by noting that the highest order term in $I(\xi,0)$ occurs as a derivative with respect to ξ. This differentiation is most conveniently performed under the integral sign in equ. 3.26. The final result is

$$\Delta C_{P_2} = -2C_{P_1}^{(u)} + \Delta C_{P_{12}} e^{-i\mu} \qquad 3.35a$$

where the interference pressure loading coefficient is

$$\Delta C_{P_{12}} = 2C_{P_1}^{(u)} + \frac{i2k}{\beta^3}\left\{2M^2\beta d - 2\beta^2 m\right\}$$

$$+\frac{k^2}{2\beta^5}\left\{-M^2\xi^2+[-4m(M^2-1)-2M^2\beta d(2M^2-5)]\xi+[-m(2M^2-3)+m^2\beta d+2b\beta^2]2M^2\beta d\right\}$$

$$+\frac{ik^3M^2}{2\beta^7}\left\{(6M^2+2)/3\xi^3+[2m(4M^2-3)-8d\beta]\xi^2+[8m(M^2-2)-4M^2\beta d(M^2-3)\right.$$
$$-3b\beta^2]\xi\beta d$$
$$\left.+[-2m^2-4M^4\beta^2d^2/3+4M^2m\beta d(M^2-2)-4\beta^2d(M^2\beta d+m)]\beta d\right\}$$

3.35b

Considerable reduction is involved in determining this result. However, the expression contains only the three basic geometric cascade parameters m, d and b (fig. 3.1), together with Mach number and frequency. To first order in frequency, the preinterference pressure loading of the second of two blades oscillating in-phase is thus seen to be independent of chordwise coordinate ξ and pivot location b. This somewhat surprising result applies for low frequency oscillations. To the next highest order in frequency, unsteady air forces on the second blade depend on both of these quantities.

A second interesting observation is that when quadratic and cubic terms in frequency are neglected, there results, for $\mu = 0$, simply $R_e(\Delta C_{P_2}) = 0$ and $I_m(\Delta C_P) = 4k/\beta\ (M^2d/\beta - m)$. This is precisely Kurosaka's periodic solution for the pre-interference zone of the infinite two-dimensional cascade [9]. It is surprising that Kurosaka's solution, the derivation of

which requires the inversion of an integral equation, should be the same as the solution obtained here for the second blade in the finite cascade. An elementary approach to the rectilinear periodic cascade problem is given in Section 4.

Before generalizing the present analysis, fig. 3.3 summarizes the solution obtained for two blades. The real component of generalized aerodynamic pressure acts on the blade at maximum angle-of-attack and is therefore in-phase with the angle-of-attack. Further, $R_e[C_p^{(u)}] = -2/\beta$ as the frequency of oscillation approaches zero, as given by Ackeret theory. The imaginary air forces, however, are 270° out-of-phase and therefore act on the blade as it passes through zero angle-of-attack with the trailing edge moving down.

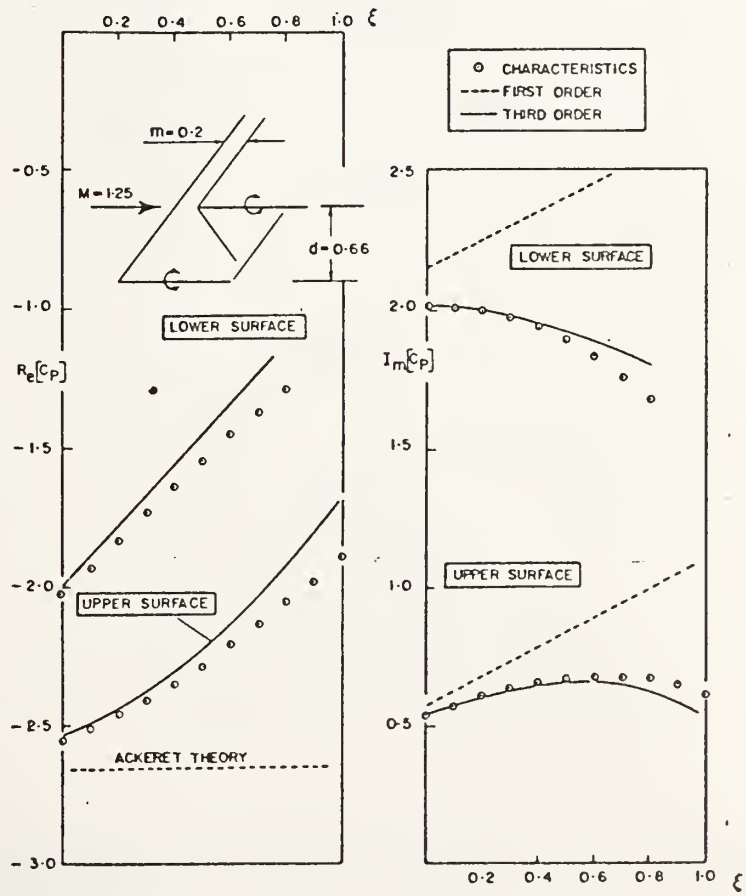

fig. 3.3 Upper and lower surface pressure distributions for second blade (zero interblade phase angle, k = 0.2)

The range of reduced frequencies over which the present solution compares favourably with exact calculations is indicated in fig. 3.4. For the cascades shown, the out-of-phase pressure loading of the second blade has been integrated up to the point of intersection along the chord of the trailing edge expansion wave from the first blade. At $M = 1.25$ the third-order theory gives the preinterference lift to a few percent for reduced frequencies to 0.4; at $M = 1.6$ the upper frequency bound is 0.7.

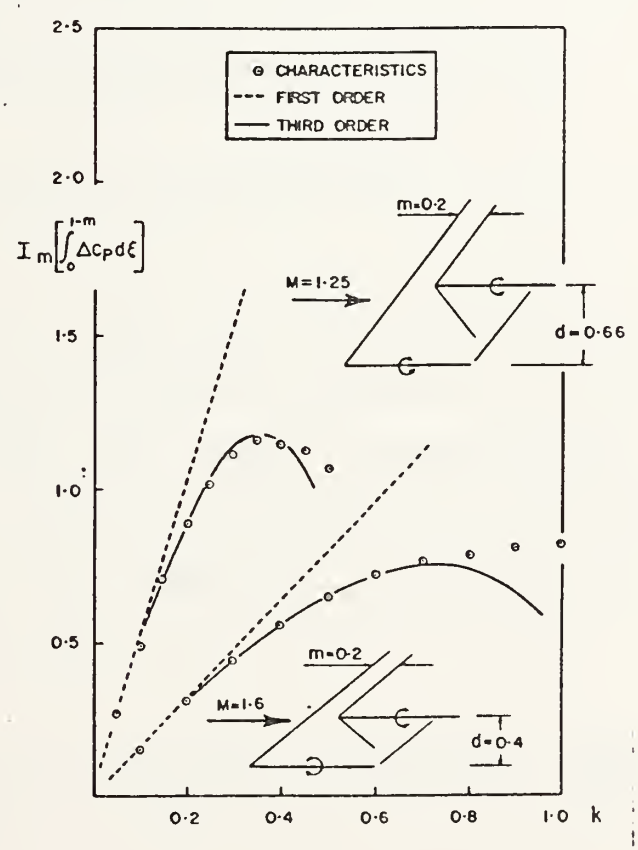

fig. 3.4 Variation of preinterference lift with reduced frequency for second blade (zero interblade phase angle)

3.3 Cascade with n-Blades

The analysis is readily extended to the n^{th} blade in the cascade. With

$$\tau = \varepsilon - \beta\gamma \qquad 3.36$$

in the preinterference zone of the third blade (fig. 3.1), continuity of the potential along the third left-running bow wave $\tau = 0$, requires

$$\phi_3(\tau=0) = \phi_2(\zeta=m) = \psi_2(\zeta=m)e^{-i\theta x} \qquad 3.37$$

The appropriate transformation of ϕ is now

$$\phi_3(\varepsilon,\gamma) = \psi_3(\varepsilon,\gamma)e^{-i\theta x} \qquad 3.38$$

where $x = \varepsilon+2l$. Equations will result which thus have an obvious bearing to those of paragraph 3.2. The tangency condition (3.19b), for example, becomes in the case of the third blade $\partial\psi_3/\partial\gamma = -w_1(\varepsilon)\exp 2i(\mu-\theta l)$ in the plane $\gamma = 0$. Recalling equ. 3.24, the following solution thus applies for $\psi_3(\varepsilon,\gamma)$, valid for $\tau > 0$

$$\psi_3(\varepsilon,\gamma) = \psi_2(\xi,\eta) + \frac{1}{\beta}\int_0^\tau \left[w_1(u)e^{2i(\mu+\theta l)} + \frac{\partial\psi_2}{\partial\eta}(\eta=d)\right]J_o(\varepsilon,\gamma,u)\,du \qquad 3.39$$

But the upwash in the plane of the third blade is now

$$\frac{\partial \psi_2}{\partial \eta}(\eta=d) = \psi_1' e^{i(\mu+\theta 1)} + \frac{\partial \psi_{12}}{\partial \eta}(\eta=d) \qquad 3.40$$

from equ. 3.27. The maximum upwash induced in the plane of the third blade is thus seen to vary from that induced in the plane of the second blade by the amount $\partial \psi_{12}/\partial \eta(\eta=d)$, which is second order in oscillation frequency. With this result, equ. 3.39 may be written

$$\psi_3(\varepsilon,\gamma) = \psi_2(\xi,\eta) + \frac{e^{i(\mu+\theta 1)}}{\beta} \int_C^{\tau} \left[w_1(u) e^{i(\mu+\theta 1)} + \psi_1 \right] J_o(\varepsilon,\gamma,u)$$

$$+ \frac{1}{\beta} \int_0^{\tau} \frac{\partial \psi_{12}}{\partial \eta}(\eta=d)\, du \qquad 3.41$$

where, because of the above observation concerning the downwash, the expansion of the Bessel function has been taken as unity in the last integral. Noting that $\partial \psi_{12}/\partial \eta(\eta=d)$ is independent of streamwise position, and employing equs. 3.24 and 3.27

$$\psi_3(\varepsilon,\gamma) = \psi_2(\varepsilon,\gamma) e^{i(\mu+\theta 1)} + \psi_{12}(\xi,\eta) + \frac{\tau}{\beta} \frac{\partial \psi_{12}}{\partial \eta}(\eta=d) \qquad 3.42$$

For the preinterference zone above the fourth blade, there would be written

$$\psi_4(p,r) = \psi_3(\varepsilon,\gamma) + \frac{1}{\beta}\int_0^t \left[w_1(u)e^{3i(\mu+\theta 1)} + \frac{\partial\psi_3}{\partial\gamma}(\eta=d)\right] J_o(p,r,u)\,du \qquad 3.43$$

where the meaning of the new coordinates is clear and where the upwash in the plane of the fourth blade is

$$\frac{\partial\psi_3}{\partial\gamma}(\gamma=d) = \psi_2' e^{i(\mu+\theta 1)} + \frac{\partial\psi_{12}}{\partial\eta}(\eta=2d) - \frac{\partial\psi_{12}}{\partial\eta}(\eta=d) \qquad 3.44$$

which may be written

$$\frac{\partial\psi_3}{\partial\gamma}(\gamma=d) = \psi_2' e^{i(\mu+\theta 1)} + \frac{\partial\psi_{12}}{\partial\eta}(\eta=d) \qquad 3.45$$

since

$$\frac{\partial\psi_{12}}{\partial\eta}(\eta=d) = -m\beta^2\eta\left[2c_3\theta^2 + i\theta^3(3md_3+2d_4)\right] \qquad 3.46$$

from equ. 2.27. It is now easy to show that

$$\psi_4(p,r) = \psi_3(p,r)e^{i(\mu+\theta 1)} + \psi_{12}(\xi,\eta) + \frac{(t+\tau)}{\beta}\frac{\partial\psi_{12}}{\partial\eta}(\eta=d) \qquad 3.47$$

where $t+\tau = 2t+m$.

In view of the simple recurrence relation for the upwash (equs. 3.40 and 3.45), it is possible to generalize equs. 3.42 and 3.47; the following result is thereby obtained for the preinterference potential of the n^{th} blade in the cascade

$$\psi_n(\xi,\eta) = \psi_{n-1}(\xi,\eta)e^{i(\mu+\theta l)} + \psi_{12}(a,b) + \left[(n-2)\zeta+m\right]\frac{\partial\psi_{12}}{\partial\eta}(\eta=d) \qquad 3.48$$

where ξ and η, with $\zeta = \xi-\beta\eta$, have been used as general coordinates for the n^{th} blade and ψ_{12} is to be evaluated at $a = \xi+(n-2)l$, $b = \eta+(n-2)d$. This simplifies to

$$\begin{aligned}\psi_n(\xi,\eta) = {} & \psi_{n-1}(\xi,\eta)e^{i(\mu+\theta l)} + \psi_{12}(\xi,\eta) \\ & + \theta^2 c_3 m^2(n-2)\left\{2\xi+nd\beta+(n-1)m\right\} \\ & + i\theta^3 m^2(n-2)\left\{d_3 m/2\left[6\xi+(3n-1)d\beta+(3n-4)m\right]\right. \\ & \left. + d_4\left[2\xi+nd\beta+(n-1)m\right]\right\} \qquad 3.49a\end{aligned}$$

as the modified potential for the n^{th} preinterference zone of the finite cascade, with the velocity potential given by

$$\phi_n(\xi,\eta) = \psi_n(\xi,\eta)e^{i\theta[\xi+(n-1)l]} \qquad 3.49b$$

It is readily shown that equ. 3.49 satisfies the differential equation and boundary conditions described at the beginning of this section. The requirement demanding continuity of $\phi(\xi,\eta)$ along the wave $\zeta=0$ may also be shown to be satisfied.

The upper-surface pressure coefficient for the n^{th} blade is given by evaluating

$$C_{P_n}^{(u)} = 2\left(\frac{i\theta}{M^2}\,\psi_n - \frac{\partial\psi_n}{\partial\xi}\right) \exp -i\left\{\theta\,[\xi+(n-1)\,l] + (n-1)\,\mu\right\} \qquad 3.50$$

where $\psi_n = \psi_n(\xi,0)$, and $C_{P_n}^{(u)}$ corresponds to $\alpha_n(\max)$. Carrying out the simplification, with $k = M^2\theta/\beta^2$

$$C_{P_n}^{(u)} = C_{P_{n-1}}^{(u)} + e^{-i(n-1)\mu}\left[C_{P_{12}}^{(u)} + \bar{C}_P^{(u)}\right] \qquad 3.51a$$

where the term of second order in frequency is

$$\bar{C}_P^{(u)} = k^2/\beta^5(n-2)M^2m(3m+2d\beta)$$

$$+ ik^3/\beta^7(n-2)M^2m\left\{-[m(4M^2+1)+3M^2d\beta]\xi + ml(5M^2-2) + M^2m^2\right.$$

$$\left. - b\beta^2(3m+2d\beta) - [m(4M^2+1)+2M^2d\beta]\,\frac{nl}{2}\right\} \qquad 3.51b$$

which embraces the case n-2. The solution may be written

$$C_{P_n}^{(u)} = C_{P_1}^{(u)} + C_{P_{12}}^{(u)} \sum_{p=1}^{n-1} e^{-ip\mu} + \sum_{p=3}^{n} \overline{C}_P^{(u)} e^{-i(p-1)\mu}$$

3.51c

where $C_{P_1}^{(u)}$ is the upper-surface pressure coefficient for the isolated blade and $C_{P_{12}}^{(u)}$ the previously defined interference coefficient associated with the first and second blades. Equation 3.51 is compared with the method of characteristics in fig. 3.5. Comments on the solution are given in paragraph 3.4 below.

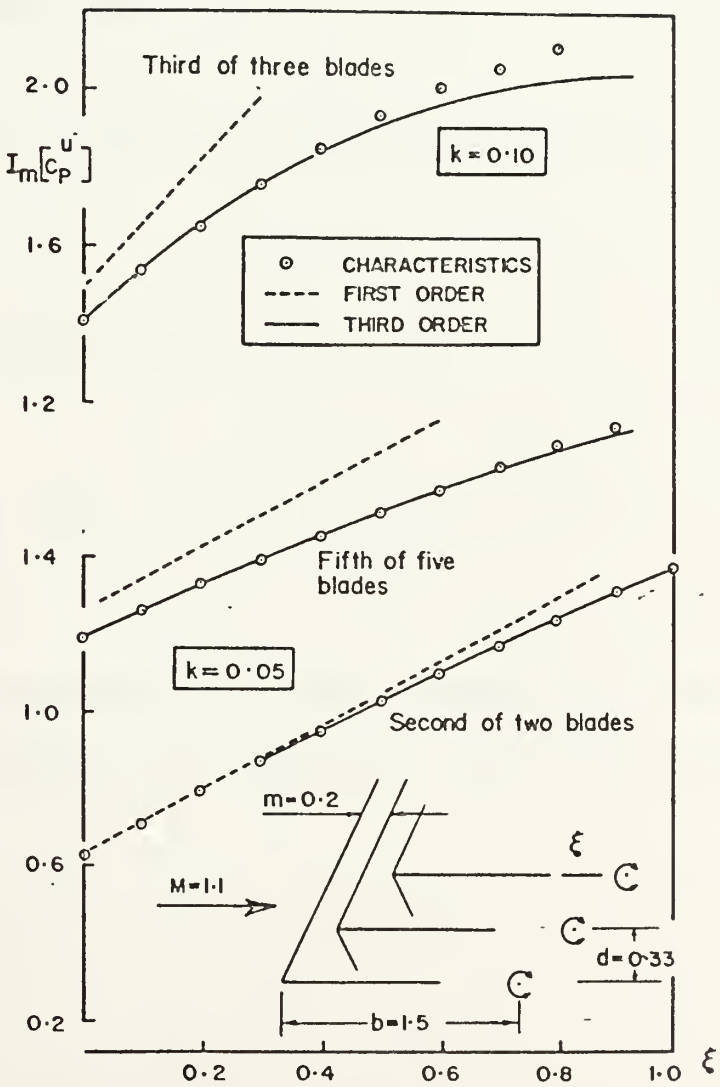

fig. 3.5 Upper surface pressure distribution for the n^{th} blade (zer interblade phase angle)

The potential difference through the plane of the n^{th} blade is

$$\Delta\psi_n(\xi) = \Delta\psi_{n-1}(\xi)e^{i(\mu+\theta 1)} - 2\xi \frac{\partial\psi_{12}}{\partial\eta} \quad (\eta=d) \qquad 3.52$$

which gives

$$\Delta C_{P_n} = \Delta C_{P_{n-1}} + e^{-i(n-1)\mu}\Delta\bar{C}_P \qquad 3.53a$$

where the second order term is

$$\Delta\bar{C}_P = \frac{k^2}{\beta^4} 2mdM^2 + \frac{ik^3}{\beta^6} mdM^2[-2(M^2+1)\xi - 2M^2 ln + m(4M^2-1) + 2M^2 d\beta - 2b\beta^2] \qquad 3.53b$$

Equation 3.53a may be written

$$\Delta C_{P_n} = \Delta C_{P_2} + \sum_{p=3}^{n} \Delta\bar{C}_P e^{-i(p-1)\mu} \qquad 3.53c$$

where the last term is zero for the case of n=2 and where ΔC_{P_2} is the loading coefficient for the second blade.

3.4 Further Discussion of the Solution

A solution which is exact to first-order in oscillation frequency is easily extracted from the more general solution. Written for the component of pressure which is out-of-phase with the angle-of-attack, this result for the n^{th} blade is

$$I_m\left[C_{P_n}^{(u)}\right] = I_m\left[C_{P_1}^{(u)}\right] + \frac{2km}{\beta^3} \sum_{p=1}^{n-1} \cos p\mu$$

$$I_m\left[\Delta C_{P_n}\right] = \frac{4}{\beta} \sin \mu + \frac{4k}{\beta}\left(\frac{M^2 d}{\beta} - m\right) \cos \mu$$

According to the elementary theory, the out-of-phase surface pressure thus exhibits a sustained oscillation with blade index, except in the case $\mu=0$, when the solution diverges. In this case, $C_{P_n}^{(u)}$ increases by the constant amount $2km/\beta^3$ from blade-to-blade. However, the pressure loading or total damping force remains finite and independent of blade index for all μ. Further, ΔC_{P_n} is uniform across the chord of the blade and is independent of pivot position.

The failure of first-order theory in the far field of the cascade, for the case when the blades oscillate in-phase, was the main reason for seeking the third-order solution. This solution is further compared with the method of characteristics in fig. 3.6, giving out-of-phase preinterference lift for several reduced frequencies and interblade phase angles. The following observations are to be noted

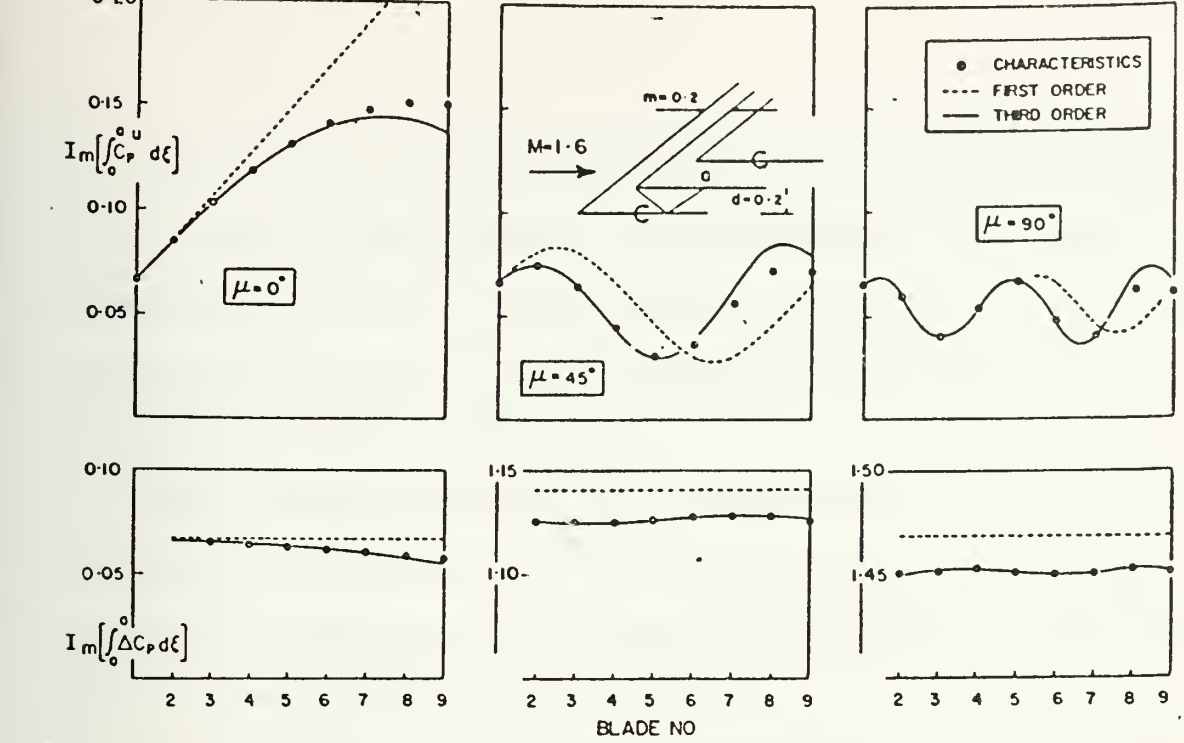

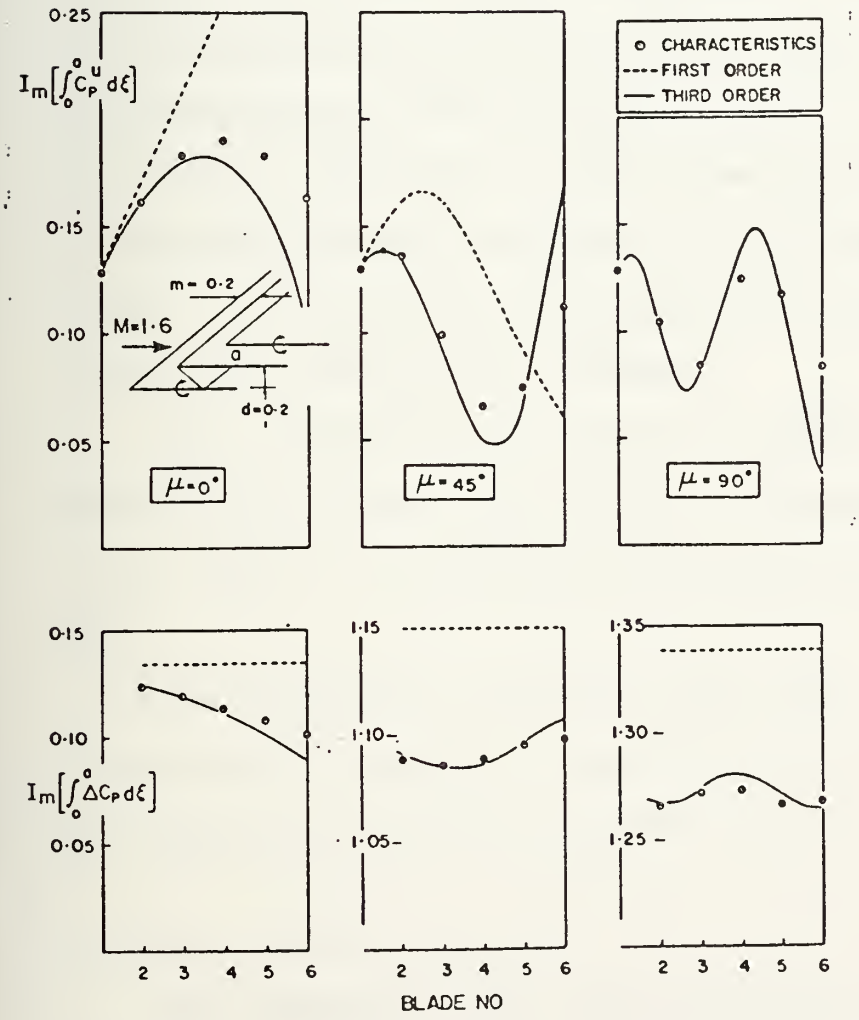

fig.3.6 Variation of preinterference lift with blade index for several interblade phase angles

fig. 3.6 Variation of preinterference lift with blade index for several interblade phase angles

(a) for zero interblade phase angle, upper-surface air loads given by the method of characteristics fall below the first-order solution, which becomes unbounded as the effect of more and more blades is considered. The third-order solution is much better.

(b) the exact results for the surface lift ($\mu = 0$) continue to oscillate out to large blade index, although the first segments only of these oscillations are shown in fig. 3.6 (see, however, fig. 4.2).

(c) for finite μ the approximate theory and the method of characteristics predict a strong sinusoidal modulation of upper-surface lift with blade index. There is also a sinusoidal modulation in total pressure loading, but of considerably reduced magnitude. This important practical result is accurately predicted by the third-order theory in the near field of the cascade.*

(d) the third-order solution diverges in the far field. This is most clearly seen by the occurrence directly of blade index in the second-order expressions for $\overline{C}_{P_n}^{(u)}$ and $\Delta\overline{C}_{P_n}$.

Notwithstanding the above limitation, the simple closed-form solution provides a useful means for estimating generalized air forces in the finite cascade over a range of practical

---

*The behavior of the exact solution in the increasingly far field of the cascade is considered in paragraph 4.2.

oscillation frequencies. Possible applications include (i) preliminary blade design, (ii) validation of computer models based on exact solutions of the linearized equations and, less obviously, (iii) as a basis for comparison with a possible periodic solution for the infinite cascade, exact to the third-power of oscillation frequency. In the next Section, such a solution is derived which is exact to the first-power of oscillation frequency; the surface pressure is shown to agree with the mean level of the present first-order oscillatory solution. It seems highly likely, on this basis, that a periodic solution to the third-power in oscillation frequency would agree with the mean level of the present divergent oscillatory solution.

4 PERIODIC SOLUTION FOR THE UNSTEADY SUPERSONIC CASCADE WITH A SUBSONIC LEADING EDGE

Flutter calculations presently employ generalized air forces determined by applying linearized flow theory to finite rectilinear cascades [20]. However, no proof has been given that these forces are representative of the infinite rotor. Indeed, it is frequently very difficult to obtain convergence of the surface pressures in practical calculations. This has been shown by Verdon [6]. It has been repeatedly demonstrated over a wide range of oscillation frequencies during the course of the present investigation.

The work of the final Section of this dissertation attempts to relate the finite cascade theory of the previous Section with an elementary periodic solution derived for the infinite cascade. The periodic analysis is based on a generalization of Sauers solution for the flat plate oscillating slowly in unbounded supersonic flow [18]. It is exact to the first power of the oscillation frequency. Kurosaka gives a difficult mathematical treatment of this problem [9]. The present approach, however, is much simpler.

4.1 The Periodic Solution

The dimensionless linearized perturbation equations describing the supersonic flow, tangency condition and pressure coefficient for the single flat-plate aerofoil are

$$\beta^2 \frac{\partial^2 \phi_1}{\partial x^2} - \frac{\partial^2 \phi_1}{\partial y^2} = k^2 M^2 \phi_1 - i2kM^2 \frac{\partial \phi_1}{\partial x} \qquad 4.1a$$

$$\frac{\partial \phi_1}{\partial y} = -[1 + ik(x-b)]; \quad y = 0 \qquad 4.1b$$

$$C_{p_1} = -2\left(\frac{\partial \phi_1}{\partial x} + ik\phi_1\right) \qquad 4.1c$$

as previously given. The coordinate x is measured downstream from the leading edge, b is the pivot and k the reduced frequency of oscillation. Upon expressing ϕ_1 as a first-order power series based on frequency, Sauer gives the following particular solution

$$\phi_1(x,y) = f_1(s) + k[h_1(s) - iM^2 y/\beta f_1(s)] \qquad 4.2a$$

$$f_1(s) = h_1(s) = 0; \quad s < 0 \qquad 4.2b$$

$$s = x - \beta y \qquad 4.3$$

which thus vanishes upstream of the left running leading edge bow wave. Apply the flow tangency condition of equ. 4.1b

$$[1+ik(s-b)] = \beta f_1' + k(\beta h_1' + iM^2/\beta f_1) \qquad 4.4$$

where the prime denotes differentiation with respect to argument and where, since y = 0, s has been written for x. It follows that

$$f_1(s) = s/\beta \qquad 4.5a$$

$$h_1(s) = - is/\beta^3(s/2 + b\beta^2) \qquad 4.5b$$

The velocity potential for s > 0 is then

$$\phi_1(x,y) = \frac{s}{\beta} - i \frac{ks}{\beta^3} (\frac{s}{2} + b\beta^2 + M^2\beta y) \qquad 4.6$$

and by substituting directly into equ. 4.1c, the upper surface pressure coefficient, exact to the first power of oscillation frequency

$$C_{p_1}^{(u)} = - \frac{2}{\beta} + i \frac{2k}{\beta^3} [(2-M^2)x+b\beta^2] \qquad 4.7$$

in agreement with the result derived in paragraph 3.1 using the Laplace transform.

Consider now the infinite array and denote by x,y the coordinates of the flow referenced to the n^{th} blade.* At

---

*No confusion should arise from the use of the same x,y coordinates as in the unbounded flow case.

time t = 0, as shown in fig. 4.1, the angle-of-attack of the n^{th} blade is $\alpha_n = 1$. That of the $(n+1)^{th}$ blade, denoted the q^{th} blade, is $\alpha_q = \exp(i\mu)$. The preinterference zone potential $\phi_n(x,y)$ in the shaded region of fig. 4.1 clearly must satisfy equ. 4.1a. Accordingly

$$\phi_n(x,y) = f_n(s) + k\left[h_n(s) - iM^2 y/\beta f_n(s)\right] \qquad 4.8$$

where $s = x - \beta y$, as in the previous case. However, while

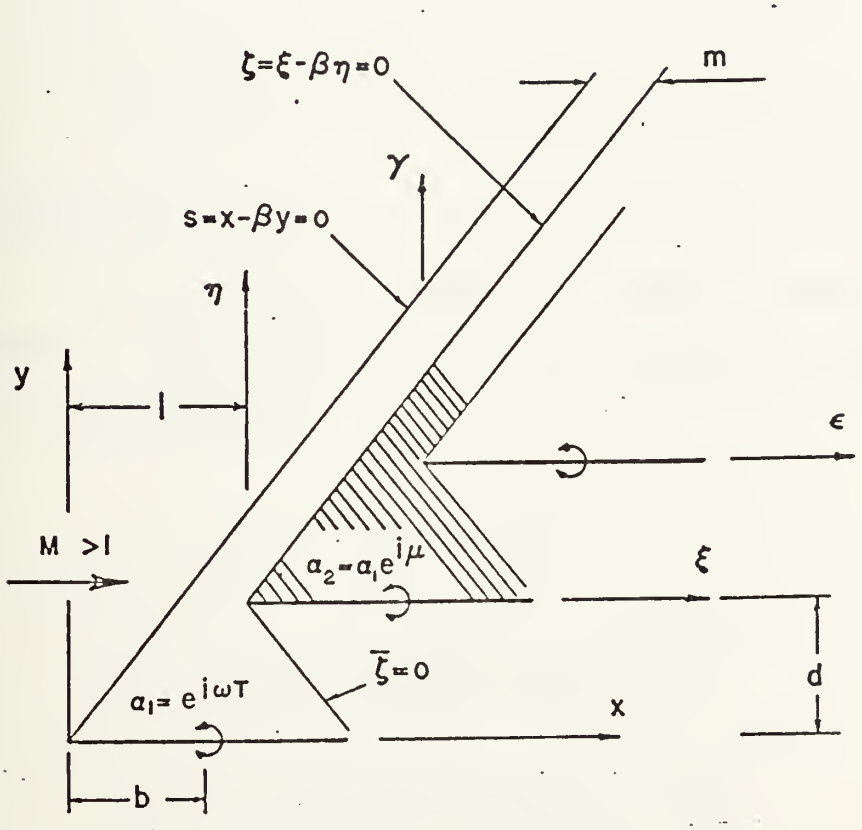

fig. 4.1 Cascade geometry

the functions $f_1(s)$ and $h_1(s)$ previously vanished ahead of the leading-edge bow wave, this is no longer so. Similarly for the preinterference zone immediately above the q^{th} blade

$$\phi_q(\xi,\eta) = f_q(\zeta) + k\left[h_q(\zeta)-iM^2\eta/\beta f_q(\zeta)\right] \qquad 4.9$$

$$\zeta = \xi - \beta\eta \qquad 4.10$$

Apply the flow tangency condition to both regions

$$1+ik(s-b) = \beta f_n'+k(\beta h_n'+iM^2/\beta f_n) \qquad 4.11a$$

$$e^{i\mu}\left[1+ik(\zeta-b)\right] = \beta f_q'+k(\beta h_q'+iM^2/\beta f_q) \qquad 4.11b$$

in the planes $y = 0$ $(0 < s < 1;\ s = x)$ and $\eta = 0$ $(0 < \zeta < 1;\ \xi = \zeta)$, respectively. There immediately results for the steady-state and first-order frequency terms, respectively

$$f_n(s) = s/\beta + A_n \qquad 4.12a$$

$$f_q(\zeta) = \zeta/\beta e^{i\mu} + A_q \qquad 4.12b$$

$$h_n(s) = -\frac{is}{\beta^3}\left(\frac{s}{2}+b\beta^2+M^2\beta A_n\right) - ikB_n \qquad 4.12c$$

$$h_q(\zeta) = -\frac{i\zeta}{\beta^3}\left(\frac{\zeta}{2}+b\beta^2\right)e^{i\mu} + M^2\beta A_q - ikB_q \qquad 4.12d$$

where A and B are integration constants. Thus it is found that

$$\phi_n(x,y) = \left[\frac{s}{\beta}+A_n\right] - \frac{iks}{\beta^3}\left[\frac{s}{2}+b\beta^2+M^2\beta y+M^2\beta A_n\right] - ik\left[\frac{M^2}{\beta}yA_n - B_n\right] \quad 4.13a$$

$$\phi_q(\xi,\eta) = \left[\frac{\zeta}{\beta}e^{i\mu}+A_q\right] - \frac{ik\zeta}{\beta^3}\left[(\frac{\zeta}{2}+b\beta^2+M^2\beta\eta)e^{i\mu}+M^2\beta A_q\right]$$

$$- ik\left[\frac{M^2}{\beta}\eta A_q - B_q\right] \quad 4.13b$$

The requirement for continuity of the velocity potential across the bow wave s = m or ζ = 0 may be written

$$\phi_n(s = m) = \phi_q(\zeta = 0) \quad 4.14$$

which leads to

$$\frac{m}{\beta} + A_n = A_q \quad 4.15$$

by virtue of the steady-state terms in equ. 3.13.

The velocity potential in the n^{th} preinterference zone at the instant when the angle-of-attack of the n^{th} blade is α_n = 1 has been denoted $\phi_n(s)$ and at this same time in the q^{th} zone when $\alpha_q = \exp(i\mu)$ by $\phi_q(\zeta)$. Thus, at the somewhat earlier time when α_q = 1 the potential in the q^{th} zone will be $\phi_q(\zeta)\exp(-i\mu)$ by virtue of the assumed harmonic time

dependence. For periodicity of the flow

$$\phi_n(s) = \phi_q(\zeta)\ e^{-i\mu} \qquad 4.16$$

Applying this result to equ. 4.13

$$A_n = A_q\ e^{-i\mu} \qquad 4.17$$

and using equ. 4.15

$$A_n = \frac{m/\beta}{e^{i\mu}-1} \qquad 4.18$$

The preinterference pressure coefficient for the upper surface of the n^{th} blade in the infinite cascade, exact to the first power of oscillation frequency, follows without B_n

$$C_{p_n}^{(u)} = -\frac{2}{\beta} + i\,\frac{2k}{\beta^3}\left[(2-M^2)x+b\beta^2+\frac{m}{e^{i\mu}-1}\right] \qquad 4.19a$$

which may be written as a modification to $C_{p_1}^{(u)}$, the upper surface pressure coefficient for the isolated blade in unbounded supersonic flow

$$C_{p_n}^{(u)} = C_{p_1}^{(u)} + \frac{i2km/\beta^3}{e^{i\mu} - 1} \qquad 4.19b$$

Consider the flow in the blade passage bounded by the right-running bow wave from the q^{th} blade and its reflection from the n^{th} blade. The potential may be constructed by superimposing upon the previous solution of left-running waves a similar family of right-running waves

$$\bar{\phi}_q(\xi,\eta) = \phi_n(x,y) + g_q(\bar{\zeta}) + k\left[r_q(\bar{\zeta})+iM^2\eta/\beta g_q(\bar{\zeta})\right] \quad 4.20$$

$$\bar{\zeta} = \xi + \beta\eta \quad 4.21$$

It is seen immediately that

$$g_q(0) = 0 \quad 4.22$$

continuity of the steady-state potential requiring $\phi_q = \phi_n$ when $\bar{\zeta} = 0$. With the observation $s = \zeta+m$, $y = \eta+d$, the potential $\phi_n(x,y)$ may be expressed in terms of the local coordinates ξ,η of the q^{th} blade; equ. 4.20 is then

$$\bar{\phi}_q(\xi,\eta) = \phi_n(\xi,\eta) + \frac{m}{\beta} - i\frac{k}{\beta^3}\left[\zeta(m+d\beta M^2)+m\eta\beta M^2+C\right]$$
$$+ g_q(\bar{\zeta}) + k\left[r_q(\bar{\zeta})+i\frac{M^2}{\beta}\eta g_q(\bar{\zeta})\right] \quad 4.23$$

where C is a constant involving A_n, cascade geometry, and Mach number. The flow tangency condition applied to the lower surface of the q^{th} blade may therefore be written

$$-e^{i\mu}\left[1+ik(\bar{\zeta}-b)\right] = -\left[1+ik(\bar{\zeta}-b)\right] + ik\left(\frac{M^2 d}{\beta} - m\right)$$

$$+ \beta r_q' + k(\beta\gamma_q' + i\frac{M^2}{\beta} g_q) \qquad 4.24$$

where $\bar{\zeta}$ has been written for ξ, since $\eta = 0$. From the steady-state terms, together with equ. 4.22

$$g_q(\bar{\zeta}) = \frac{(1-e^{i\mu})}{\beta}\bar{\zeta} \qquad 4.25$$

while from the first-order frequency dependence

$$r_q' = -i/\beta^3\left[(1-e^{i\mu})(\bar{\zeta}+b\beta^2) + M^2 d\beta - m\beta^2\right] \qquad 4.26$$

Hence, the lower surface pressure coefficient for the q^{th} blade, from equs. 4.1c and 4.23

$$C_{p_q}^{(l)} = C_{p_n}^{(u)} - 2\left\{g_q'+kr_q'+ik\left[g_q+m/\beta-(m+d\beta M^2)/\beta^3\right]\right\} \qquad 4.27a$$

$$= C_{p_n}^{(u)} + (1-e^{i\mu})C_{p_l}^{(u)} + i\frac{4k}{\beta}\left(\frac{M^2 d}{\beta} - m\right) + i\frac{2km}{\beta^3} \qquad 4.27b$$

where, as previously defined, $C_{p_n}^{(u)}$ and $C_{p_l}^{(u)}$ are the upper surface pressure coefficients for the n^{th} blade and for the isolated blade, respectively, Finally, there may be written for the preinterference pressure loading for the q^{th}, or $(n+1)^{th}$ blade, the following expression

$$\Delta C_{p_{n+1}} = C_{p_{n+1}}^{(1)} - C_{p_n}^{(u)} e^{i\mu} \qquad 4.28a$$

using the periodicity of $C_p^{(u)}$, and which reduces to

$$\Delta C_{p_{n+1}} = 2C_{p_1}^{(u)} (1-e^{i\mu}) + i \frac{4k}{\beta} \left(\frac{M^2 d}{\beta} - m\right) \qquad 4.28b$$

These should now be rewritten to correspond to the time of maximum angle-of-attack for the $(n+1)^{th}$ blade. Thus, multiply equ. 4.28b by $\exp(-i\mu)$ and there may be written the following general expressions for the preinterference pressures in the infinite cascade

$$C_p^{(u)} = C_{p_1}^{(u)} + i \frac{2km/\beta^3}{e^{i\mu} - 1} \qquad 4.29$$

$$\Delta C_p = 2C_{p_1}^{(u)} (e^{-i\mu} - 1) + i \frac{4k}{\beta} \left(\frac{M^2 d}{\beta} - m\right) e^{-i\mu} \qquad 4.30$$

4.2 Comparison with Finite Cascade Theory

The analysis of Section 3 gives the following solution for preinterference pressures when terms of quadratic and cubic frequency dependence are neglected

$$C_{p_n}^{(u)} = C_{p_1}^{(u)} + i \frac{2km}{\beta^3} \sum_{p=1}^{n-1} e^{-ip\mu} \qquad 4.31$$

$$\Delta C_{p_n} = 2C_{p_1}^{(u)} (e^{-i\mu} - 1) + i \frac{4k}{\beta} \left(\frac{M^2 d}{\beta} - m\right) e^{-i\mu} \qquad 4.32$$

for the n^{th} blade of the finite supersonic cascade, with $C_{P_1}^{(u)}$ denoting the upper surface pressure coefficient for the isolated blade. Consider equ. 4.31 and for $\mu \neq 2\pi m$ (where m is integer) write

$$I_m\left[C_{P_n}^{(u)} - C_{P_1}^{(u)}\right] = \frac{2km}{\beta^3} \sum_{1}^{n-1} \cos p\mu$$

$$= \frac{2km}{\beta^3} \left\{ \frac{-1}{2} + \frac{\sin(n-\frac{1}{2})\mu}{2 \sin \mu/2} \right\} \qquad 4.33a$$

$$R_e\left[C_{P_n}^{(u)} - C_{P_1}^{(u)}\right] = \frac{2km}{\beta^3} \sum_{1}^{n-1} \sin p\mu$$

$$= \frac{2km}{\beta^3} \left\{ \frac{\sin \mu}{2(1-\cos \mu)} - \frac{\cos(n-\frac{1}{2})\mu}{2 \sin \mu/2} \right\} \qquad 4.33b$$

where it may be noted that interblade phasing introduces into the real part of equ. 4.33 terms of first order in frequency.

The upper surface pressures in the unsteady finite cascade are thus predicted on the basis of the elementary theory to oscillate indefinitely with blade index, except for the case of zero interblade phase angle, when the component of unsteady aerodynamic force which is out-of-phase with the angle-of-attack evidently diverges. This divergence is due to the approximate representation of the velocity potential by terms of first order in oscillation frequency,

or to some other limitation of the elementary theory, as illustrated in fig. 4.2 giving the results of exact calculations of unsteady preinterference lift. Considered, with zero inter-blade phase angle, are torsional oscillations at reduced frequencies of 0.3 and 1.0. The results show an almost undamped oscillation in upper and lower surface lift with blade index out to the 35^{th} blade.

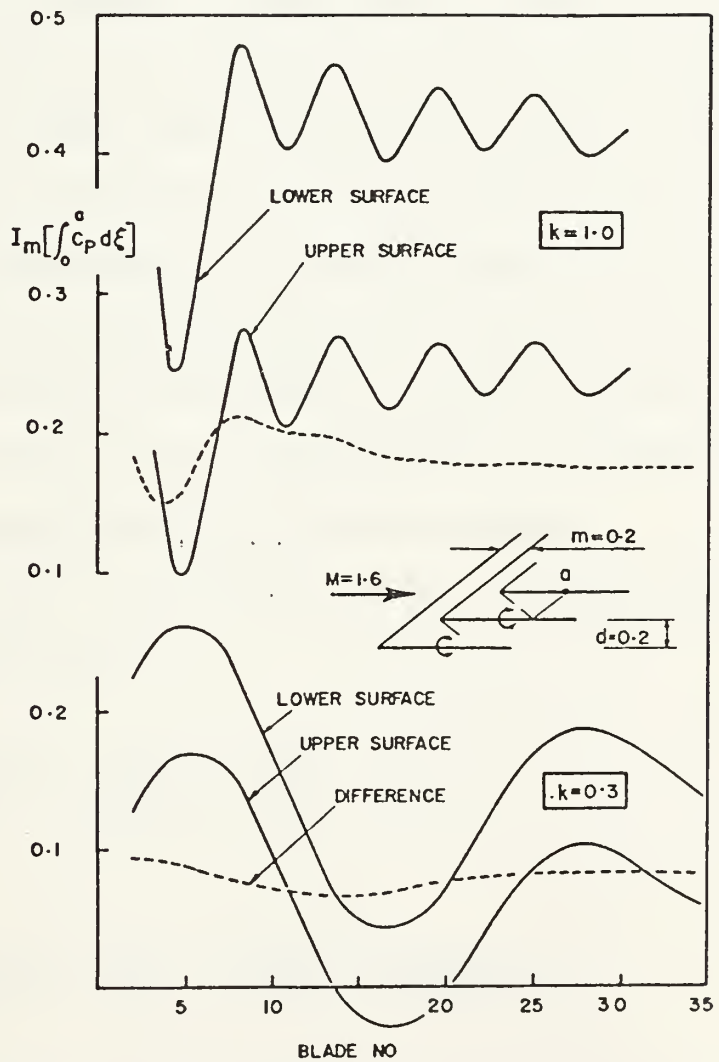

fig. 4.2 Variation of preinterference lift with blade index. Method of characteristics with zero interblade phase angle

On the basis of the low frequency theory of the finite cascade, together with the results of fig. 4.2 (see also fig. 3.6) it is possible to conclude that surface pressures in finite cascade calculations will exhibit a very lightly damped oscillation with blade index for most frequencies of practical interest in flutter analysis and for all inter-blade phase angles.

Sustained oscillations in surface pressure with blade index are not possible in the infinite rotor. Without proof, Verdon suggests that a periodic solution may be obtained by estimating the mean level of these oscillations [6]. This assumption has indeed been the basis for past work on supersonic unstalled compressor blade flutter. As outlined below, the present work provides some justification for this approach. At low oscillation frequencies, a proof is given that the average of finite cascade calculations is in fact the desired periodic solution for the infinite cascade.

Rewrite equ. 4.29 for the infinite array in terms of real and imaginary parts

$$I_m\left[C_P^{(u)} - C_{P_1}^{(u)}\right] = \frac{2km}{\beta^3}\left[-\frac{1}{2}\right]$$

$$R_e\left[C_P^{(u)} - C_{P_1}^{(u)}\right] = \frac{2km}{\beta^3}\left[\frac{\sin\mu}{2(1-\cos\mu)}\right] \qquad 4.34$$

which are precisely the mean values of the two undamped oscillatory series given in equ. 4.33 for the finite cascade.

The solution for the finite cascade involves the divergent series

$$\sum_{1}^{n} e^{ip\mu}$$

which does not converge to a sum in the ordinary sense of the word. However, the series is capable of generalized summation, using the method of arithmetic means [25]. In this sense, the Cesâro generalized sum is

$$R_e\left[\sum_{1}^{\infty}{}' e^{ip\mu}\right] = -\frac{1}{2} + \sum_{m=-\infty}^{m=\infty} \delta\left(\frac{\mu}{2\pi} - m\right) \qquad 4.35a$$

$$I_m\left[\sum_{1}^{\infty} e^{ip\mu}\right] = \frac{\sin \mu}{2(1 - \cos \mu)} \qquad 4.35b$$

where δ is the delta function. It may thus be said that the solution for the finite array converges in the Cesâro sense to the desired periodic solution ($\mu \neq 0$).

The divergent series for the finite cascade may be interpreted conveniently by representing the partial sums

$$S_n = \sum_{1}^{n} e^{ip\mu}$$

as points in the complex plane. From equ. 4.33 it is then easy to show that these points are equally spaced about the

circumference of a circle which passes through the origin of coordinates and whose center is at the point shown (fig. 4.3). The amplitude of oscillations is 1/2 cosec μ/2 .

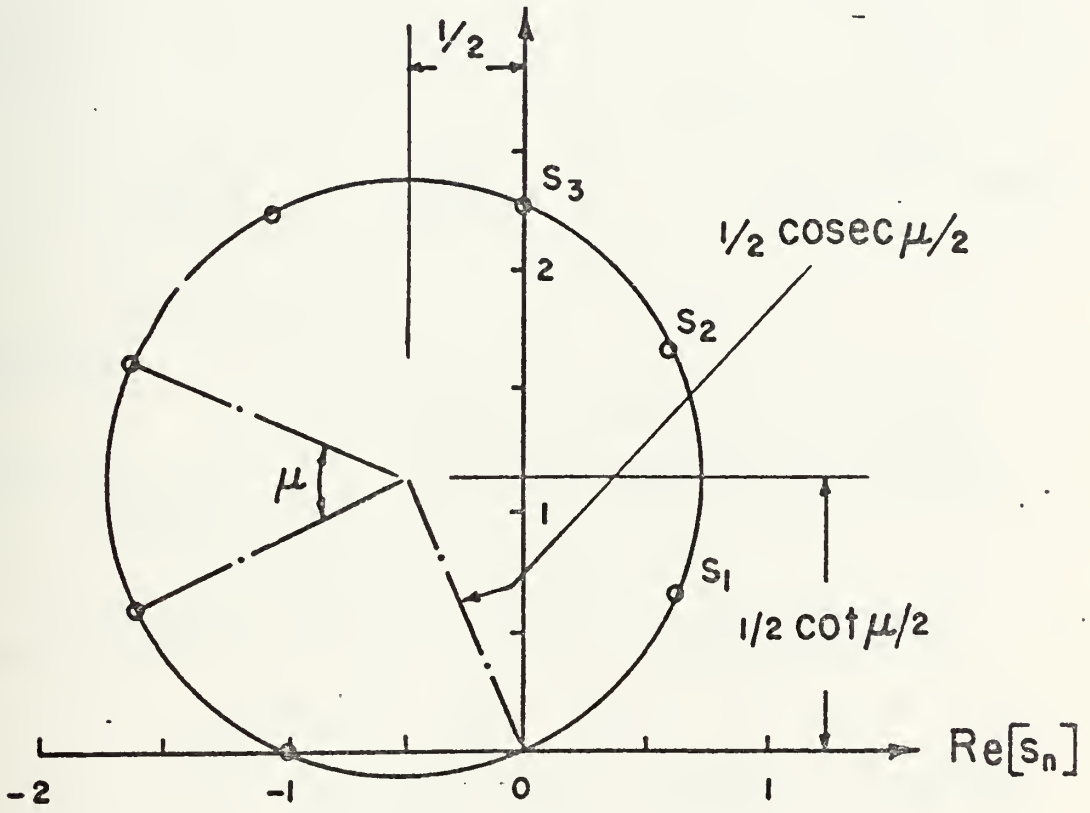

fig. 4.3 Geometrical interpretation of the divergent series for the finite cascade array

The finite and infinite cascade solutions are compared in fig. 4.4. Presented against blade index are in-phase and out-of-phase components of upper surface lift. The results

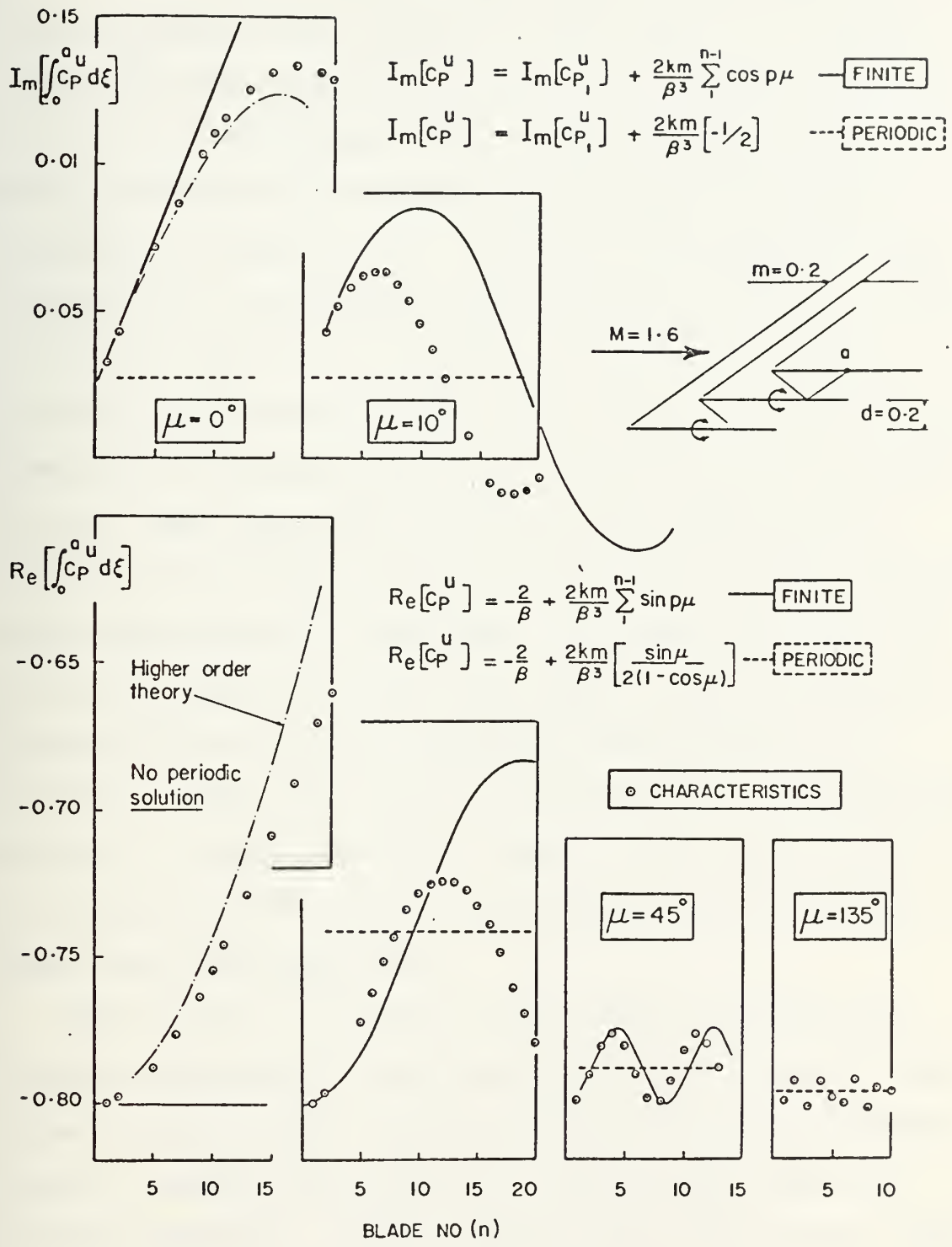

fig. 4.4 Comparison of finite and infinite (periodic) solutions for upper surface lift (k=0.1)

given include exact calculations based on the method of characteristics which extend to blade index 20. Several interblade phase angles are considered. Reduced frequency is 0.1. It is important to note that no periodic solution exists according to the present theory when the blades oscillate in phase ($\mu = 0$). In fig. 4.4, however, making allowance for the expected limitations of first order theory in the far field of the cascade, it is clear that for μ greater than some small value, the lift in the finite cascade commences to oscillate about the derived periodic solution. Further, when the blade oscillations are approximately in-phase, the pressure forces in the finite cascade oscillate with large period and amplitude. As μ approaches 180° the period and amplitude become very small. Both the method of characteristics and the elementary theory predict this behaviour. Note also that the imaginary part of the periodic solution is independent of μ; however, the real component of the pressure varies with μ, approaching Ackeret theory as the phase angle approaches 180°.

The unsteady air forces in the finite cascade do not therefore converge in the usual sense with increasing blade index to the periodic forces predicted by infinite cascade theory. Instead, they oscillate indefinitely about the periodic solution. Further, while exact calculations indicate the possibility of light damping of these oscillations, the rate of convergence is much too slow for practical purposes.

In the case of the blade pressure loading, the difficulties noted above disappear. The ΔC_{P_n} of equ. 4.32 for the finite cascade and the ΔC_p of equ. 3.30 for the infinite cascade are identical. The fact that ΔC_{P_n} is constant for all the blades of the cascade (except the first) was noted in Section 3. This finding of the elementary theory is in agreement with the results given in fig. 4.5* (see also fig. 4.2).

*Note the large component of lift in these calculations which is not associated with the pitching of the aerofoil, namely $4 \sin \mu/\beta$.

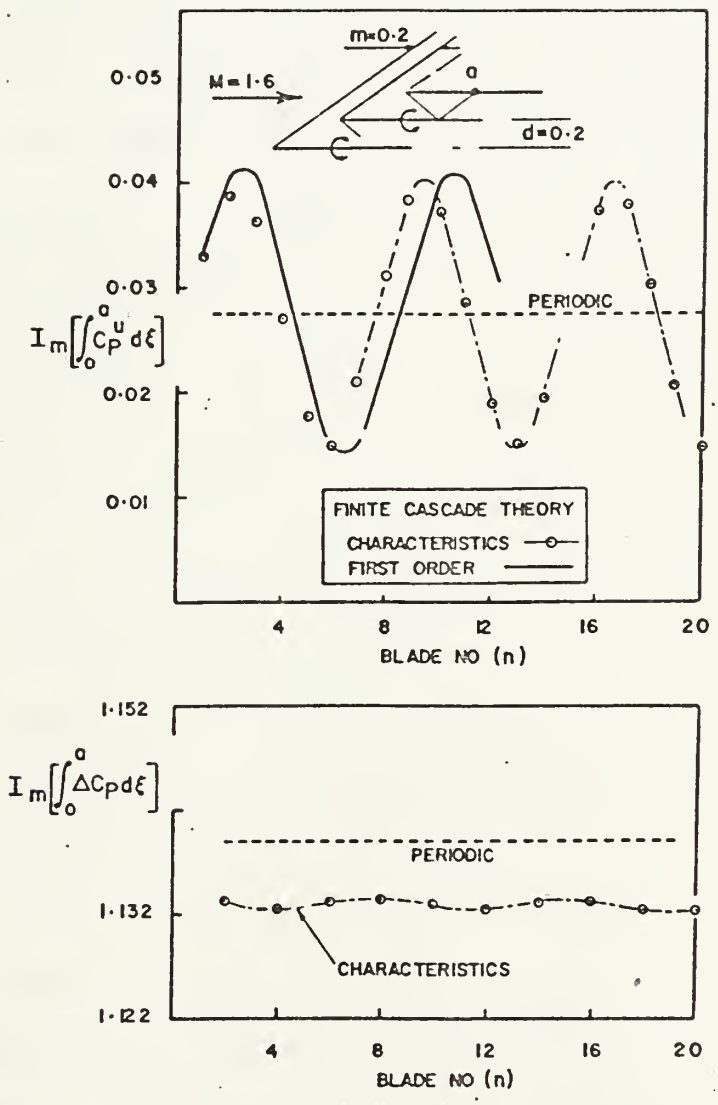

fig. 4.5 Variation of upper surface lift and total lift with blade index (45° interblade phase angle, k=0.1)

5 CONCLUSIONS

Nonlinear Effects

A numerical procedure for calculating the nonlinear effects of blade thickness in finite supersonic cascades with a subsonic leading edge locus is presented. A basic feature of the method is the application of the Rankine Hugoniot relations to determine unsteady boundary conditions immediately downstream of an oscillating bow shock wave. The solution is developed downstream of the shock using the two-dimensional nonlinear theory of characteristics. For the single oscillating wedge, the solution is in good agreement with Carrier's exact solution, even at Mach numbers close to shock detachment. There is a significant increase in the stability of the biconvex aerofoil, compared with the flat plate, for oscillations about a rearward pivot. On the other hand, for slow oscillations about a forward pivot, this aerofoil exhibits a level of instability which is somewhat higher than that given by the classical linear theory. The equivalent single wedge, however, is dramatically unstable and in this case the pressures show very poor agreement with linear theory. The general nonlinear thickness solution for the finite cascade reduces correctly in the limit as blade thickness vanishes. There is also an indication that thickness effects may be reduced by cascading.

Linear Theory

The finite flat plate array is solved analytically to the third power in oscillation frequency, using the Laplace transform. Notwithstanding the divergence of the solution in the far field of the cascade, owing to a Bessel function expansion which assumes small values of the argument, the simple expressions for pressure distribution have application over a useful range of oscillation frequencies. The important first-order frequency solution is also derived by generalizing Sauer's classical treatment of the oscillating flat plate in unbounded supersonic flow. This is compared with a corresponding result for the infinite array, which is obtained using a simple periodic analysis. The pressure loading in the two cases is shown to be identical. For the case when the blades oscillate with some phase difference, surface pressures in the finite cascade exhibit a continuing oscillation with blade index. The mean value of this oscillation is shown to be the correct periodic solution.

APPENDIX

Alternative Derivation of the First-Order Solution for the Finite Cascade

A solution for the finite cascade, exact to first-order in oscillation frequency, may be obtained by suitably extending Sauer's solution for the isolated blade oscillating slowly in unbounded supersonic flow [18]. The flow in the n^{th} preinterference zone of the cascade must satisfy

$$\beta^2 \frac{\partial^2 \phi_n}{\partial x^2} - \frac{\partial^2 \phi_n}{\partial y^2} = k^2 M^2 \phi_n - i2kM^2 \frac{\partial \phi_n}{\partial x} \qquad \text{A.1a}$$

$$\frac{\partial \phi_n}{\partial y} = -[1 + ik(x-b)]\, e^{i(n-1)\mu} \; ; \; y = 0 \qquad \text{A.1b}$$

where x and y are local coordinates for the n^{th} blade. A particular solution is

$$\phi_n(x,y) = f_n(s) + k[h_n(s) - iM^2 y f_n(s)/\beta] \qquad \text{A.2}$$

where $$s = x - \beta y \qquad \text{A.3}$$

and where, for the isolated aerofoil, the functions f(s) and h(s) vanish upstream of the left-running bow wave s=0. Apply the flow tangency condition

$$[1 + ik(s-b)]e^{i(n-1)\mu} = \beta f_n' + k(\beta h_n' + iM^2 f_n/\beta) \qquad A.4$$

where the prime denotes differentiation with respect to argument and where, since y=0, s has been written for x. It follows that

$$f_n(s) = s/\beta e^{i(n-1)\mu} + A_n \qquad A.5a$$

$$h_n(s) = is/\beta^3[(s/2+b\beta^2)e^{i(n-1)\mu} + M^2\beta A_n] + B_n \qquad A.5b$$

where A_n and B_n are integration constants. Thus

$$\phi_n(x,y) = \frac{s}{\beta} e^{i(n-1)\mu} + A_n - \frac{ik}{\beta^3}\left[(\frac{s}{2}+b\beta^2+M^2\beta y)e^{i(n-1)\mu} + M^2\beta A_n\right]$$

$$- ik(M^2 y A_n/\beta - B_n) \qquad A.6$$

To determine the pressure coefficient

$$C_{P_n}(x,y) = -2[f_n' + k(h_n' + if_n')]\, e^{-i(n-1)\mu} \qquad A.7$$

corresponding to maximum angle-of-attack of the n^{th} blade, the integration constant A_n is required. This is obtained by matching steady potentials in adjacent preinterference regions along the common left-running bow wave. Thus, with $A_1=0$, the continuity requirement $\phi_n(s=m) = \phi_{n+1}(s=0)$ leads to

$$A_n = \frac{m}{\beta} \sum_{p=0}^{n-2} e^{ip\mu} \qquad A.8$$

and the upper surface pressure coefficient for the n^{th} blade in the cascade in the preinterference zone is

$$C_{P_n}^{(u)} = C_{P_1}^{(u)} + ik \frac{2m}{\beta^3} \sum_{p=1}^{n-1} e^{-ip\mu} \qquad A.9$$

where $C_{P_1}^{(u)}$ corresponds to the isolated blade. To O(k) this agrees with equ. 3.51c derived using the Laplace transform.

If consideration is now given to the flow field bounded by the right-running bow wave from the $(n+1)^{th}$ blade and its reflection from the n^{th} blade, then the potential in this region may be constructed by superimposing upon the previous solution of left-running waves from the n^{th} blade an analogous family of right waves. The basic procedure is given in Section 4, where the Sauer approach is applied to the infinite cascade. The pressure loading is found to be

$$\Delta C_{P_n} = 2C_{P_1}^{(u)} \left[e^{-i\mu} - 1 \right] + \frac{i4k}{\beta} \left[\frac{M^2 d}{\beta} - m \right] e^{-i\mu} \qquad A.10$$

which is again in agreement with a result of Section 3.

LIST OF REFERENCES

1. Fleeter, S., Proceedings of a Workshop on Aeroelasticity in Turbomachines held at Detroit Diesel Allison, Indianapolis, June 1972, Project Squid, ONR.

2. Okurounmu, O. and McCune, J.E., Lifting Surface Theory of Axial Compressor Blade Rows: Parts 1 and 2, AIAA Journal, Vol. 12, No. 10, Oct. 1974, pp. 1363-1380.

3. Lane, F., Supersonic Flow Past an Oscillating Cascade with Supersonic Leading Edge Locus, Journal of Aeronautical Sciences, Vol. 24, June 1957, pp. 65-66.

4. Platzer, M.F., and Chalkley, H.G., Theoretical Investigation of Supersonic Cascade Flutter and Related Interference Problems, AIAA/ASME/SAE 13th Structures, Structural Dynamics, and Materials Meeting, San Antonio, Texas, April 1972, Paper No. 72-377.

5. Brix, C.W., and Platzer, M.F., Theoretical Investigation of Supersonic Flow Past Oscillating Cascades with Subsonic Leading Edge Locus, AIAA 12th Aerospace Sciences Meeting, Washington, D.C., Jan. 1974, Paper No. 74-14.

6. Verdon, J.M., The Unsteady Aerodynamics of a Finite Supersonic Cascade with Subsonic Axial Flow, Transactions of ASME, Journal of Applied Mechanics, Vol. 40, No. 3, Sept. 1973, pp. 667-671.

7. Sisto, F. and Ni, Ron Ho, Research on the Flutter of Axial-Turbomachine Blading, Stevens Institute of Technology, Tech. Rep. ME-RT74-008, May 1974.

8. Nagashima, T. and Whitehead, D.S., Aerodynamic Forces and Moments for Supersonic Vibrating Blades, CUED/A-Turbo/TR-59, Cambridge University, 1974.

9. Kurosaka, M., On the Unsteady Supersonic Cascade with a Subsonic Leading Edge - An Exact First Order Theory, Parts 1 and 2, Transactions of ASME, Journal of Engineering for Power, Vol. 96, No. 1, Jan., 1974, pp. 13-31.

10. Verdon, J.M. and McCune, J.E., The Unsteady Supersonic Cascade in Subsonic Axial Flow, AIAA Journal, Vol. 15, No. 2, Feb. 1975, pp. 193-201.

11. Busemann, A., Aerodynamischer Auftrieb bei Uberschallgeschwindigkeit, Luftfahrt forschung, Bd. 12, Nr. 6, Oct. 1935, pp. 213.

12. Van Dyke, M.D., Supersonic Flow Past Oscillating Aerofoils Including Nonlinear Thickness Effects, NACA Technical Note 2982, July 1953.

13. Teipel, I., Die Berechnung instationarer Luftkrafte im schallnahen Bereich, Journal de Mecanique, Vol. 4, No. 3, Sept. 1965, pp. 335-360.

14. Teipel, I., Die Verdichtungsstosswelle an einem oszillierenden Keil, DVL - Bericht Nr. 424, 1965.

15. Carrier, G.F., The Oscillating Wedge in a Supersonic Stream, Journal of Aeronautical Sciences, Vol. 16, No. 3, March 1949, pp. 150-152.

16. Garrick, I.E., and Rubinow, S.J., Flutter and Oscillating Air Force Calculations for an Aerofoil in Two-Dimensional Supersonic Flow, NACA Report No. 846, 1946.

17. Lichtfuss, H.J. and Starken, H., Supersonic Exit Flow of Two-Dimensional Cascades, ASME Publication, Presented at the Gas Turbine and Fluids Engineering Conference and Products Show, San Francisco, Calif., March 1972.

18. Sauer, R., Elementare Theorie des langsam schwingenden Uberschallflugels, ZAMP, 1950, pp. 248-253.

19. Landahl, M., Unsteady Transonic Flow, Permagon Press, London, 1961.

20. Snyder, L.E., and Commerford, G.L., Supersonic Unstalled Flutter in Fan Rotors; Analytical and Experimental Results, ASME Paper No. 74-GT-40, Nov. 1973.

21. Oswatitsch, K., Die Berechnung wirbelfreier achsensymmetrischer Uberschallfelder, Oesterr. Ing-Archiv X, Bd. 4, 1956, pp. 359-382.

22. Owazarek, J.A., Fundamentals of Gas Dynamics, International Text Book Company, Pennsylvania, 1964, pp. 366-378.

23. Van Dyke, M.D., On Supersonic Flow Past an Oscillating Wedge, Quarterly of Applied Mathematics, Vol. 11, No. 3, Oct. 1953, pp. 360-363.

24. Jones, W.P. and Skan, W., Aerodynamic Forces on Biconvex Aerofoils Oscillating in a Supersonic Air Stream, Aeronautical Research Council R&M No. 2749, August 1951.

25. Kantrowitz, A., The Supersonic Axial-Flow Compressor, NACA Report No. 974, 1950.

26. Lyusternik, L.A., and Yanpol'skii, A.R., Mathematical Analysis, Permagon Press, London, 1965.

INITIAL DISTRIBUTION LIST

		No. Copies
1.	Defense Documentation Center Cameron Station Alexandria, Virginia 22314	2
2.	Library, Code 0212 Naval Postgraduate School Monterey, California 93940	2
3.	Associate Professor M.F. Platzer, Code 57Pl Department of Aeronautics Naval Postgraduate School Monterey, California 93940	15
4.	Professor D.J. Collins, Code 57Co Department of Aeronautics Naval Postgraduate School Monterey, California 93940	1
5.	Professor T.H. Gawain, Code 57Gn Department of Aeronautics Naval Postgraduate School Monterey, California 93940	1
6.	Associate Professor R.P. Shreeve, Code 57Sf Department of Aeronautics Naval Postgraduate School Monterey, California 93940	1
7.	Professor C. Comstock, Code 53Zk Department of Mathematics Naval Postgraduate School Monterey, California 93940	1
8.	Professor K.E. Woehler, Code 61Wh Department of Physics and Chemistry Naval Postgraduate School Monterey, California 93940	1
9.	William Richard Chadwick Research Associate Surface Warfare Department U.S. Naval Weapons Center Dahlgren, Virginia	1
10.	Dr. H. J. Mueller, Code AIR-310 Naval Air Systems Command Washington, DC 20360	1

Thesis
C33863
c.1

182229

Chadwick
Unsteady supersonic cascade theory including nonlinear thickness effects.